Universidad Autónoma de Nuevo León

Facultad de Ingeniería Mecánica y Eléctrica

Subdirección de Estudios de Posgrado

Distance and Overcurrent relay coordination considering non standardized inverse time curves

por

M.C. Carlos Alberto Castillo Salazar

en opción al grado de

Doctor en Ingeniería Eléctrica

Diciembre 2015

UNIVERSIDAD AUTÓNOMA DE NUEVO LEÓN

FACULTAD DE INGENIERÍA MECÁNICA Y ELÉCTRICA

SUBDIRECCIÓN DE ESTUDIOS DE POSGRADO

DISTANCE AND OVERCURRENT RELAY COORDINATION CONSIDERING NON STANDARDIZED INVERSE TIME CURVES

POR

M.C. CARLOS ALBERTO CASTILLO SALAZAR

EN OPCIÓN AL GRADO DE

DOCTOR EN INGENIERÍA ELÉCTRICA

DICIEMBRE 2015

Universidad Autónoma de Nuevo León

Facultad de Ingeniería Mecánica y Eléctrica

Subdirección de Estudios de Posgrado

Los miembros del Comité de Tesis recomendamos que la Tesis «**Distance and Overcurrent relay coordination considering non standardized inverse time curves**», realizada por el alumno **M.C. Carlos Alberto Castillo Salazar**, con número de matrícula **1249685**, sea aceptada para su defensa como requisito parcial para obtener el grado de **Doctor en Ingeniería Eléctrica**.

El Comité de Tesis

Dr. Arturo Conde Enríquez
Asesor

Dra. Satu Elisa Schaeffer
Co-asesora

Dra. Gina María Idárraga Ospina
Revisor

Dr. Óscar Arreola Soria
Revisor

Dr. Emilio Barocio Espejo
Revisor

Vo. Bo.

Dr. Simón Martínez Martínez
Subdirección de Estudios de Posgrado

San Nicolás de los Garza, Nuevo León, México, diciembre 2015

To God, my parents, and my fiancée.

ACKNOWLEDGEMENTS

Foremost, I would like to take this chance to express my gratitude to my thesis directors, Dr. Arturo Conde Enríquez and Dr. Satu Elisa Schaeffer for their guidance, support, shared knowledge, doubts clarification, time, and patience through the development of this work. This was my second opportunity to work with both of you and I look forward to keep doing research together.

Besides my advisors I also want to thank my host during my research visit at Aalto University, Professor Harri Ehtamo for receiving, guiding, and helping me and my research project during one of the most memorable parts of my education. I would like to extend this recognition to my thesis reviewers, Dr. Gina Idárraga, Dr. Emilio Barocio, and Dr. Óscar Arreola for their fast response and valuable comments that certainly improved the quality of my work and allowed me to accelerate the graduation process.

My gratitude is extended to the Facultad de Ingeniería Mecánica y Eléctrica, the Universidad Autónoma de Nuevo León, and the Consejo Nacional de Ciencia y Tecnología for giving me the opportunity to obtain my postgraduate academic degree and reach a life goal through the assignation of a scholarship and the complete coverage of tuition and scholar fees.

I want to accentuate my thanks to my friends and fellow researchers, Raúl García, Fernando Sánchez, Fernando Salinas, Alexandro Curti, Raúl Aguirre, Demetrio Macías, and Victor Oropeza for their support, help, and most for their friendship. I will always remember the difficult paths we walked together in order to reach our goals; new paths are just beginning.

Mostly I would like thank my parents and to do so I am going to switch to my native language. Papá y Mamá, gracias por cada momento que han compartido conmigo, por basar gran parte de su alegía en la mía, por pensar en mí, amarme y demostrarlo cada día con cada una de sus acciones, por permanecer juntos y porque gracias a ustedes soy la persona en quien me he convertido. Agradezco también a mis hermanos — Luis, Junior, Laura, Esmeralda, Claudia y Dinorah — así como a mis sobrinos, por el amor y expectativas tan altas que tienen para mi, logrando así impulsarme cada día a ser la persona que creen que soy. Deseo cerrar este párrafo agradeciendo también a mi nueva familia por recibirme cálidamente, hacerme sentir un miembro más y brindarme la oportunidad de ser parte de sus vidas, gracias señor Angel, señora Cristina, Angel, Sara, Maggie, Cris, Humby y bebé.

There is an old saying that reads “whoever finds a faithful friend has found a treasure”, therefore I think I must be the luckiest person alive; I want to thank my numerous friends for doing what friends do best, share and lighten any burden.

There are not enough words in my vocabulary to express how grateful I am with life, mainly because I also have the bliss of having the most kind and beautiful woman to share my life with. I want to thank you, my beloved fiancée Alejandra because the best moments of this years and probably of my whole life, I have shared them with you.

Thank you God, because your unfailing love is better than life itself.

M.C. Carlos Alberto Castillo Salazar

Abstract

Protective relaying comprehends several procedures and techniques focused on maintaining the power system working safely during and after undesired and abnormal network conditions, mostly caused by faulty events. Overcurrent relay is one of the oldest protective relays, its operation principle is straightforward: when the measured current is greater than a specified magnitude the protection trips; less variables are required from the system in comparison with other protections, causing the overcurrent relay to be the simplest and also the most difficult protection to coordinate; its simplicity is reflected in low implementation, operation, and maintenance cost.

The counterpart consists in the increased tripping times offered by this kind of relays mostly before faults located far from their location; this problem can be particularly accentuated when standardized inverse-time curves are used or when only maximum faults are considered to carry out relay coordination. These limitations have caused overcurrent relay to be slowly relegated and replaced by more sophisticated protection principles, it is still widely applied in subtransmission, distribution, and industrial systems.

In this work, the use of non standardized inverse-time curves, the model and implementation of optimization algorithms capable to carry out the coordination process, the use of different levels of short circuit currents, and the inclusion of distance relays to replace insensitive overcurrent ones are proposed methodologies focused on the overcurrent relay performance improvement. These techniques may transform the typical overcurrent relay into a more sophisticated one without changing its fundamental principles and advantages. Consequently a more secure and still economical alternative can be obtained, increasing its implementation area.

Contents

List of Figures

List of Tables

NOMENCLATURE

α	Weighting factor for main relays
β	Weighting factor for backup relays
δ	Weighting factor for distance-relays
ϵ	Penalty factor for negative coordination errors
η	Sensitivity index
γ	Weighting factor for main relays
ι, κ, τ	Weighting constants for I_{sc} magnitudes
$\mathbf{B}_n$	Hessian matrix approximation
$\mathbf{P}_{\mathbf{C_x}}$	Population matrix
$\mathbf{Z}$	Population matrix distance times
$\mathrm{A}, \mathrm{B}, \mathrm{p}$	Time curve characteristic constants
t	Tripping time
$\mathrm{C_x}$	Chromosome
$\mathrm{CTI_d}$	Coordination time interval for distance-relays
CTI	Coordination time interval
$\mathrm{E_{CTI}}$	Coordination error

F_b Fitness of the fittest element

F_w Fitness of the worst element

F Fitness of an individual

I_c Coordination current

I_{load} Load current

I_{pickup} Pickup current

I_{sc} Short circuit current

$mc_d\%$ Overcurrent and distance-relays miscoordination percentage

P_s Population size

P_m Pickup current multiplier

S_{rM} Maximum possible assigned seeds

S_{rm} Minimum possible assigned seeds

S Seeds

t_b^d Backup relays desired tripping time

T_i Total iterations

t_m Main relays tripping time

T_r Total overcurrent relays

T_S Total seeds

T_{C_x} Total of chromosomes

T_{dr} Total of distance-relays

T_{mc} Total miscoordinations

$\nabla f(x)$ Vector of gradients

$\nabla^2 f(x)$ Hessian matrix

de_b Coordination error OC+D

de_m Coordination error D+OC

f Fitness

s Total samples of each parameter

T_c Total combinations

x^* Local optimum

x_0 Initial solution

ABC Artificial bees colony

ACO Ant-colony optimization

D+OC Distance as main and Overcurrent as backup pair

DE Differential-evolution

DOCR Directional-overcurrent relays

EI Extremely inverse

EPS Electrical power system

FLOPS Floating-point operations per second

GA Genetic algorithms

IEC International electrotechnical commission

IEEE Institute of electrical and electronics engineers

IWO Invasive-weed optimization

mc% Overcurrent miscoordination percentage

MI Moderately Inverse

NLP Nonlinear programming

OC+D Overcurrent as main and as backup pair

OC+D Overcurrent as main and distance as backup pair

OCR Overcurrent relay

OF Objective function

P(D) Probability of dispersing

P(D) Probability of mutation

P(S) Probability of crossover

P(S) Probability of elite parents

P(S) Probability of rolling-down

P(S) Probability of spreading

PSO Particle-swarm optimization

SQP Sequential quadratic programming

TCP Total coordination points

TDS Time dial setting

VI Very inverse

Chapter 1

Introduction

A brief introduction to power systems, power systems protection and their importance is presented in the first section of this chapter. In the next section, the power system protection importance is highlighted, thereupon the state-of-the-art related work is listed and described, then the motivation and problem statement as well as the hypothesis, objectives, and thesis structure are presented.

1.1 Power System Protection

An *Electrical Power System* (EPS) is a network of electrical components used to generate, transmit, and supply electric power. The basic power system structure is illustrated in Figure 1.1. The EPS can be seen as a huge monster that has to remain immovable before any unpredictable event and hold stoic while supplying the required demand; if the system collapses and a blackout is presented, it has to be reestablished as soon as possible in order to keep business running and maintain us satisfied and comfortable.

In some way the system is in fact a beast not easily affected by every undesired event, moreover it can regain equilibrium after events occurrence. The previous statement is founded in two main reasons, the first one is that the power system is usually too big to be affected by daily events, characteristic related with a research field named power system *stability* [1].

The second reason — and most important for this thesis — is the hard task carried

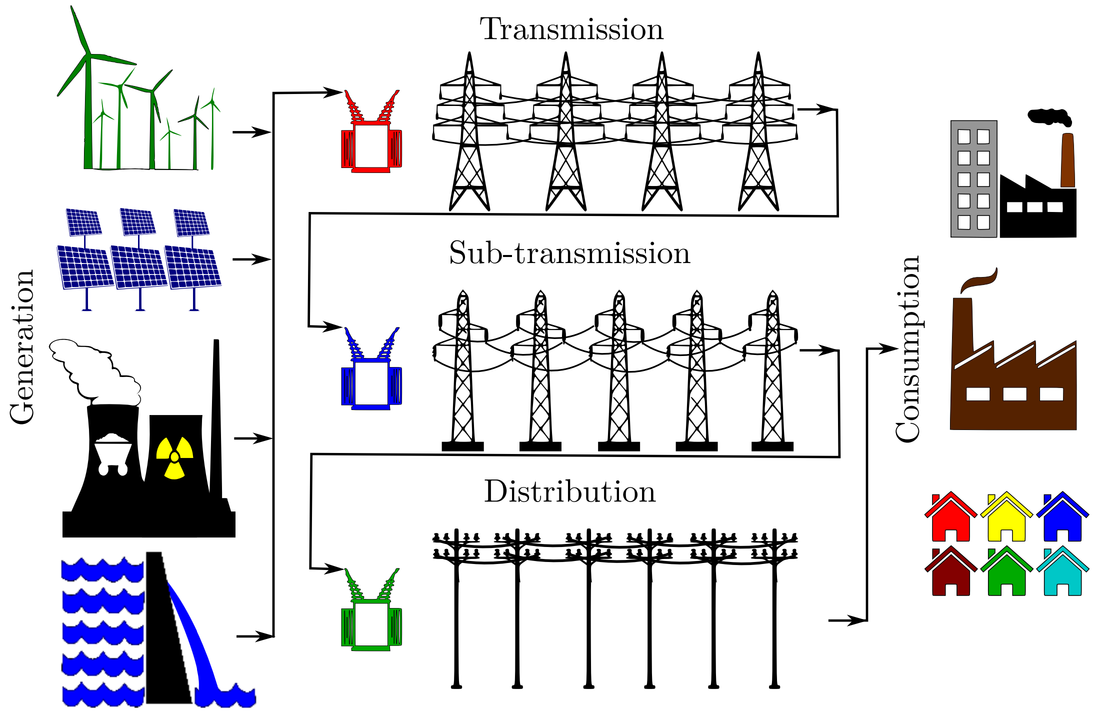

Figure 1.1: Basic structure of an electric power system. The electrical energy is generated, transmitted, and delivered for customer consumption.

out by the *protection system* and protection engineers charged with the crucial duty of isolating the system, preventing it from collapsing before undesirable and possibly harmful events, most often caused by short circuits.

A protective relay is an electric device that receives inputs as temperature, voltage, and current, measures and compares them to make a diagnosis, and takes decisions about the actions that have to be performed to keep the protected system safe; the output signal of protective relays may lead to abrupt changes on their related power circuits. The monitored events are in the order of milliseconds and must be faced as quickly as possible, making the human intervention impractical; consequently a relay is designed to operate autonomously in a prescribed manner. One of the most interesting and complex applications of a protective relay is the protection of electric power systems [2].

The distribution systems deliver the energy to the final customer either in residential or industrial areas, typically within a range of voltages from 2 to 35 kV; distribution are the most interconnected networks, the conductors may be buried or carried on overhead poles. The subtransmission systems connect the distribution substations around a city or relatively small regions with voltages from 35 up to 110 kV, although in some countries voltages of 138 kV are often used. Finally, the transmission lines are responsible to carry on the energy from the generation substations to the subtransmission ones at high and ultra-high voltages from 110 to +800 kV [2, 3].

The protections system is not useful while the system is operating in a normal manner; however, when a fault condition is presented, the stability of the whole EPS depends on its proper operation. The consequences of a malfunction could lead the system to a concatenation of errors or faults, resulting at worst case in a massive collapse and blackout, depriving of electric service to industrial and residential zones and possibly causing a large scale damage to the EPS.

1.2 State-of-the-Art

Because of the complex nature of the overcurrent relay coordination problem and encouraged by the constant increase of computer capabilities [4], looking to facilitate and improve the protection engineering practices, fifty years ago some efforts were made in order to automate the solution process, then for almost three decades the Overcurrent Relay (OCR) coordination problem has been faced as an optimization one.

On this section, several related works are going to be described and compared in order to clearly identify the novelties presented in this work. A short description of articles that have been published between 1963 and 2015 regarding this topic can be seen in the following paragraphs.

1.2.1 Overcurrent Relay Coordination Works

Some of the first effective tries to automate the coordination process and to set some fundamentals in this topic are presented by Radke [5], Albrecht et al. [6], Tsien [7], Kennedy and Curtis [8], and Whiting and Lidgate [9]. First, Radke [5] propose an accurate curve-fitting method with the advantage of small computer storage requirements.

In 1964 Albrecht et al. [6] published an article describing a digital computer protective device co-ordination program, the objective of the program was to compute and check the settings of the relays system. Late in the same year, in a similar work Tsien [7] proposes another method with the advantage of not requiring previous short-circuit calculations, since the program perform them by itself.

The method presented by Kennedy and Curtis [8] is capable to compute an inverse-time curve for industrial applications. Whiting and Lidgate [9] improve previously obtained results by proposing a method capable to perform short-circuit analysis, obtain relay settings, offer limited interactive functions, and check the performance of the relays. All these methodologies pursued and achieved saving time to the protections engineer and they were successfully used for several years [10], until the advances in computation industry allowed the implementation of more complex procedures.

Almost three decades ago, Urdaneta et al. [10] introduced a multiple criteria linear optimization method that give solution to the problem by obtaining optimal time dial settings (TDS) results. This work opened a new research area, where a specific objective function is minimized and the OCR coordination problem is seen as an optimization one.

The computer capacities of the time permit the coordination to be carried out just for faults at the midpoint of lines. The same authors present a more effective approach based in linear programming [11], it is used to compute the same optimal setting when a local structure change has been performed in the system. In a similar work, Urdaneta and Pérez [12] use linear programming to solve the problem considering dynamic changes in the network's topology due to the effect of transient configurations.

The main issue in linear programming approaches is the requirement of a good initial guess and also the high probability of being trapped in local minima solutions. In a successful attempt to overcome those limitations, So et al. [13, 14] start with the adaptation and implementation of natural imitation algorithms to solve coordination problems, the Genetic Algorithms (GA) offer multiple initial search and a quick obtention of optimum relay settings. The use of evolutionary programming by So and Li [15] increases the chance of obtaining global minimum settings, and also considers the addition of dynamic changes in the network's topology. The approaches presented by Urdaneta et al. [16] and Karegar et al. [17] propose a linear programming interior-point algorithm; presolution techniques are used to filter and simplify the problem; reducing its complexity and improving the performance of mathematical optimization algorithms.

As an alternative to linear and nonlinear programming, Zeienldin et al. [18] present a Mixed Integer Non Linear Programming method (MINLP), they conclude that computing continuous pickup currents to later round them to their nearing discrete value could lead to infeasible solutions. This work is improved by Zeineldin et al. [19]; the robustness increases by adding additional constraints, avoiding nonlinearities caused by the discrete magnitudes of the I_{pickup}.

In another publication, Zeineldin et al. [20] recognize the limitations of deterministic methods and apply a Particle-Swarm Optimization (PSO) technique in another attempt to overcome those limitations. It is demonstrated that for larger problems, the PSO find faster and much better solutions in comparison with MINLP. Similar results are obtained by Gholinezhad et al. [21] when they use MINLP considering two variables as adjustable settings.

Birla et al. [22] optimize the problem settings in a nonlinear environment using SQP and considering one fault point. The results show that solving the coordination problem based on only close-end faults does not affect significantly the results in small systems; the drawback is that in some scenarios, specially in bigger systems, this consideration can lead to miscoordinations for far-end faults. This conclusion helps to highlight the importance of considering more than one magnitude of short-circuit current to carry out the coordination process, as done in this thesis. As a complement of their previous work, Birla et al. [23] propose an approach to prevent sympathy trips that may appear by considering only near-end faults.

The genetic algorithms prove to be a fast and robust method suitable to solve the coordination problem; Lee and Chen [24] implement this metaheuristic to achieve coordination in an industrial radial system, improving the results obtained by traditional methods. Razavi et al. [25] introduce a novel — and later widely used — objective function capable to handle miscoordination problems (Equation 1.1); the tripping time of the main relay is represented by t_i and the coordination error by Δt_{mb}. This approach considers only the TDS as adjustable setting.

$$OF = \alpha_1 \sum (t_i)^2 + \alpha_2 \sum (\Delta t_{mb}) - \beta_1 (\Delta t_{mb}) - \|\Delta t_{mb}\|)^2. \tag{1.1}$$

Kamangar et al. [26] present a new GA method, in addition to the coordination of overcurrent relays, this method also coordinates earth fault ones. Uthitsunthorn and Kulworawanichpong [27] optimize the TDS in another simple but effective implementation of GA. Bedekar et al. [28, 29] introduce the use of simplex and dual-simplex methods to optimize the TDS in small radial and interconnected distribution systems. Noghabi et al. [30] obtain optimal relay settings for a set of different network topologies; in the first work, a hybrid method is developed with the objective of taking advantage of the search space exploration and the local exploitation capabilities of GA and LP to find optimal TDS and pickup tap settings.

Furthermore, Noghabi et al. [31] optimize the TDS by implementing an interval linear programming method; this methodology is tested in bigger systems in comparison with the previous contribution. In a research with a similar objective, Bedekar and Bhide [32] propose a GA-NLP hybrid method to optimize the pickup current and the TDS; nevertheless, the same authors obtain satisfactory results in small distribution systems using only a continuous genetic algorithm [33].

Damchi et al. [34] use a hybrid PSO-LP methodology to obtain optimal discrete I_{pickup} and continuous TDS settings for microgrid systems. Singh et al. [35] present a simple GA capable to solve the OCR coordination for small systems. Mohammadi et al. [36] also implement a genetic algorithm that considers the priority of constraints in order to reduce the total of miscoordinations.

Ezzeddine and Kaczmarek [37] introduce the consideration of three parameters as adjustable settings, in addition to the commonly used TDS and I_{pickup}, the algorithm is capable of selecting an inverse-time characteristic curve. This solution considers all three settings discrete. Moirangthem et al. [38] present the implementation of a differential evolution algorithm to solve the coordination considering distributed generation. Uthitsunthorn [39] and El-Mesallamy et al. [40] introduce in different works the use of the Artificial Bees Colony (ABC) algorithm, concluding that this method can be faster while achieving similar results in comparison with linear, nonlinear and PSO methods.

Thangaraj et al. [41] have worked with the adaptation and implementation of three modified Differential-Evolution (DE) algorithms which mutation operators were based on Laplace, Cauchy, and Gaussian probability distributions, improving the results obtained by the basic DE. Singh et al. [42] develop a Covariance Matrix Adaptation Evolution Strategy as a minimization strategy to obtain optimal I_{pickup} and time multiplier settings. Sueiro et al. [43] present a new method using evolutionary and linear programming, this implementation allows the elimination of restrictions, seeking to achieve partial coordination of relays prone to miscoordinate.

Mahari and Seyedi [44] propose an analytic approach to compute two optimal settings; the iterative numerical technique's main objective is the reduction of the total operating time instead of the magnitude of the adjustable settings. Chen et al. [45] introduce a fast GA with the objective of optimizing two settings in an industrial radial system. In similar works, Bottura et al. [46, 47] optimize the discrete settings to achieve coordination in a real meshed power system via the implementation of a hybrid linear programming and genetic algorithm.

Even tough the following two works are not presenting novelties in coordination related topics, they are interesting to mention. Hussain et al. [48] depict a review of OCR coordination methods, focusing in artificial intelligence and nature-inspired techniques. Lu and Chung [49] present a method to detecting and solving curve intersection problems.

Singh et al. came out with the implementation of a differential evolution algorithm to achieve coordination considering a fault in the middle of the line [50] and faults located at close and far-ends [51]. In a similar but improved work, Chelliah et al. [52] show the results of an opposition chaotic differential evolution algorithm; the main idea of this method is the simultaneous consideration of an estimate and its opposite point.

Hussain et al. [53] introduce the use of a Modified Swarm Firefly Algorithm, which is a improved version of PSO that accelerate the convergence speed and enhance its capability to obtain optimal settings.

Shih et al. [54] compare the performance of GA, PSO, and DE algorithms to achieve online coordination results of Directional-Overcurrent Relays (DOCR) considering two adjustable settings. Arreola Soria et al. [55] introduce the implementation of unconventional curves in industrial power systems; by considering the interaction of the digital representation of the moving induction disc and the TDS, the software is able to design a specific OCR curve that fits in the studied industrial power system. This work shows that the introduction of unconventional inverse-time curves reduces the mechanical stress and thermal effects, preventing damage and increasing the lifetime of the protection elements.

The related work is also shown in a condensed manner in Table 1.1. The columns of the table indicate the reference, year of publication, total of adjustable settings, methods implemented to solve the problem, and the total of busses and relays of the systems where each proposal is tested. All the related work consider conventional time curves and one, two, or three parameters as adjustable settings. The implemented methods are diversified, including linear and nonlinear, numerical, and nature-inspired algorithms.

Table 1.1: Related work for overcurrent relay coordination.

Reference	Year	AS	Method	System Buses	Total Relays
Urdaneta et al. [10]	1988	1	NLP	3, 6, 30	6, 30, 68
Urdaneta et al. [11]	1996	1	LP	18	74
Urdaneta and Pérez [12]	1997	2	LP	2, 6	6, 16
So et al. [13]	1997	2	GA	6	8
So et al. [14]	1997	2	GA	6	8
So and Li [15]	2000	2	EP	6	8
Urdaneta et al. [16]	2001	1	LP	9, 108	11, 97
Karegar et al. [17]	2005	1	LP	8, 11	6, 14, 39
Zeienldin et al. [18]	2004	1	NLP	3	6
Zeineldin et al. [19]	2005	2	MIP	8	14
Zeineldin et al. [20]	2006	2	PSO	8, 14	14, 40
Gholinezhad et al. [21]	2011	2	MIP/PSO	6, 30	14, 86
Birla et al. [22]	2006	2	SQP	6, 30	14, 68
Birla et al. [23]	2007	2	SQP	30	68
Lee and Chen [24]	2007	2	GA	2	8
Razavi et al. [25]	2008	1	GA	6, 8	14
Kamangar et al. [26]	2009	1	GA	8	14
Uthitsunthorn et al. [27]	2010	1	GA	6	14
Bedekar et al. [28]	2009	1	LP	4, 6	5, 8
Bedekar et al. [29]	2009	1	LP	2	2, 4
Noghabi et al. [30]	2009	2	LP	8	14
Noghabi et al. [31]	2010	1	ILP	14, 30	39, 76
Bedekar and Bhide [32]	2011	2	SQP/GA	9	24
Bedekar and Bhide [33]	2011	2	GA	3,	5, 6
Damchi et al. [34]	2011	2	PSO	6	11
Singh et al. [35]	2011	1	GA	3	8
Mohammadi et al. [36]	2011	1	GA	30, 59	39, 90
Ezzeddine and Kaczmarek [37]	2011	3	LP/NLP	8, 30	14, 78
Moirangthem et al. [38]	2011	2	DE	19	23
Uthitsunthorn et al. [39]	2011	2	GA	9	11
El-Mesallamy et al. [40]	2013	2	GA	3, 6, 8	6, 14, 14
Thangaraj et al. [41]	2012	2	DE	3, 4, 6	6, 8, 14
Singh et al. [42]	2012	2	CMA-ES	30	30
Sueiro et al. [43]	2012	2	LP	3	12
Mahari and Seyedi [44]	2013	2	LP	3, 8, 15	6, 14, 42
Chen et al. [45]	2013	2	GA	2,7	8, 7
Bottura et al. [46]	2013	2	LP/GA	18	22
Bottura et al. [47]	2014	2	LP/GA	43	6
Lu and Chung [49]	2013	2	Numerical	6, 7	16, 14
Singh et al. [50]	2014	2	DE	9, 30	24, 42
Singh and Panigrahi [51]	2014	2	DE	6	14
Chelliah et al. [52]	2014	2	OCDE	3, 4, 6, 14	6, 8, 14, 40
Hussain et al. [53]	2014	2	MSFA	8	14
Shih et al. [54]	2014	2	DE	14, 30	30, 68
Arreola Soria et al. [55]	2014	2	Numerical	3	4
Proposed work	**2015**	**5**	**GA, IWO, SQP**	**9, 14, 30, 57, 118**	**12, 30, 68, 130, 340**

1.2.2 OCR and Distance Relay Coordination Works

There have been several attempts to automate the coordination process between directional overcurrent and distance-relays [56–59]. The main objectives of these algorithms is to reduce the burden to the protections engineer while obtaining adequate solutions to this problem. In a more robust and still used work, Ramaswami et al. [60] present enhanced analytical techniques for coordinating three zones of distance-relays with overcurrent ones.

Pérez and Urdaneta [61] improve the work presented in [10] by including the timing of the second zone of distance-relays to the coordination process. An important conclusion of this research is the importance of the selected coordination time interval, in some scenarios the second zone tripping time should be greater than the classical and widely used 0.3 seconds. In a different approach, Khederzadeh [62] proposes a fixed second zone operation time while the shape of the OCR would change in accordance with the fault location. This proposal is based in the use of *universal protection devices* —which are conformed by the combination of inverse-time and definite-time overcurrent tripping shapes [63] —, instead of inverse definite minimum time relays.

Chabanloo et al. [64] propose a methodology based on the implementation of a genetic algorithm. This method is capable to optimize the TDS and the selection of a standardized OCR characteristic curve in order to coordinate it with the previously fixed tripping times of the second and third zones of distance-relays. In similar works, Sadeh et al. [65, 66] present the coordination of DOCR with the second zones of distance ones; these articles includes the second zone tripping time as a variable on their PSO formulation. Later, Chabanloo et al. [67] improve their previous work by considering more critical — coordination — points as restrictions; furthermore, the tripping time of the second zone was also considered as an adjustable setting.

Singh et al. [68] implement a DE algorithm with hybrid mutation with the objective to optimize the TDS and the I_{pickup} of an overcurrent relay while the tripping times of the distance-relays zones are fixed. Four coordination points are considered in this

Table 1.2: Related work for distance and overcurrent relay coordination.

Reference	Year	AS	Method	System Buses	Total Relays
Gastineau et al. [56]	1977	1	Numerical	-	-
Damborg et al. [57]	1984	1	Numerical	5	12
Ramaswami et al. [58]	1984	1	Numerical	6	14
Schultz and Waters [59]	1984	1	Numerical	-	-
Ramaswami et al. [60]	1986	1	Numerical	6	11
Pérez and Urdaneta [61]	2001	2	LP	8	16
Khederzadeh [62]	2006	2	LP	8	16
Kojovic and Witte [63]	2001	2	Numerical	8	7
Chabanloo et al. [64]	2008	2	GA	6	14
Sadeh et al. [65]	2008	1	GA	6	14
Sadeh et al. [66]	2011	2	PSO	8	16
Chabanloo et al. [67]	2011	3	GA	8,30	14,68
Singh et al. [68]	2012	2	DE	6	14
Moravej et al. [69]	2012	2	PSO	8	14,64
Nair and Reshma [70]	2013	2	GA	8	14
Farzinfar et al. [71]	2014	2	PSO	8,14	14,34
Haron et al. [72]	2013	2	Numerical	6	8
Proposed work	**2015**	**5**	**GA, IWO, SQP**	**9, 14, 30, 57, 118**	**12, 30, 68, 130, 340**

work. Moravej et al. [69] introduces a new approach that considers the intrusion of *series compensated* system to the coordination process. In this article, a Modified Adaptive Particle-Swarm Optimization is adapted to obtain the same two optimal OCR settings considering three critical points; in addition, the t_{z2} is also considered as adjustable.

Nair and Reshma [70] propose a GA capable to obtain optimal curve selection and time multiplier settings, the algorithm considers a fixed tripping time for the second zone and is successfully tested in a small 6-bus system. Farzinfar et al. [71] adapt a new Multiple Embedded Crossover PSO to deal with this complex nonlinear problem. The TDS, the pickup current, and the second zone operating time are optimized to achieve coordination in three critical points.

In a different methodology, Haron et al. [72] propose the coordination of overcurrent, directional overcurrent, and differential relays for distributed generation and microgrid systems. The proposals of the references described in the previous paragraphs are condensed in Table 1.2.

1.3 Motivation and Problem Statement

Despite the newer and more sophisticated protection principles, the overcurrent relay is far from entering into disuse, its simplicity and low cost are main advantages in comparison with other principles. The implementation of this technique is still widely used in subtransmission and distribution lines as well as in applications where the implementation cost of pilot, distance, or differential relays is not sustained.

The IEEE, IEC, and AREVA institutes in accordance with the computational capabilities of the time and aiming to prevent curves incompatibility established standardized inversion grades for the OCR inverse-time curves. In radial systems, designing curves with equivalent inversion grades is an advantage for coordination purposes; an example of this case was depicted in Figure 2.2(b) where the TDS is changed while the inversion grade is maintained. Given that the short-circuit current seen by a pair of relays in this kind of systems is the same and supposing similar load currents, the coordination can be ensured for practically all curve length, thus the standard is logical and applicable.

The curves performance in radial systems is remarkable nevertheless those systems coordination do not suppose a major challenge in power system protection while coordination in bilateral supplied and interconnected systems does; it is precisely in those cases when the efficiency of the standards is questionable. Figure 1.2 presents an example where a pair of relays is coordinated; both relays are using a very inverse IEEE characteristic curve and the coordination current seen by both relays is supposed to be equal. As can be appreciated the use of curves with the same inversion grade does not guarantee the avoidance of possible curve crossings; moreover on this case the coordination is lost — because the curve separation is less than the CTI — long before the crossing point is presented, as depicted by the shaded region.

Since modern digital OCR basically a computer, they are capable of calculating their own characteristics from given parameters. Furthermore, state-of-the-art optimization methods and current computer capacities allow the computation of acceptable ad-

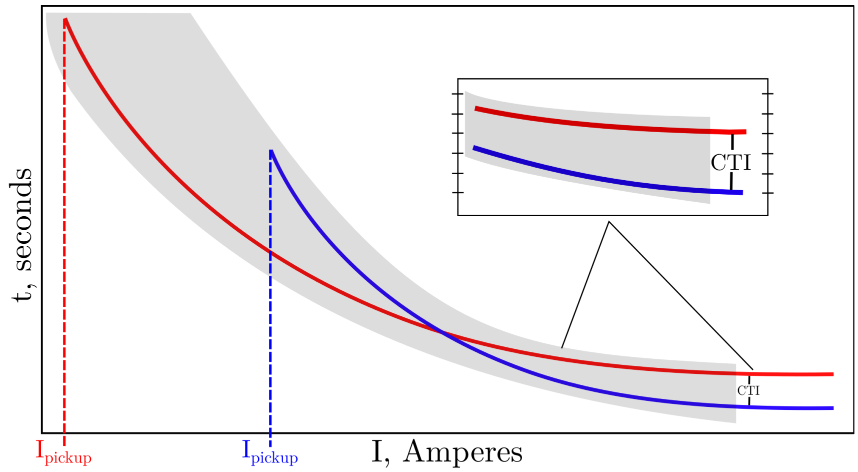

Figure 1.2: Curves crossings presented in a coordination pair.

justable settings that might reduce the relays tripping time and reduce or even avoid possible curves crossings in a reasonable short period of time; by exploiting these options the OCR coordination performance may be improved, consequently obtaining safer systems.

Another limitation of overcurrent relays is their lack of sensitivity for faults near or under the pickup current. At this moment, related works have focus their efforts to coordinate distance-relays as main protections while considering OCR as backups. Since the aim of this thesis consists in improving the overcurrent relay performance and therefore its field of application, an alternative that combines distance and overcurrent relay protection principles is also presented.

The novelty of this research is the use of all five overcurrent relay parameters as adjustable settings. The second contribution is the consideration of more than one short-circuit level to carry out the coordination process. The problem will be faced through the implementation of an exact method known as sequential quadratic programming and two heuristic algorithms, genetic algorithms and Invasive-Weed Optimization methods (IWO); while genetic algorithms have been successfully used to solve the coordination problem for several years, the implementation of the weed method has not been reported. In addition, the use of quadratic programming method with input values obtained from heuristic methods is also an original idea.

The last novelty of this proposal is the implementation of distance-relays just in lines where the overcurrent ones are insensitive, their tripping times are elevated, or when OCR coordination cannot be achieved; therefore this thesis is focused in the OCR improvement and distance-relays are used to bring an integrated solution in power system protection.

1.4 Hypothesis

The objective of the overcurrent relay coordination is keeping the inverse-time curves of the coordination pairs as close as possible — maintaining between them a gap called CTI — for a region of short-circuit currents; with the aim of preserving curves compatibility and considering computational capacities at the time, this process has been carried out considering standardized inverse-time curves.

Technology has been growing faster than several other economic sectors, as a result computers are evolving and becoming more powerful year after year; this fact impacts engineering and any other sciences, enabling possibilities that years ago seemed out of reach. The hardware of digital relays is now capable to perform simple calculations and readjustments, moreover computers are capable of running optimization algorithms and performing coordination tasks. The facts mentioned above lead us to state the hypotheses of this thesis:

- The consideration of all OCR parameters as adjustable settings may lead the protection system to improve its performance by reducing the tripping times for maximum and minimum short-circuit currents while conserving curves compatibilities.
- The use of close-end three-phase and far-end two-phase faults with the remote relay open as frontier coordination currents — as well as an intermediate magnitude between those — in the objective function, may guarantee the curves compatibilities.
- Since metaheuristic methods are robust, adaptable to different problems, non dependant of good initial guesses, and have remarkable exploration and exploitation capabilities, they seem to be the best choice to face the coordination process.

- Genetic algorithms are proven to perform well while facing the coordination problem; since invasive-weed optimization method is also a nature-inspired algorithm but based only on mutation operators, it can be adapted and implemented to solve this problem obtaining good results.

- The implementation of an exact method may be difficult because of the search space size and its good initial approximation necessities, nevertheless the implementation of a nonlinear algorithm during or after metaheuristic simulations may improve the coordination result by locating the closer optimal result.

- The addition of a routine capable of including distance-relays where overcurrent ones are not capable of achieving coordination may provide an integral solution to this problem.

1.5 Objectives

The general objective of this thesis is to implement an optimization method that, considering all the overcurrent relay parameters as adjustable settings and consequently obtaining non standardized inverse-time curves, achieves the OCR coordination for different levels of short-circuit current. Moreover, the particular objectives are listed below:

- The first particular objective is the accomplishment of a complete review of the related work, specially focused in the state-of-the-art in overcurrent relay coordination.

- The following objective is centralized to adapt and implement nonlinear and metaheuristic optimization algorithms capable to solve the coordination problem.

- A third objective is the development of a methodology adequate to achieve OCR and distance-relay coordination, followed by its adaptation and integration to the implemented algorithms.

1.6 Thesis Structure

The present thesis is divided into five chapters, the first one presents the introduction, the state-of-the-art enlists related work on this topic in order to highlight the main contributions and establish the characteristics that distinguish this work from any other. Finally the problem statement, hypothesis and objectives are also presented.

The second chapter discusses the background of this project; it is divided into two main parts, the first one introduces protective relaying coordination theory as well as the protection principles addressed on this work. The overcurrent relay limitations and the proposed techniques to face them are also postulated in those sections. The second main part describes the optimization methods implemented to solve the coordination problem either in this or different works.

Chapter 3 details the implementation of the optimization methods used to face the overcurrent and distance coordination problem. In the fourth chapter the conducted experiments and the obtained results can be seen. The last chapter is devote to present the conclusions and contributions reached from the results section, in addition future work ideas are explored.

CHAPTER 2

BACKGROUND

The aim of this chapter consists in presenting the background of this thesis. The chapter is divided in four sections: the first and second present conceptual information and general concepts about overcurrent, and overcurrent and distance-relay coordination; the last one describes different optimization methods implemented to solve the coordination problem.

2.1 OVERCURRENT RELAY

The *overcurrent relay* [73–76] is the simplest, cheapest, and oldest among all protection principles. Despite the increased use of more sophisticated protections, it is still commonly used as phase primary protection on distribution and subtransmission systems and as a phase secondary protection on transmission systems. More than a century has passed since OCR was developed and it is still used with almost any modification [77].

Based on their tripping characteristics, overcurrent relays are classified in definite current, definite time, and inverse time. The definite current characteristic immediately triggers the relay when a certain current magnitude is reached; this option allows fast tripping for faults located at long distances, nevertheless presents the drawback of lacking selectivity before overload conditions. The second approach allows the protections engineer to set a definite time operation for a determined range of measured currents, defining different tripping steps may increase the relay's selectivity however the tripping time for the biggest currents can be slow. The last and most common tripping characteristic is the

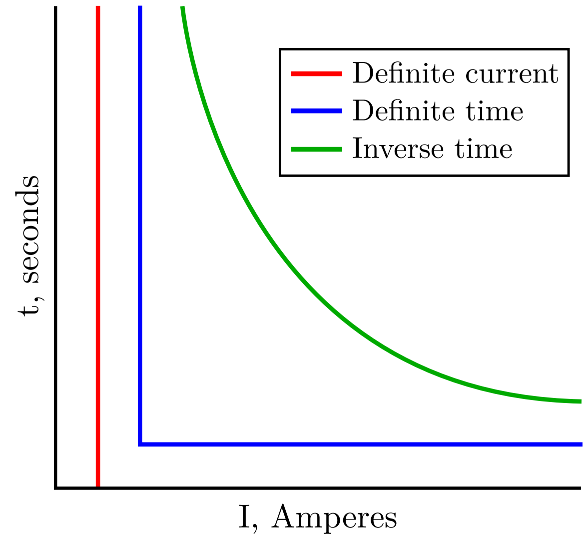

Figure 2.1: Definite current, definite time, and inverse time overcurrent characteristics.

inverse time curve, this option requests faster operations as the short-circuit current grows and vice versa; throughout this work the last approach will be the only one referred. The three overcurrent relay characteristics are illustrated in Figure 2.1.

One of the assets of the inverse time relay is its relative selectivity, that means that it is designed to operate as *main protection* for the line where it is placed and as a *backup protection* for any adjacent line. The principle is straightforward: the OCR gives a signal to trip the protected line when a measured current is greater than the previously set *pickup current* (I_{pickup}).

A common approach consists in setting the I_{pickup} to a magnitude equal to or greater than 1.5 times the maximum *load current* (I_{load}) flowing trough the line where the relay operates as a main protection; nevertheless in some of the reported works detailed in the following chapters, the *pickup current multiplier* (P_m) is reduced to 1.25. The objective of the P_m is the avoidance of relay operation under temporary overload conditions that can be considered as normal system operation. Thus the I_{pickup} is computed as shown by Equation 2.1.

$$I_{pickup} = I_{load} \times P_m. \tag{2.1}$$

The tripping time of an overcurrent relay for a given short-circuit current I_{sc} is computed using Equation 2.2, defined by the Institute of Electrical and Electronics Engineers (IEEE) in the standard C37.112-1996 [78]:

$$\mathrm{t} = \left[\frac{\mathrm{A}}{\left[\frac{\mathrm{I_{sc}}}{\mathrm{I_{pickup}}}\right]^{\mathrm{p}} - 1} + \mathrm{B} \right] \times \mathrm{TDS}, \tag{2.2}$$

where

$$\begin{aligned} \mathrm{t} &= \text{tripping time,} \\ \mathrm{I_{sc}} &= \text{short-circuit current,} \\ \mathrm{I_{pickup}} &= \text{pickup current,} \\ \mathrm{TDS} &= \text{time dial setting, and} \\ \mathrm{A, B, p} &= \text{Time curve characteristic constants.} \end{aligned}$$

An *inverse-time characteristic curve* is designed for each relay of the system, it can be obtained by evaluating the previous equation for different $\mathrm{I_{sc}}$ magnitudes. The curve indicates the time that the relay will take to trip a fault of a given magnitude; it is asymptotic to the $\mathrm{I_{pickup}}$, consequently the tripping times for currents near to that value tend to infinite. The characteristic constants are responsible to give the inversion grade to the curve, and the TDS is a time multiplier which moves the curve along the vertical axis while keeping its inversion grade unaltered.

The methodology followed to design an inverse-time curve consists of the selection of proper values of TDS, $\mathrm{P_m}$, and one of the three sets of characteristic constants established in the IEEE standard [78]. Diverse curve constants are used by different institutes, for example the sets used by AREVA [79] and the International Electrotechnical Commission (IEC) [80] as listed in Table 2.1. Since the relay employs a single adjust to operate as main and backup protection, the security of the protected system relays on a correct parameter selection and curve design. The aim of limiting the curve to certain inversion grades consists in giving more compatibility among all the OCR curves in the system. The topic is discussed in further etail in the next section.

The IEEE defines three standardized inverse-time curves known as the *Moderately*

Table 2.1: IEEE standardized curves characteristic constants.

Institute	Curve	A	B	p
IEEE	Moderately Inverse	0.0515	0.114	0.02
	Very Inverse	19.61	0.491	2
	Extremely Inverse	28.2	0.1217	2
IEC	Normal Inverse	0.14	0	0.02
	Very Inverse	13.5	0	1
	Extremely Inverse	80	0	2
AREVA	Short-time Inverse	0.05	0	0.04
	Long-time Inverse	120	0	1

Inverse (MI), *Very Inverse* (VI), and *Extremely Inverse* (EI), their predefined characteristic constants are illustrated in Table 2.1. Figure 2.2(a) shows an example of the three curves plotted in a bilogarithmic scale; the inversion grade is remarkably different for each one of them, so that their names are appropriate to distinguish one from another. In Figure 2.2(b), the previously mentioned multiplicative effect of the TDS on the inverse-time curves is depicted; generally, values from 0.5 to 15 can be defined as time dial settings for overcurrent relays. Nevertheless, given that the tripping time is directly proportional to TDS magnitude, big values are not often used. The TDS selection range can be considered continuous for digital relays or discrete for electromechanical ones.

As stated in previous paragraphs the tripping time tends to infinity while I_{sc} becomes closer to the pickup current. This behavior is exemplified in the case used to compute the curves depicted in Figure 2.2(a); in this example the I_{pickup} equals 460 A but the tripping time of the very and extremely inverse-time curves for a current near 600 A is respectively around 20 and 60 seconds, a slow operation time for coordination purposes. Because of that, the region comprehended from 1 to 1.5 times the I_{pickup} is commonly not considered during the coordination process.

With the objective of ensuring that the relay is capable of detecting a fault magnitude and tripping the line in a reasonable amount of time, before the coordination process is carried out overcurrent relays that exercise as backups are subjected to a sensitivity filter. A sensitivity index η is given by Equation 2.3; it consists in the quotient of the pickup

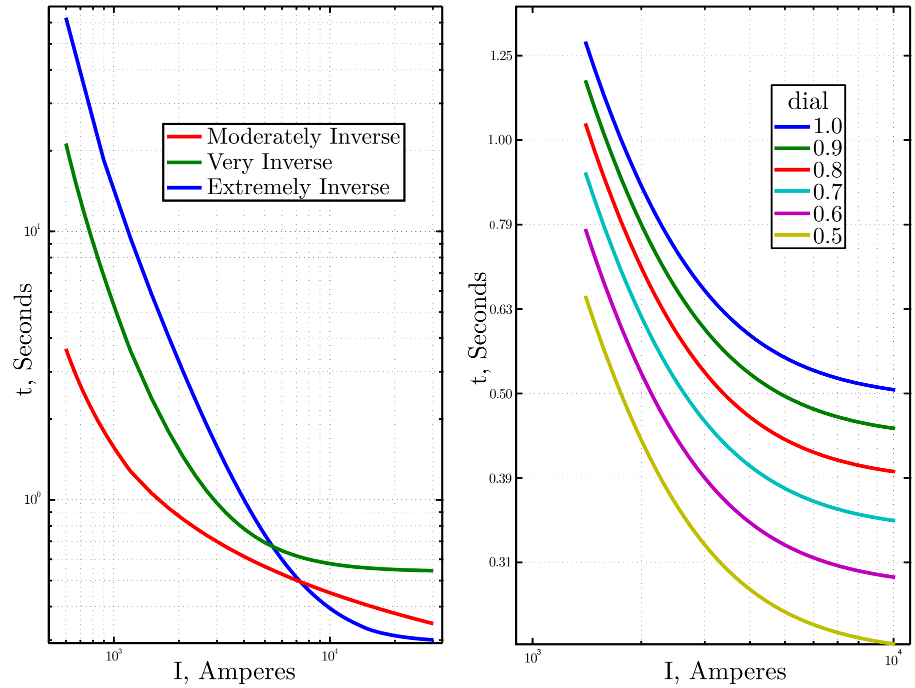

(a) Conventional inverse-time curves. (b) Dial effect on inverse-time curves.

Figure 2.2: IEEE standardized inverse-time curves and the TDS effect on the curves design.

current and the two-phase (2ϕ) fault located at the far-end of the adjacent line with the remote relay open. The relays that obtain $\eta \leq 1.5$ are considered insensitive and taken out of the coordination process; since each relay may be backup of different protections, it is important to clarify that it can be insensitive for certain pair and sensitive for others:

$$\eta = \frac{\mathrm{I}_{\mathrm{sc}}^{2\phi}}{\mathrm{I}_{\mathrm{pickup}}}. \tag{2.3}$$

2.1.1 Overcurrent Relay Coordination

The main task of protective relaying engineering is coordinating the protective devices. Overcurrent protections are set to clear the faults on the main lines and to operate as back-ups for adjacent lines. The complexity of the problem increases exponentially as the power system grows; for example, the *radial* system of four buses and three relays shown in Figure 2.3(a) can be easily coordinated, nevertheless, the addition of one interconnected node

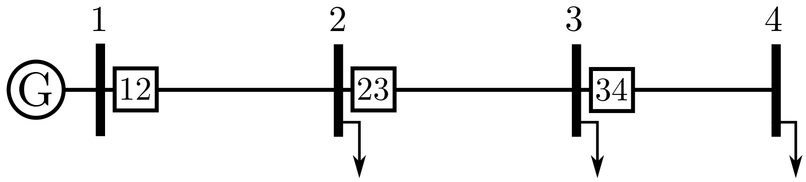

(a) Example of a four bus radial system.

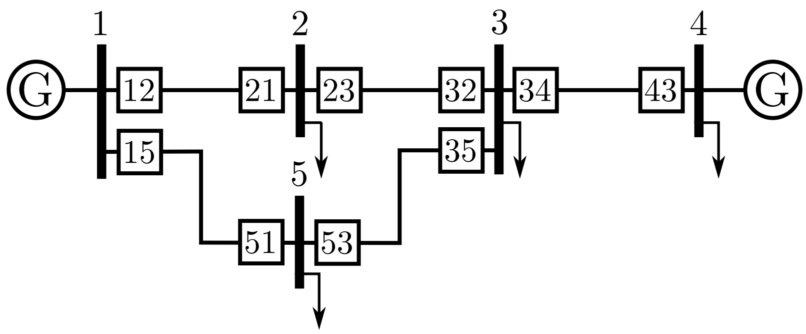

(b) Example of a five bus interconnected system with bilateral generation.

Figure 2.3: Two examples of power systems.

and bilateral generation, can transform this task to a rather difficult one. The number of relays to coordinate increases from three to ten with this slight modification as illustrated in Figure 2.3(b).

The I_{load} is necessary to calculate the I_{pickup}, moreover the coordination process is performed considering the maximum fault magnitude, commonly caused by three-phase (3ϕ) faults, consequently flow and fault analysis have to be carried out since their results are needed to coordinate the protections. The load demand and the results obtained by a fault analysis are well known by the system operators, consequently they could be either computed or retrieved from historical data.

The main characteristic of radial systems is their load-flow direction; considering loads connected in nodes 2, 3, and 4 of Figure 2.3(a) and a short circuit occurrence in bus 4, the current will flow from node 1 to the fault point, i.e., in *downstream* direction. The coordination process starts by setting the curve parameters of downstream protections, setting relay 34 to trip its main line as fast as possible for a I_{sc}^{max}; the load connected to node 4 is considered as I_{load}^{34}. Moreover the relay 23 is adjusted as main protection for the line 2–3 and also as backup of the relay 34; the I_{load}^{23} will be equal to the sum of loads connected to nodes 3 and 4. This process will continue until the relay closest to the generator is coordinated.

The unilateral load-flow in radial systems makes the use of *directional-overcurrent relays* unnecessary. On the other hand, in an *interconnected* power system the current flows in both directions, and consequently the use of DOCR is required. Let us consider a fault located at the 80% of the line 2-3 of the system depicted in Figure 2.3(b), it can be seen that the fault contribution will come from both sides of the line; the *electric distance* between relays 32, 34, and 35 and the fault location — and consequently the measured fault magnitude — is practically identical. The relay 32 must trip its main line, but an operation of the relays 34 and 35 will implicate an undesirable outage of non faulted lines. Broadly speaking, the directional function will allow or prevent the operation of the relay for faults occurred in an specific direction [75].

The coordination process will be explained using Figure 2.4. Supposing a three-phase fault f_1 occurring in the line 2–3, the relays 32 and 23 had to clear the fault as main protections nevertheless let us assume that just the first of them accomplished its task. As a consequence of that malfunction, the fault is still being fed by the generators located at the nodes 1 and 4.

Directional function prevents relays 21 and 24 from detecting this fault, therefore the protections 12 and 42 are appropriate to operate as backups of the faulted relay, isolating the fault and preventing it from keeping spreading towards the rest of the system. The relays 12 and 23, as well as the relays 42 and 23 form *coordination pairs*, namely, a pair of relays in which one of them is backup of the other. A relay can be part of as much coordination pairs as adjacent lines are located in its trip direction, meaning that each relay can be backup of multiple relays, as well as multiple relays can be its backups.

The *coordination current* (I_c) is the maximum current seen by the backup relay after the occurrence of a fault located on the main zone of its pair. As its name suggests, the I_c is the current used to carry out the coordination. In Figure 2.4 the fault magnitude seen by relay 23 after correct operation of relay 32 is equal to x+y A, which is a combination

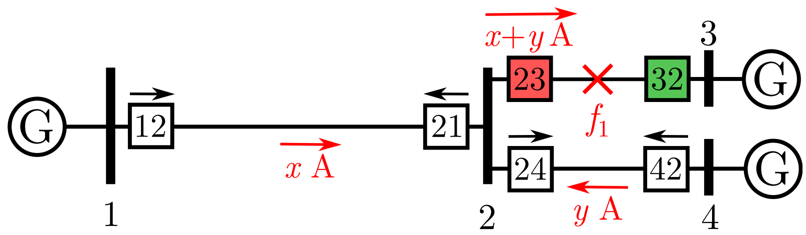

Figure 2.4: Relay coordination is performed considering that one of the relays operates correctly.

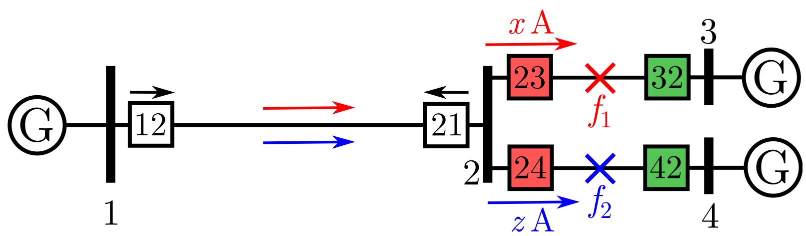

Figure 2.5: Two independent faults in a four bus system where a main relay fails to trip.

of the contributions coming from the lines 1–2 and 4–2, following the Kirchhoff's first law. The contributions do not necessarily have the same magnitude, so it can be said that each coordination pair has an individual coordination current. Further, while the tripping time of the main relay will be computed considering the full amount of current — $x+y$ A in this example —, the backup tripping time will be calculated considering just the contribution of its line (x A). This situation is an example of an effect known as *infeed* current, presented in interconnected and bidirectional power systems.

The definitions of the latter paragraphs are complemented using Figure 2.5. It can be noted that the relay 12 is a coordination pair of the relays 23 and 24, therefore it has to be adjusted to respond as backup if any of them fails. Assuming two independent faults f_1 and f_2 occurring in different moments. It is supposed that for each case the relay on the right operate correctly and the relay on the left fails to trip; the contribution from the line 1–2 to each fault surely will have a different magnitude, consequently the relay 12 will operate as backup for more than one relay considering different coordination currents. The complexity of the problem increases when the same relay has to be coordinated with its own backups, although this example is not the case. While the coordination process is simple to achieve for small systems, the complexity grows rapidly as the system grows either in nodes or interconnections.

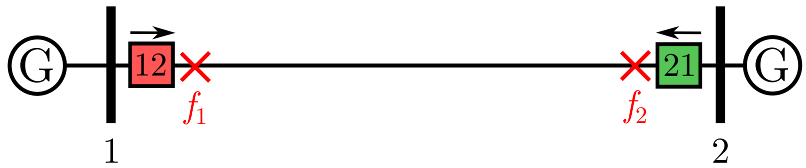

Figure 2.6: Close-end (f_1) and far-end (f_2) faults with open end.

In order to ensure that the backups will respond only if the main relay failed to operate or if its operation is taking too long, the backup relays should not trip the line immediately, but after a time delay called *Coordination Time Interval* (CTI); in this thesis the CTI magnitude is assumed to be 0.3 seconds when overcurrent relays are coordinated between them. Thus, the desired tripping time of a backup relay ($\mathrm{t_b^d}$) is equal to the sum of the main relay tripping time ($\mathrm{t_m}$) and the CTI, as shown in Equation 2.4:

$$\mathrm{t_b^d} = \mathrm{t_m} + \mathrm{CTI}. \tag{2.4}$$

This section is concluded by defining the fault locations considered in this thesis, close-end and far-end faults are depicted in Figure 2.6. A common assumption in protective relaying is that one of the main relays will operate correctly; in this example, relay 21 is supposed to do so, consequently considering a fault with open end.

2.1.2 Coordination Examples

A numerical example of the overcurrent relay coordination process will be described in the following paragraphs. Figure 2.7 illustrates a section of the IEEE 14 bus system [81], widely used to test power system protection contributions. Considering a fault $\mathrm{f_1}$ located in the close-end of the line 1–5, it is assumed that the relay 15 operates correctly while the relay 51 fails to trip. The fault magnitude seen by the 51 relay is equal to the sum of the fault contributions coming from nodes 2, 4, and the rest of the system. Let us consider $\mathrm{f_1}$ = 6638 A while the fault contribution seen by the relays 25 and 45 is respectively 2005 A and 3133 A. The data that will be used to solve this problem is condensed in Table 2.2.

The first step consists in computing the $\mathrm{I_{pickup}}$ and $\mathrm{t_m}$ using Equations 2.1 and 2.2.

Table 2.2: Parameters used for the coordination example.

RelayID	51	25	45
I_c	6638 A	2005 A	3133 A
I_{load}	350 A	195 A	304 A
P_m	1.5	1.5	1.5
Curve	VI	VI	VI

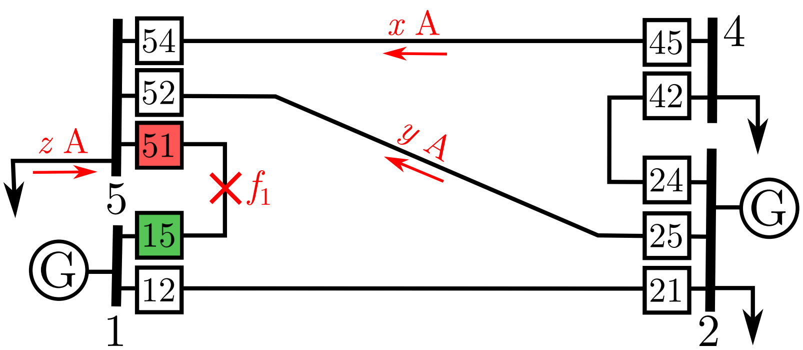

Figure 2.7: Fault event on a section of the IEEE 14 bus system.

The main relay must trip as fast as possible, therefore the initial TDS is set to 0.5:

$$\begin{aligned} I^{51}_{pickup} &= 350 \times 1.5 = 525\text{A}, \\ t^{@6638\text{A}}_{51} &= \left[\frac{19.61}{\left[\frac{6638\text{A}}{525\text{A}}\right]^2 - 1} + 0.491 \right] \times 0.5, \\ t^{@6638\text{A}}_{51} &= 0.3071\text{s}. \end{aligned}$$

The tripping time of the relay 51 for a short-circuit magnitude of 6638 A is equal to 0.3071 s; therefore, the desired tripping time of the backup relays 25 and 45 for their respective coordination currents is calculated using Equation 2.4, as follows:

$$t^{@2005\text{A}}_{25} = t^{@3133\text{A}}_{45} = (0.3071 + 0.3)\text{s} = 0.6071\text{s}.$$

Since in this exercise the only modifiable variable considered is the TDS, it has to be isolated in order to obtain its magnitude for the backup relays. Equation 2.5 shows the isolated equation, then, the TDS for the backup relays is calculated.

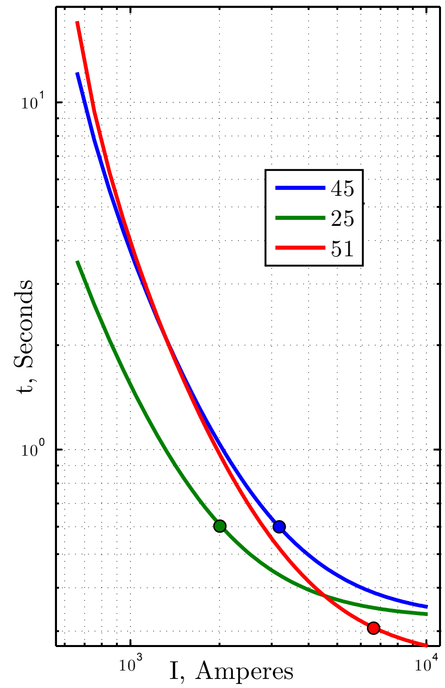

Figure 2.8: Characteristic curves for the relays 25, 45, and 51.

$$\mathrm{TDS} = \frac{t_b^d}{\left[\frac{A}{\left[\frac{I_{sc}}{\mathrm{I_{pickup}}}\right]^p - 1} + B\right]}. \tag{2.5}$$

$$\mathrm{I}_{\mathrm{pickup}}^{25} = 195 \times 1.5 = 292.5\mathrm{A}. \qquad \mathrm{I}_{\mathrm{pickup}}^{45} = 195 \times 1.5 = 456\mathrm{A}.$$

$$\mathrm{TDS}_{25} = \frac{t_b^d}{\left[\frac{19.61}{\left[\frac{2005\mathrm{A}}{292.5\mathrm{A}}\right]^2 - 1} + 0.491\right]}, \qquad \mathrm{TDS}_{45} = \frac{t_b^d}{\left[\frac{19.61}{\left[\frac{3133\mathrm{A}}{456\mathrm{A}}\right]^2 - 1} + 0.491\right]},$$

$$\mathrm{TDS}_{25} = 0.6619. \qquad \mathrm{TDS}_{45} = 0.6634.$$

After selecting and calculating all the parameters, the inverse-time curves can be obtained by evaluating Equation 2.2 for different levels of $\mathrm{I_{sc}}$. Figure 2.8 shows the characteristic curves of the relays 25, 45, and 51. The dot marks represent the tripping time for the coordination current.

The next step of the process would be the coordination a new pair of relays, for example the relay 12 as a backup protection and the 25 as a main one. A three-phase fault with the relay 52 open will be simulated and the current of the main and backup relays obtained. A similar process will be followed and after some iterations the coordination will be completed. It is important to recall that all the relays have to operate without any change on their configuration, i.e, the relay 25 with the same settings has to be backup for the relays 51 and 54, and also be backed up by the relays 12 and 42.

The last sentence leads to affirm that the coordination is an iterative process; if the coordination between the pair conformed by the relays 12 and 25 is not permissible, the tripping time do not meet the expectations, or the obtained settings cannot be permitted by the relay, several protections must be readjusted. Furthermore, since almost all the relays have certain linkages any change on one of them might affect others, consequently it is likely that the protections engineer might has to restart the whole process.

The previous calculations ensure the coordination of the relays for the commonly used case, namely a *close-end* maximum fault with open end; however, a short circuit of that magnitude occurs in less than the 5% of the fault cases. For a two-phase fault the currents seen by the relays 51, 25, and 45 will be 4601, 1536, and 2941 Amperes. The coordination error ($\mathrm{E_{CTI}}$) is calculated by subtracting the desired time from the obtained time ($\mathrm{t^o}$), namely the computed tripping time of the backup protection, as can be seen in Equation 2.6. In order to obtain better coordination results, the error must be nonnegative and as close as possible to zero. The tripping times of the relays for the mentioned two-phase faults as well as the $\mathrm{E_{CTI}}$ are shown in Table 2.3.

$$\mathrm{E_{CTI}} = t_b^o - \mathrm{t_b^d}. \tag{2.6}$$

As can be appreciated, the coordination error is negative for one of the cases, meaning that the relays will fail to coordinate for faults of that magnitude. From this example it can be concluded that even using the same kind of curves, the coordination is not guaranteed for a whole interval of fault currents. This problem is accentuated when the whole coordination process is carried out for a whole system instead of just a couple of pairs.

Another point to conclude from this section is the need of an optimization algorithm capable to deal with the coordination process. The complexity of the “hand-made” calcu-

Table 2.3: Tripping times and coordination errors for a two-phase fault.

	Relay ID		
Result	51	25	45
t	0.374	0.813	0.646
E_{CTI}	-	0.138	-0.028

lations and the required iterations increase rapidly as the system grows; several researches have been dealing with this problem over the last thirty years. Most of those works just consider the TDS as a variable setting, the remaining ones consider also the pickup multiplier as another variable. Linear programming and heuristic methods have been used to face the problem, as will be discussed in the following sections.

2.2 Overcurrent and Distance Relay Coordination

Distance-relays [73–76] are one of the most used protections; this protection principle is widely implemented to protect transmission lines and it is commonly used when the overcurrent relay is insensitive or it presents slow tripping times. The principle is based on the relay response to the ratio of voltage to current, namely the *impedance* at the relay location. Broadly speaking impedance may refer to resistance, reactance, or both combined; given that the impedance of transmission lines is directly proportional to their length — and also fairly constant — distance-relays obtain their name since they operate according to the distance between them and the fault location.

The operation principle of distance-relays can be easily described considering electromechanical elements. The principle is based in the equilibrium between the positive torque produced by current — pickup torque — and the negative one produced by voltage — reset torque —. During normal operation the voltage torque is greater than pickup one, maintaining the relay unaltered; although, as a result of short-circuit events the current and consequently the pickup torque increases whilst the voltage and reset torque will decrease or remain the same, causing the protection to trigger. Neglecting the control-spring effect, the torque equation is given by:

$$T = K_1\mathrm{I}^2 - K_2\mathrm{V}^2, \tag{2.7}$$

where K_1 and K_2 are the current (I) and voltage (V) springs constants using I and V as root media square magnitudes. The equilibrium point is the edge that defines the moment when the relay is about to operate; in this situation both torques are equivalent as described by Equation 2.8. Isolating the ratio between V and I from this equation, the constant impedance value that defines the protection tripping zone is defined by Equation 2.9.

$$K_1\mathrm{I}^2 = K_2\mathrm{V}^2, \tag{2.8}$$

$$\frac{V}{I} = Z = \sqrt{\frac{K_1}{K_2}}. \tag{2.9}$$

The tripping characteristic that indicates the tripping and non tripping zones considering the voltage and current is shown in Figure 2.9(a). Moreover, Figure 2.9(b) shows a more common and useful characteristic known as impedance or *R-X diagram*. The impedance is represented by a vector with magnitude and phase and whenever the vector lies inside of the circle the protection trigger. The impedance design operates in the four quadrants, encouraging the need of an additional directional element to discriminate between fault locations; this design is now out of use and has been replaced for different characteristics.

The *Mho* characteristic — depicted in Figure 2.9(c) — overcomes the impedance one limitations by moving the position of the circle and make it pass through the origin. This design is directional without the need of additional implementations. Moreover an inductive load current is known for lagging voltage roughly from 0° to 30°, heavy loads might move the impedance vector towards the origin and be identified as faults; mho characteristic reduces sensitivity to possible load currents and increases it for currents lagging from 60° to 85° degrees. There are different designs applicable to diverse situations for example the offset mho and the lens characteristics illustrated in Figures 2.9(d) and 2.9(e); those examples among others can be further reviewed in the referenced books and articles.

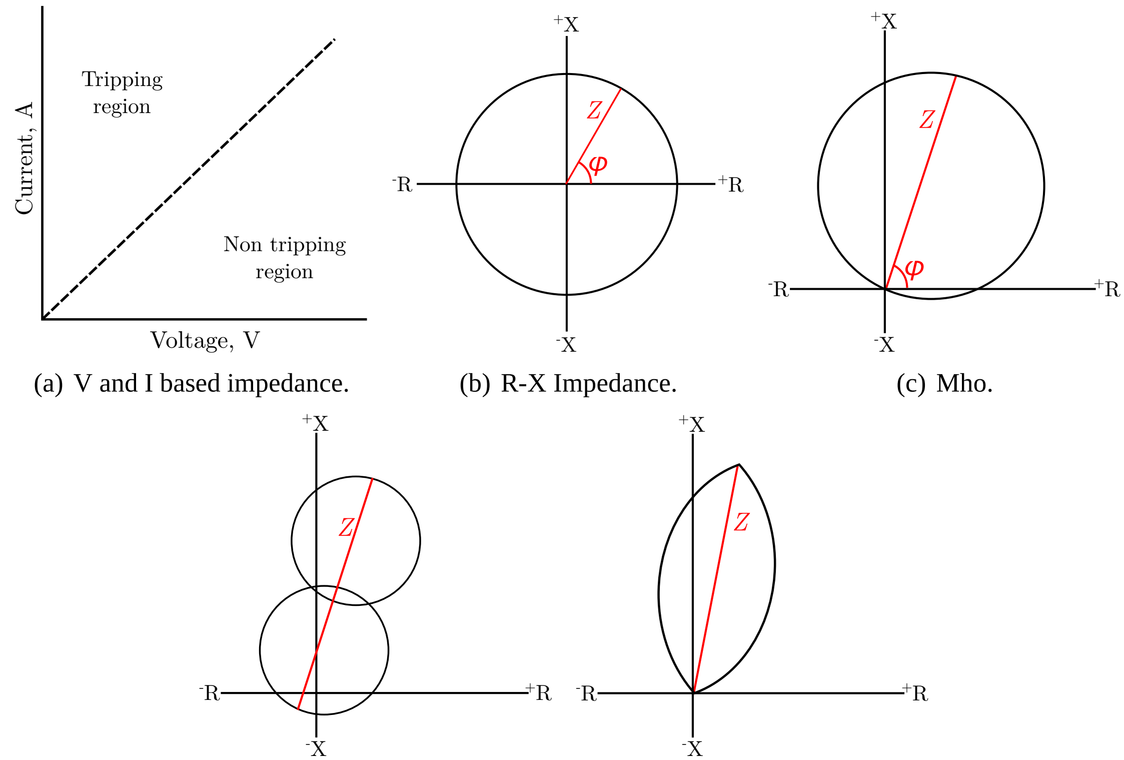

(a) V and I based impedance. (b) R-X Impedance. (c) Mho.

(d) Offset mho. (e) Lens.

Figure 2.9: Examples of different distance-relay characteristics.

Distance-relay provides protection for the line where it is located and can be adjusted to function as backup for adjacent lines or remote sections. The adjust consists in defining up to three definite time tripping steps known as protection zones. The first zone is set to protect around 80% of the main line, the second one must protect the rest of the first line and at least 20% of the adjacent one, lastly the third zone protects the remaining percentage of the adjacent line and sometimes up to 30% of the second adjacent line; each zone has its own tripping time that will be referred as t_{z1}, t_{z2}, and t_{z3}.

Figure 2.10 illustrates the three zones of protection; the R-X mho diagram with the three operating circles of the relay 12 is shown in Figure 2.10(a) while the line coverage of each relay and their zones can be seen in Figure 2.10(b). The directional relays coordination problem seeks to define the percentage of the line covered by each protection zone as well as the tripping time of the second and third zones, considering that no intentional delay is assigned to the first one.

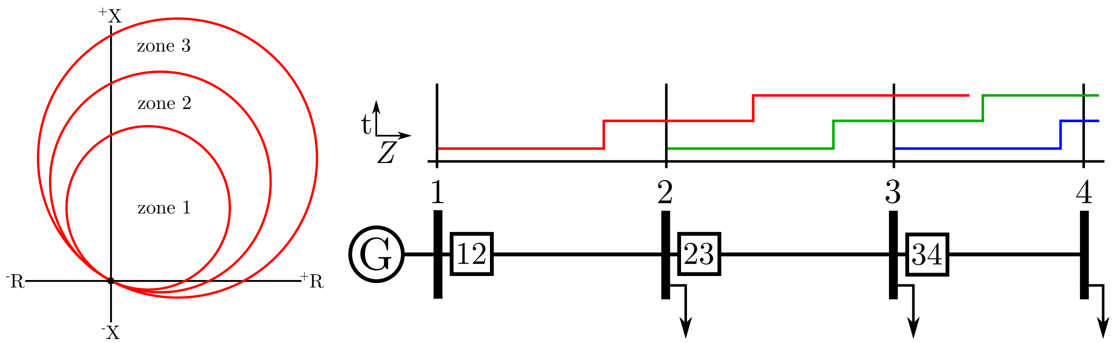

(a) Mho design for zones. (b) Zones coverage and coordination.

Figure 2.10: Distance-relay coordination.

The coordination process increases its complexity in real-life applications where multiple adjacent lines with different lengths and bilateral generation are common factors. The line lengths will cause the second zone to under or overreach the desired coverage — depending on which line percentage is used to compute the second zone distance — while the infeed effect will cause the protection to detect an impedance greater than the real, underreaching the fault and causing an increased tripping time.

A possible solution to this among other problems consists in the redundancy provided by the implementation of different protection principles like *pilot* and overcurrent protection; nevertheless the coordination complexity increases even more when a protection principle has to be coordinated with different ones. The following paragraphs will describe the general coordination process between distance and overcurrent relays.

The coordination between different protection principles has become an important topic explored by different researchers in recent years as will be discussed in Section 1.2.2. Since the protection principles combination increases the problem variables and restrictions, the coordination problem complexity grows.

Figure 2.11 represent a radial system with mixed distance and overcurrent protection principles; distance-relay 23 backups OCR 34 and it is backed up by OCR 12. The attained case presents six critical points that need to be coordinated by obtaining a time gap equal or greater than the CTI; each point is represented with letters A to F.

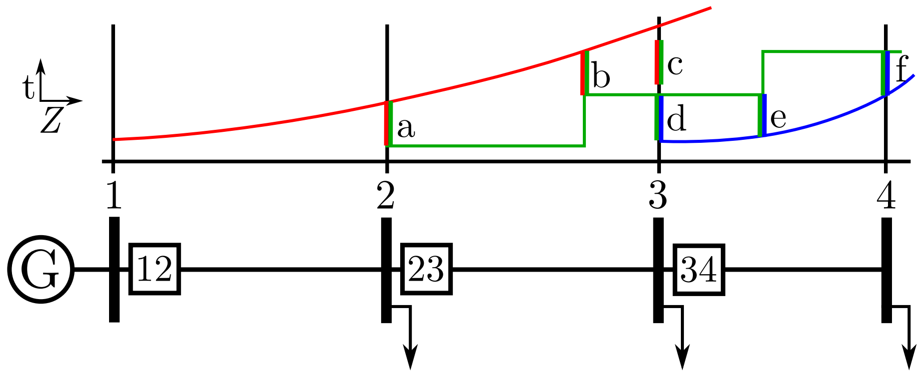

Figure 2.11: Coordination points in distance and overcurrent relays coordination.

The first and third zones do not represent a mayor challenge since they just have one critical point located in the close-end and far-end positions of lines 2–3 and 3–4; although the second zone presents two coordination points with each of the overcurrent relays. All six restrictions have to be added to the ones presented in the OCR-OCR and distance-distance-relay coordination.

2.3 Optimization Methods

Some of the common definitions of optimization include: to make something as good or perfect as possible, to look for the better way to carry out an activity, or to find the best solution candidate among a given population. The term *best* implies that there can be other solutions with less qualifications. A *variable* is a symbol that represents an unknown number, a *solution* is conformed by one variable or a set of them.

Depending on the faced problem, variables can be allowed to take just certain magnitudes; these limitations are called system *restrictions*. A solution that overcomes the systems restrictions is called *feasible*. An *Objective Function* (OF) identifies the aptitudes that a solution has to have in order to be considered better than others, it can also contemplate penalties for solutions that infringe the system restrictions. The *search space* is the region where all possible solutions can be found, the feasible region comprehends all possible feasible solutions [82–84].

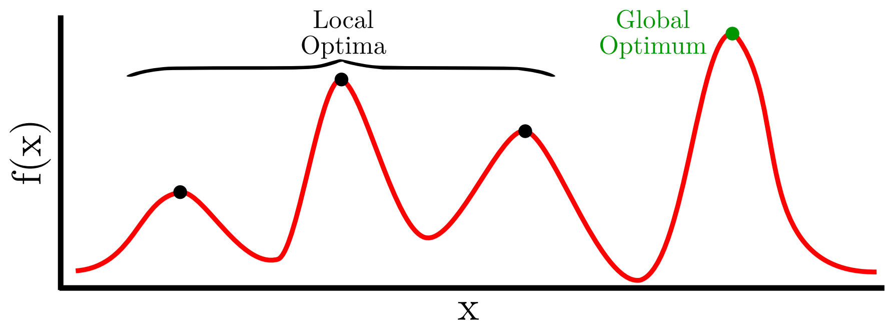

Figure 2.12: Global and local optimal solutions. The global optimum is the best solution of the entire search space while local optima are the best of their surroundings.

If the goal of the problem is to find the minimum value of a function, the OF is commonly known as *cost* function; on the other hand, for problems where the objective is maximizing a function value, the OF is also called *fitness* function. The result that an individual obtains after being evaluated by the objective function is known as Fitness (f).

A feasible solution that satisfies the objective function and minimizes — or maximizes — it is called *optimal*. A *global optimum* is a solution that is better than — or at least as good as — any other feasible solution of the problem; moreover, a *local optimum* is a solution that is better or equal to the solution obtained by its *neighbors*, or the elements located in the surroundings of the search space. An example of local and global optima concepts is illustrated in Figure 2.12. The size of the search space plays an important role on the difficulty of finding a local or global optimal solution, it grows if more variables are considered or if their sampling interval is modified.

Optimization does not necessarily imply perfection. An optimal solution can be found for a determined system and yet, not be perfect. Systems with restrictions based on time minimization, thresholds, and tolerances may serve as examples of this affirmation. Nonlinear optimization problems may have several locally optimal solutions; *heuristic* and gradient based methods converge to one of these configurations and the user should be aware that this may or may not be a global optimum solution. Despite this, there may exist some scenarios where it can be assured that the local optimum is in fact a global one, for example in concave or convex optimization problems.

Combinatorial optimization [85–87] consists in finding the best solution among all feasible ones considering a finite set of candidates. This kind of problems are considered complex because their search space is commonly big. Perhaps the most common and important problem on this field is the Traveling Salesman Problem [88], roughly its objective is to find the shortest tour through a given set of cities.

As stated in Chapter 1, in the the simplest case of the protective devices coordination problem a configuration of discrete settings is computed and selected within a predefined selection range, the above description allows to treat this problem as a case of combinatorial optimization. The total of possible combinations increases exponentially in accordance with the total variables considered as adjustable settings, the sampling interval of those settings, and the total of relays or system size; this exponential growing is known as *combinatorial explosion* [89]. *Brute-force search* methods seek to perform either a systematic or random search among all possible solutions, i.e., an exhaustive search; this approach or related ones should not be implemented when the coordination problem is treated, the reasons are discussed in the following paragraphs.

Supposing a small ten relays system that is going to be coordinated considering just one adjustable setting with five possible values or samples. The total generated combinations would be equal to 5^{10} — 9,765,625 combinations —. The size of this search space should not be a problem for current computers and the solution might be obtained performing an exhaustive search. Nevertheless if five adjustable settings are considered, the total combinations is given by Equation 2.10:

$$\mathrm{T_c} = (s_{\mathrm{A}} \times s_{\mathrm{B}} \times s_{\mathrm{p}} \times s_{\mathrm{P_m}} \times s_{\mathrm{TDS}})^{\mathrm{T_r}}, \tag{2.10}$$

where:

$$\begin{aligned} \mathrm{T_c} &= \text{Total combinations,} \\ s &= \text{Total samples of each parameter,} \\ \mathrm{T_r} &= \text{Total relays.} \end{aligned}$$

In order to get closer to the problem treated on this thesis, five adjustable settings are used in the next example. Considering from one up to ten relays and assuming that each setting

Table 2.4: Combinatorial explosion in a protection system.

T_r	T_c	t_{sim}		T_r	T_c	t_{sim}	
1	3.13E+03	92.3	fs	6	9.31E+20	7.64	hours
2	9.77E+06	288.41	ps	7	2.91E+24	2.76	years
3	3.05E+10	901.28	ns	8	9.09E+27	8.63	thousand years
4	9.54E+13	2.82	ms	9	2.84E+31	26.98	million years
5	2.98E+17	8.8	s	10	8.88E+34	84.33	billion years

can be adjusted to one value among five, Table 2.4 shows the combinatory explosion produced in this problem. A computer performance can be measured in Floating-point Operations Per Second (FLOPS) [90]. At present, the China's Tianhe-2 is the world's fastest supercomputer and can perform an average of 33.86 PFLOPS [91, 92]; the time that this supercomputer would take to perform those calculations — if we assume that the full system coordination consists in just one floating point operation — is shown on the third column of Table 2.4.

Let us put these numbers into perspective; first, consider a base area that is equal to five times the pitch size of the Wembley Stadium — 105 $\times$ 68 square meters $\times$ 5 —, then each possible solution is represented with a Lego brick identical to the one illustrated in Figure 2.13(a). Each brick is aligned to cover the complete base area and the bricks are joined to build layers. The Burj Khalifa is currently the tallest building in the world with 828 meters of height and roughly 100 meters of base diameter — if we consider a round area —. The surface used in our example would be 4.54 times the base area of this building and still, considering just four relays, a 1053.50 meters tower could be build as illustrated in Figure 2.13(b). The Tianhe-2 supercomputer is so fast that performing an exhaustive search, it would theoretically take just 2.82 milliseconds to find the best brick in our Lego building.

The computer performance is still fast when five relays are considered, but from that point the combinatorial explosion starts to become an important factor. The length of the tower combining six relays would be equal to 12.68 round trips to the moon, an exhaustive search for a system with this search space dimension would last almost eight hours.

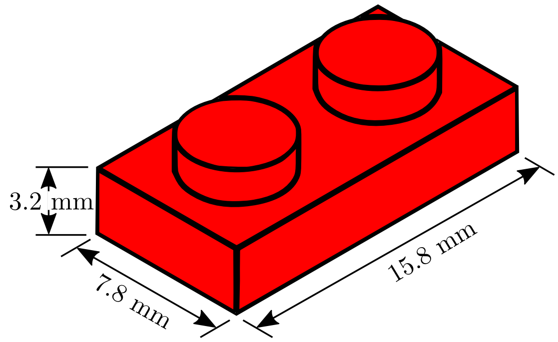

(a) Dimensions of a Lego brick.

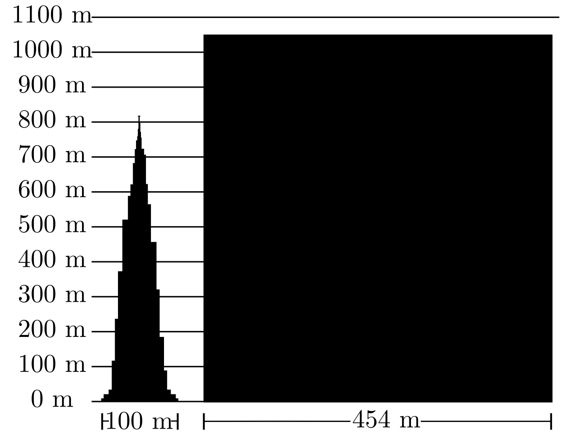

(b) Lego tower compared with the Burj Khalifa.

Figure 2.13: A tower taller than the Burj Khalifa can be build if each solution is represented with a Lego brick.

Programming the same methodology adding just one more relay would be equivalent to a search space length equal to 107.46 round trips to the sun and the computer would take almost three years to obtain a result.

Unreachable computing times are obtained after this point; the computation time would be greater than eight thousand years and the tower length equal to 10.62 light-years considering just eight relays, five adjustable settings, and five samples per setting. The simulation time if 10 relays are considered would be greater than 18 times the age of the planet earth.

The importance of this analysis grows if we consider three facts: 1) a small power system, for example the IEEE 9-bus test system has up to 12 line protection relays [93]; 2) the protection system relays settings are commonly considered continuous, or at least with a smaller sampling interval, and 3) the conventional computer used in this thesis has 8.0 GB of RAM and an Intel Core i7 3537U 2GHz processor, enough to perform an average of 63 GFLOPS [94], and consequently being half a million times slower than the supercomputer used in the example. The size of the search space of this problem tend to infinite proportions, in consequence the protections engineer should avoid using brute-force or similar methods to solve it.

Heuristics are methods adapted to solve an specific problem reducing the computational effort while increasing the *exploration* of the search space [95]; in contrast with analytical methods, rather than exact solutions they offer good enough results in a reasonably small time. Moreover, *metaheuristics* are heuristic methods oriented to solve general problems, or those that do not have an specific algorithm or heuristic capable to solve them [96]. Metaheuristics have grown in popularity over the last years because they offer good approximations to complex problems and are quite easy to adapt.

The provided information about the complexity of this problem helps to aim to the implementation of this kind of methods in order to solve it. With the objective of locating optimal regions, metaheuristics can be implemented to analyze and explore the search space in the shortest amount of time. Once this regions are found, exact methods might offer good *exploitation* of those regions. On the following subsections, the optimization methods implemented to solve the problem on this thesis are going to be described.

2.3.1 Calculus-Based Optimization Methods

Calculus-based optimization schemes are perhaps the most popular optimization techniques [97], and these methods are the elementary form of *nonlinear programming*. The general idea is to search for local optima by finding extremal points obtained when the derivative of the analyzed function is equal to zero.

Nonlinear Programming (NLP) [98–101] is a mathematical sub-field defined as the process of solving an optimization problem where either the objective function or one of the constraints are nonlinear. A function or system is nonlinear when the superposition principle is not satisfied, i.e., its output is not directly proportional to its input, the effects of the input factors is not completely additive, and the parts conforming the system cannot be reassembled obtaining the same output [102].

Nonlinear programming can be comprised by *constrained* and *unconstrained* problems. While unconstrained optimization does not require to delimitate the magnitudes of the parameters to optimize, constrained problems demand those settings to possess a desired characteristic, dealing with equality and inequality constraints.

The search algorithms used in NLP can be roughly classified into direct and indirect search algorithms. The direct algorithms depend only on the objective function and does not take into account its partial derivatives. This methods apply to single-variable functions; successive search points are iteratively determined with the goal of narrowing the *interval of uncertainty*, i.e., the zone that it is known to contain the optimal solution point, until the termination condition is met. On the other hand, the indirect algorithms are based on matrices of the first (Jacobian) and often second (Hessian) derivatives or gradients of the objective function. The basic idea of indirect methods is to generate a route following the direction of the function gradient until it becomes null [103, 104].

Nonlinear programming methods have limited information about the problem and still are effective to find extremal points of the evaluated function; the current solution point, the value of the objective function at the current point, the results of the constraints, and the jacobian and hessian matrices are sufficient information to determine if the actual solution is a minimum or maximum point [83]. Nevertheless, unless the evaluated function has only one solution, it is not possible to know if there is a better local optimum or if the method found the global one.

As can be deducted, NLP methods are highly dependant on the initial solution, consequently different inputs may converge to different solutions, something that it is not completely desirable when it comes to optimize. This situation is caused by the methodology followed by this kind of algorithms, where the function gradient is tracked in order to ascend or descend towards an optimal solution.

In addition to these complications, unlike linear programming problems, the optimal point is not necessarily located in an extreme point, but it can be on the boundary of the feasible region or in an interior point as depicted in Figure 2.14. Furthermore, the problem constraints might lead to a discontinuous solution space, increasing the difficulty of finding a feasible initial solution [97, 105].

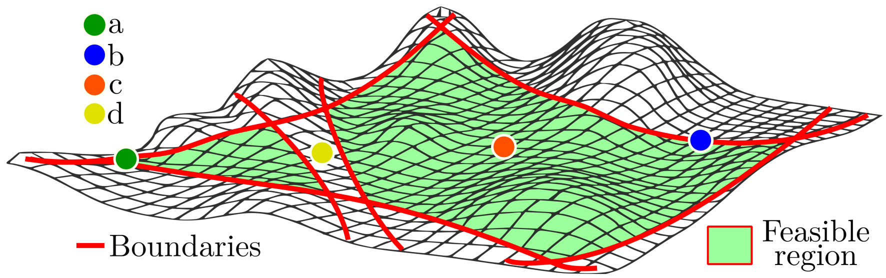

Figure 2.14: An optimal solution for a nonlinear system may be located in a) an extreme point, b) a non extreme boundary, or c) an interior point. The search space might present discontinuities (d) caused by the restrictions.

The dependence of computing the gradient in order to direct the search path can achieve optimal results on a local scale, for relatively simple problems with a small amount of variables and boundaries, these methods can be the best option; but for systems involving complex search spaces that contain multiple peaks and discontinuities this approach may face different drawbacks. The construction of a feasible initial solution may be a hard work, the algorithm might has to try several random initial points or even use a different approach in order to get a feasible point and start the convergence process. Given that an initial guess is found, there is no guarantee that this point is even close to the absolute best solution, consequently more random points have to be tested in order to achieve a solution that might not be as good as expected. This problem can be faced by using an exhaustive search, an option that is clearly not a good one when solving the coordination problem. Another important requirement that cannot be always fulfilled is the existence of derivatives, a medullar part of some of these methodologies.

Robustness is a significant asset of every optimization method. When an optimization technique is applied to solve a problem and obtain the desired settings, configuration, or any result required by a given scientific research, industrial application, et cetera, it is important to test and then to inform how well this methodology might perform in case of different initial conditions, restrictions, dimensions, characteristics, and any other features that lead to a dissimilar system.

The last two paragraphs help to conclude that, even when they perform well obtaining the optimal settings within the surrounding neighborhood, calculus-based optimization methods are not capable to provide robust search for some complex systems [84, 97]. Newton's-based methods and sequential quadratic programming concepts are described on the following paragraphs.

2.3.2 Newton's-Based Methods

Newton's method is a numerical analysis method used to find a sequence of approximations to the zeros of a function. Given an initial guess x_0 for a real differentiable function f and its first derivative f', a better approximation of the function root is given by Equation 2.11. This process is followed until a root is found. An example of Newton's method considering a one-dimensional function and three iterations is shown in Figure 2.15. The point where the tangent of the initial solution crosses the horizontal axis is considered as second point; the process is repeated until a stopping criteria is met;

$$x_1 = x_0 - \frac{f(x_0)}{f'(x_0)}. \tag{2.11}$$

In unconstrained optimization, Newton's method is an iterative method oriented to find the roots of a twice differentiable function. The generalized method consists of creating a sequence of solutions (x_n) that converges towards a local maximum or minimum (x^*) by using the vector of partial derivatives ($\nabla f(x)$ in Equation 2.13) and the inverse of its Hessian matrix ($\nabla^2 f(x)$) — matrix of second-order partial derivatives in Equation

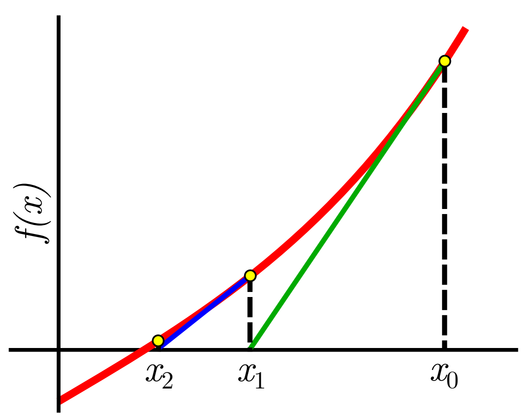

Figure 2.15: Example of Newton's method.

2.14 —. The method is defined in Equation 2.12. The iterative process is repeated until $f(x_{n+1})$ is sufficiently close to a root of the function $f(x)$:

$$x_{n+1} = x_n - [\nabla^2 f(x_n)]^{-1} \nabla f(x), \tag{2.12}$$

$$\nabla f(x) = \frac{\partial y}{\partial x}\left(\frac{\partial f(x)}{\partial x_1} + \frac{\partial f(x)}{\partial x_2} + \ldots + \frac{\partial f(x)}{\partial x_n}\right), \tag{2.13}$$

$$\nabla^2 f(x_n) = \frac{\partial^2 y}{\partial x_i x_j} = \begin{bmatrix} \frac{\partial^2 f}{\partial x_1^2} & \frac{\partial^2 f}{\partial x_1 \partial x_2} & \cdots & \frac{\partial^2 f}{\partial x_1 \partial x_n} \\ \frac{\partial^2 f}{\partial x_2 \partial x_1} & \frac{\partial^2 f}{\partial x_2^2} & \cdots & \frac{\partial^2 f}{\partial x_2 \partial x_n} \\ \vdots & \vdots & \ddots & \vdots \\ \frac{\partial^2 f}{\partial x_n \partial x_1} & \frac{\partial^2 f}{\partial x_n \partial x_2} & \cdots & \frac{\partial^2 f}{\partial x_n^2} \end{bmatrix}. \tag{2.14}$$

Newton's method is known for obtaining excellent results on local convergence if the initial approximation is close enough to the optimal value. The need for twice differentiable functions allows this method to change the step size on each iteration, obtaining rapid convergence for some cases and consequently performing better than other methods; nevertheless, the computation of the Hessian is not possible for some scenarios, it can also be expensive to compute, and the result of the iteration is undefined when this matrix is singular.

An alternative that can reduce the computational effort produced by computing the partial derivatives on each iteration is que quasi-Newton method. This method can be used even when the Jacobian or Hessian are not available or when they are expensive or difficult to compute. The general idea of this methods consists of applying successive approximations — defined in Equation 2.15 — of the inverse of the Hessian matrix ($\mathbf{B}_n$) to improve the convergence process. The $\mathbf{B}_n$ matrix is recursively computed using for example the approach proposed by Broyden [106]:

$$\mathbf{B}_n = \mathbf{B}_{n-1} + \frac{(y_n - \mathbf{B}_{n-1} s_n)}{|s_n|^2} s_n^{\intercal}, \tag{2.15}$$

$$y_n = \nabla f(x_n) - \nabla f(x_{n-1}), \tag{2.16}$$

$$s_n = x_n - x_{n-1}. \tag{2.17}$$

2.3.3 SEQUENTIAL QUADRATIC PROGRAMMING

Sequential Quadratic Programming (SQP) [107–110] — proposed by Wilson [111] in 1963 — can be seen as a general form of Newton's method. SQP has evolve to become one of the most effective and successful methods for the numerical solution of nonlinear constrained optimization problems, it generates sequential steps from the initial point by minimizing quadratic subproblems. The simplest form of SQP algorithm uses a quadratic approximation (Equation 2.18) subject to linearized constraints to replace the objective function.

$$q_n(d) = \nabla f(x_n)^\intercal d + \frac{1}{2} d^\intercal \nabla^2_{xx} \mathcal{L}(x_n, \lambda_n) d, \tag{2.18}$$

where d is the difference between two successive points. The hessian matrix of the lagrangian function is denoted by $\nabla^2_{xx}\mathcal{L}(x_n, \lambda_n)$; an approximation of this matrix is performed on each iteration using a quasi-Newton method. The quadratic approximation of the Lagrange function (Equation 2.19) is the base of the problem formulation.

$$\mathcal{L}(x_n, \lambda_n) = f(x) + \sum_{i=1}^{m} \lambda_i g_i(x). \tag{2.19}$$

Given a nonlinear programming problem:

$$\begin{aligned} \text{minimize} f(x) & \\ \text{subject to} b(x) &\leq 0, \\ c(x) &= 0. \end{aligned} \tag{2.20}$$

Simplifying the general nonlinear problem, a quadratic subproblem is obtained by linearizing the nonlinar restrictions, the subproblem is defined as follows:

$$\begin{aligned} \text{minimize} \quad & \nabla f(x_n)^\intercal d + \frac{1}{2} d^\intercal \mathbf{H}_n d \\ \text{subject to} \quad & \nabla b(x_n)^\intercal + b(x_n) \leq \quad 0, \\ & \nabla c(x_n)^\intercal + c(x_n) = \quad 0, \end{aligned} \tag{2.21}$$

where $\mathbf{H}_n$ is the BFGS (Broyden–Fletcher–Goldfarb–Shanno) approximation of the hessian matrix of the lagrangian function computation, required by the quadratic program and updated on each iteration. The approximation $\mathbf{H}_n$ is computed by:

$$\mathbf{H}_{n+1} = \mathbf{H}_n + \frac{y_n y_n^\intercal}{y_n^\intercal s_n} - \frac{\mathbf{H}_n^\intercal s_n^\intercal s_n \mathbf{H}_n}{s_n^\intercal \mathbf{H}_n s_n}, \tag{2.22}$$

$$y_n = \nabla_x \mathcal{L}(x_{n+1}, \lambda_n) - \nabla \mathcal{L}(x_n, \lambda_n), \tag{2.23}$$

$$= \left[\nabla f(x_{n+1}) + \sum_{i=1}^{m} \lambda_i \nabla g_i(x_{n+1})\right] - \left[\nabla f(x_n) + \sum_{i=1}^{m} \lambda_i \nabla g_i(x_n)\right], \tag{2.24}$$

$$s_n = x_{n+1} - x_n. \tag{2.25}$$

The Hessian is recommended to be maintained positive by keeping $y_n^\intercal s_n$ positive on each actualization by initializing the method with a positive $\mathbf{H}_n$. If $\mathbf{H}_n$ is not positive, y_n is modified until this requirement is achieved.

2.3.4 Nature-Inspired and Evolutionary Computation

Nature-inspired algorithms [112–114] are problem-solving techniques that emulate processes observed in different parts of the physical universe. Evolutionary Computation [115–118] is a computer science area that refers to optimization techniques involving evolutionary terms or Darwinian [119] principles such as reproduction, mutation, competition, selection, struggle for survival, et cetera. The main idea is that given an initial population, the natural selection will lead to the survival of the fittest, causing an improvement of the population fitness over the generations.

Natural selection is a powerful heuristic, stochastic, trial and error competition where the environment is previously defined and the same survival rules apply to every individual. Their chances of survival and leave legacy are increased in accordance with their quality or fitness, which depends on their adaptation ability. Each individual configuration or *genome* can be slightly or significantly different from another, bringing system diversification. For example, some individuals can be better hunters while others can be adapted to survive just with the leftovers; both of them might survive, giving plurality to the next generation. The wild world is challenging and the best asset of a fit individual is adaptation; in order to preserve the existence of it species, the individuals have to adjust their performance based on the feedback received from the environment.

Sometimes the classic deterministic optimization techniques cannot satisfy the non-linear, non-differentiable, or other unconventional optimization problems — especially in search spaces surrounded by local minima —, but this kind of problems have been solved pretty well by nature [115]. As said before, optimization does not imply perfection, nevertheless nature inspiration algorithms can find results that satisfy the problem requirements in a reasonable time.

Heuristic algorithms sacrifice the guarantee of obtaining a global optimum but they can boast of robust adaptation characteristics. The nature-inspired algorithms can be adapted to successfully solve an endless variety of problems involving planning, scheduling, designing, modeling, simulating or setting almost any kind of activity or problem. Several researchers, developers, and students of different research fields prefer to implement an already proven and robust evolutionary or nature-inspired algorithm rather than spending time and effort on the design of an specific software tool for any new problem they face.

Roughly, the natural selection process or evolution cycle is illustrated in Figure 2.16 and described as follows: On each generation, the best individuals have more possibilities of being chosen to be either mutated, reproduced, or both, leading to a new set of candidates or offspring. An example of the so called *genetic operators* is depicted in Figure 2.17. Considering functions of randomness or uncertainty, usually the average quality of the next generation is improved. This process is repeated until one or more stopping criteria is reached; for example, the simulations can be stopped when a desired goal is obtained, a limit of time or generations is exceeded, or if the convergence slope is not descending significantly.

The first attempt of emulating natural behavior in order to implement optimization algorithms goes back to long time before the computers started to become a common factor. In 1948 Alan Touring proposed a *genetical search* [120, 121] as a mean to configure his *unorganized machines*, he stated that the complex brain-like networks used to train the machines to perform particular tasks can be well approached from the evolution and

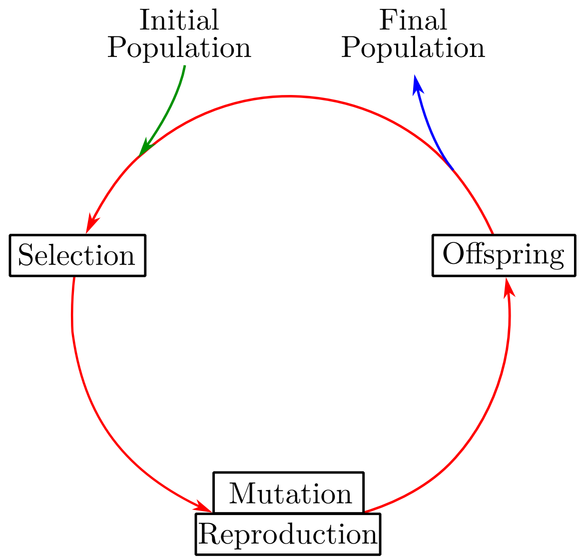

Figure 2.16: The cycle of evolution.

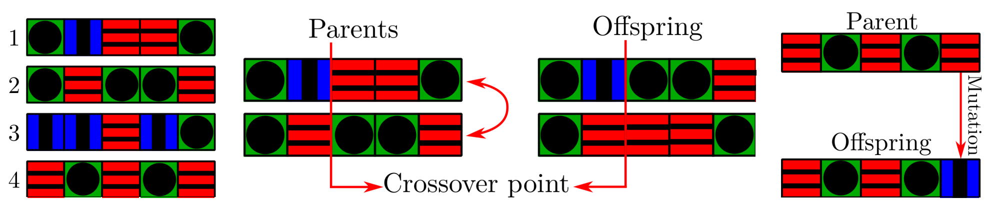

(a) Initialization. (b) Reproduction. (c) Mutation.

Figure 2.17: The concept of a genetic algorithm.

genetics point of view. It was until the 1960s when John H. Holland introduced the *genetic algorithms* [122–124], a metaheuristic method that is going to be described in the following section. Simultaneously, Lawrence J. Fogel et al. [125–127] proposed the *evolutionary programming*; in this method, adaptive mutation is the main *genetic operator* while reproduction or crossover is mostly discarded. The progeny competes with their parents and the fittest elements are selected to survive.

Later, Rechenberg and Schwefel [128–133] developed the *evolution strategies*; this method uses both crossover and a self-adapted strategy of parameters mutation [134]. The fourth strong evolutionary algorithm is a machine learning technique that considers elitism, crossover, mutation, and architecture-altering operations; the *genetic programming* method was presented by John Koza [135–138].

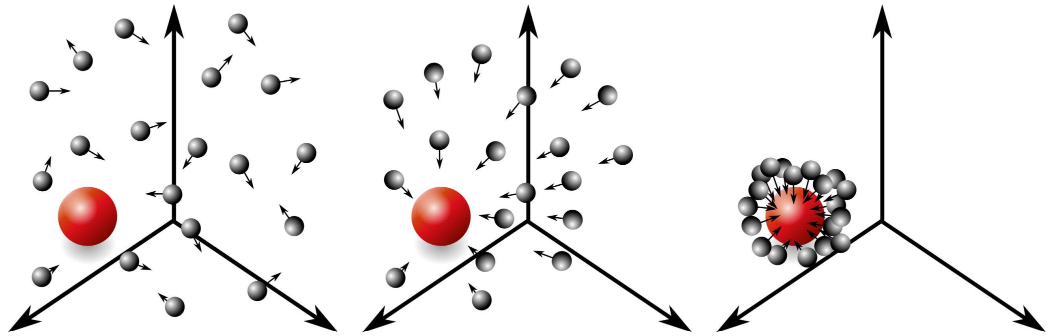

(a) The initial population is spread with random velocities.

(b) The food source position is communicated.

(c) The swarm travels and converge to the food source.

Figure 2.18: The concept of particle-swarm optimization.

This algorithm has produced human-competitive results for several instances and its field of implementation is growing [137, 138]. In the 1990s this set of methods started to be considered as subareas of a major field named evolutionary computation [117]. In addition, the *differential-evolution* algorithm [139–143] is another evolutionary computation, stochastic, and population-based strategy that was introduced years later than the other algorithms; it has been proven that it is a good strategy capable of solving problems over a continuous space [144].

There is some other nature-inspired algorithms that are not part of the evolutionary computation, nevertheless they keep some similarities in the formulation, objective, category, and of course in the inspiration source. The *particle-swarm optimization* [145–147] is a powerful technique which demonstrates robustness to solve several problems in different research areas [148]. The PSO keeps many similarities in comparison with a genetic algorithm, but the main difference is that every solution has an assigned velocity, so it is capable to travel over the search space.

Another method related to swarms is known as the *Ant-Colony Optimization* (ACO) algorithm [149–152]. Introduced in 1992 by Dorigo [153] as part of his PhD thesis, it is a method that emulates the behavior of an ant-colony while looking for food, pheromone is left in by the ants in different places until an optimized path from the anthill to the food source is found.

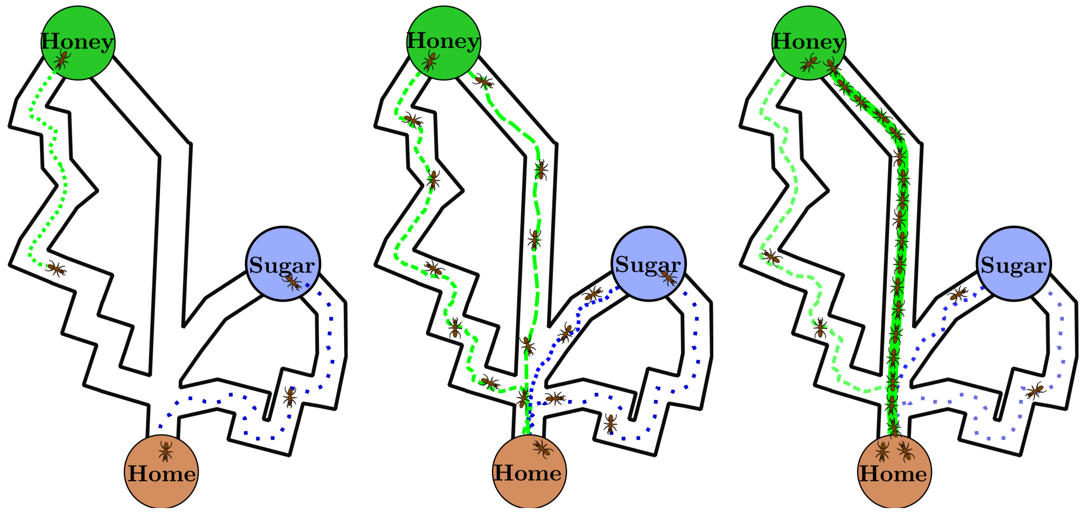

(a) Some ants find food sources. (b) Pheromone paths are left in accordance with the food quality. (c) The shortest path to the best food source is followed.

Figure 2.19: The concept of ant-colony optimization.

In addition, there is a relatively new metaheuristic algorithm named *invasive-weed optimization* method [154–157]. The strategy is based in a high exploration of the search space by performing different mutation operators.

Some of the optimization algorithms introduced in the previous paragraphs have been adapted to solve overcurrent and distance-relays coordination problems. The genetic algorithms and the invasive-weed optimization method are used to solve the problem in this thesis, consequently they are going to be described in a more detailed manner.

2.3.5 Genetic Algorithms

Genetic algorithms [82, 124, 158] are iterative, population-based metaheuristics developed in the 1960s by John Holland, his students, and colleagues. GA are based on the natural selection theory proposed in parallel [159] by Darwin [119] and Wallace [160] in the late 1850s. This methods are part of the evolutionary computation and were developed to solve optimization problems and to study the self-adaptation of molecules in biological processes; by combining *directed* and *stochastic* searches, they obtain a balance between the exploration and the exploitation of the search space [161].

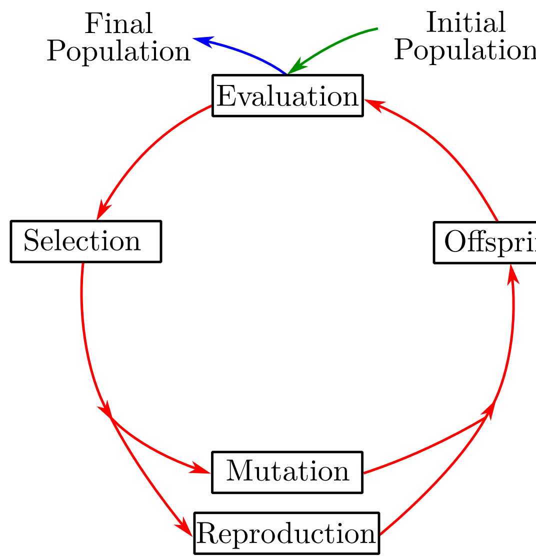

Figure 2.20: Genetic algorithms methodology.

The methodology followed by the GA is depicted in Figure 2.20 and each step is briefly described next. At first, the population is randomly generated using *uniform distribution*; each member of the population is called *Chromosome* ($\mathrm{C_x}$). Conformed by *genes* or settings for all the system variables, chromosomes are candidates to obtain a complete system solution. The population size commonly remains unaltered during the simulation. Individuals are evaluated according to the objective function on each iteration or *generation* with the objective of identifying the fittest elements, which will have better chances to survive.

The next step is a matter of life and death; it consists of selecting the chromosomes that will be used to leave offspring and consequently discarding some elements of the population. Several schemes may be implemented to carry out this process [162, 163]. *Truncation* selects the first n elements according to their fitness and *tournament* selection is based on the competition of a set of chromosomes.

In this thesis *stochastic universal sampling* and *roulette-wheel* selection are implemented. Both methods consist on sorting the chromosomes from the fittest to the least adapted; the individuals are then mapped to contiguous segments computed using Equation 2.26, these portions can consider *fitness-based* or *ranking-based* approaches. While the universal sampling selects by placing equally spaced pointers over the line of ranked chromosomes, the roulette-wheel spins to select each parent. Figure 2.21 depicts an example of both methods.

$$P_i = \frac{x_i}{\sum_{j=1}^{N} x_j}, \tag{2.26}$$

where:

P_i = Portion of the roulette assigned to the chromosome i,

x = Fitness or ranking value of the chromosome,

N = Total of chromosomes.

Suppose a rough example where wireless sensors have to be automatically deployed in a mountain — as illustrated in Figure 2.22 — with the aim of conform a network and report hazardous situations by communicating the compiled environmental information. The position of the sensors and the distance between them are used by the objective function. Considering a four chromosomes population, the supposed fitness results of each one are displayed in the second column of Table 2.5 and the roulette portion assigned by the fitness-based option on the third. There might be generations — specially the initial ones — where the fittest element is much better than the others, on this example the best element would cover the 70% of the roulette-wheel. This situation may cause the population of selected parents to be dominated by this element, reducing the diversity and increasing the possibility of premature convergence.

The second option is to designate a value equal to the inverse of the chromosome's ranking position; this action increases the selection possibilities of the least adapted and brings population diversity. Another benefit of this approach is that the ranking values and consequently the roulette portions can be defined since the beginning of the simulation, avoiding further calculations on each generation and reducing the computational effort. The roulette portions are also illustrated in Figure 2.21.

The offspring is generated through the implementation of *genetic operators*; reproduction or *crossover*, *mutation*, and *elitism* are the most common ones. Crossover is the main genetic operator. Two or more selected parents are randomly chosen to interchange

Table 2.5: Roulette-wheel portion based on fitness and ranking approaches.

C_x	Fitness	Roulette portion	Ranking	Value	Roulette portion
1	$x-1$	6%	3	1	48%
2	$2x+1$	15%	2	$1/2$	24%
3	x^2+3x	70%	4	$1/3$	16%
4	$x+2$	9%	1	$1/4$	12%

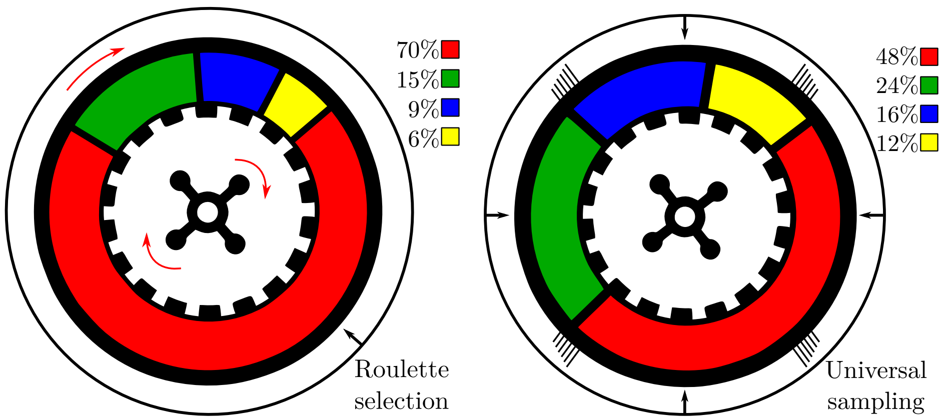

(a) Fitness-based roulette selection. (b) Ranking-based universal sampling.

Figure 2.21: Roulette-wheel and universal sampling selection method can use fitness or ranked-based approaches.

their genes considering one or more crossover points as can be seen in Figures 2.17(b) and 2.22(b). The objective of mutation is to bring diversity to the population by randomly changing one or more genes of the selected chromosome (see Figures 2.17(c) and 2.22(c)). Almost all the new chromosomes are derived from crossover, a small percentage comes from mutated elements, and occasionally an even smaller portion is conformed by elite parents, i.e., the fittest elements of the previous generation. The aim of elitism is to ensure that the solution will not worsen over the generations. The operator's probability of occurrence sums up to one:

$$\mathrm{P(C)} + \mathrm{P(M)} + \mathrm{P(E)} = 1. \tag{2.27}$$

In order to explore the search space, genetic algorithms starts the simulation randomizing the initial population, the crossover operator helps by interchanging the fittest elements genes while the mutation one introduces diversity; as the generations pass the algorithm detects optimal zones and exploit their neighborhoods.

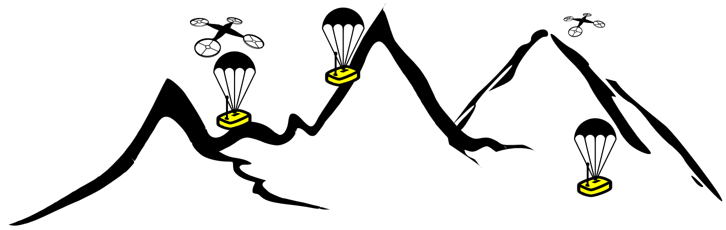

(a) The sensors are automatically deployed.

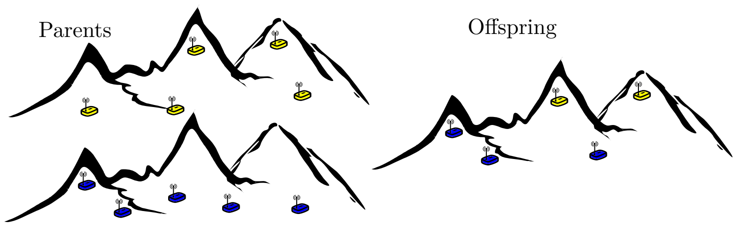

(b) Crossover is applied to selected parents.

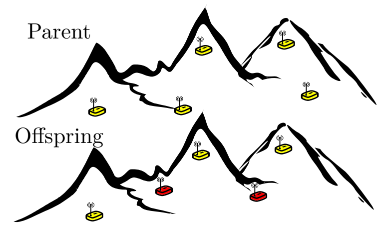

(c) Mutation operator is applied.

Figure 2.22: Genetic algorithm example. The deployment position of wireless sensors oriented to report hazardous situations is optimized.

Genetic algorithms methodology is highly conformed by randomized elements as the selected parents, the percentage of reproductions and mutations, the crossover points, among others. The influence of these elements excludes the possibility to guarantee the obtention of an optimal solution; it is even possible to obtain different solutions on every simulation. Over and above these disadvantages, the implementation of these algorithms present diverse benefits:

- The implementation of genetic algorithms is straightforward and does not require deep mathematical basis.
- GA are robust and flexible to be adapted to different problems. They may not obtain optimal solutions, but in some cases close is enough.
- They can be adapted to solve different objective functions allowing any kind of restrictions.
- This algorithms explore the search space before it is exploited, lightening the computational effort.

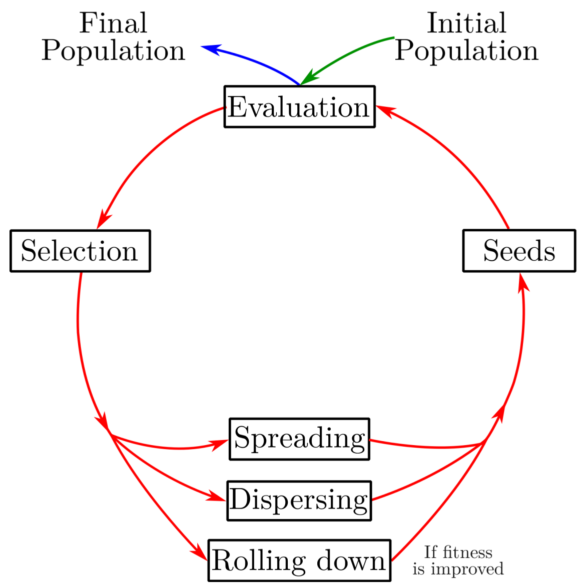

Figure 2.23: Invasive-weed optimization methodology.

2.3.6 Invasive-Weed Optimization

Weeds are plants with vigorous invasive habits that commonly grow on undesirable places; these kind of plants tend to invade crops in order to find and absorb water resources and nutrients to keep growing and reproduce, becoming a threat difficult to eliminate [164]. Weeds have survived tillage and herbicides, they cannot be fully eradicated and keep spreading and mutating stronger.

This description depicts a robust, stubborn, and self adapted to environmental adversities system, properties that can be harnessed by an optimization method. Invasive-weed optimization is a numerical stochastic metaheuristic that mimics the behavior of colonizing weeds; it was proposed by Mehrabian and Lucas [154] in 2006 with the objective of emulating the successful persistence of these plants. The IWO methodology is illustrated in Figure 2.23.

The initial steps are similar to a GA implementation, a possible system solution is known as *weed* and the weed population is randomly created and then evaluated. The members of the population are allowed to leave a n *seeds* (S) depending on their own and on the highest and lowest population fitness as described by Equation 2.28.

$$\mathrm{S}_i = \mathrm{S}_{\min}\left[(\mathrm{F}_i - \mathrm{F}_{\min})\frac{\mathrm{S}_{\max} - \mathrm{S}_{\min}}{\mathrm{F}_{\max} - \mathrm{F}_{\min}}\right], \tag{2.28}$$

where:

$$\begin{aligned}
\mathrm{S}_i &= \text{Total seeds of the weed } i,\\
[\mathrm{S}_{\min}, \mathrm{S}_{\max}] &= \text{Range of allowed seeds,}\\
\mathrm{F}_i &= \text{Fitness of weed } i,\\
[\mathrm{F}_{\min}, \mathrm{F}_{\max}] &= \text{Minimum and maximum population fitness.}
\end{aligned}$$

Once the total seeds of each weed is defined the main characteristic of this method is the introduced; the seeds are subject to invasive-weed operators based on mutation schemes, they are called *spreading*, *dispersing*, and *rolling-down*; these operators — described below — are responsible of the seeds dissemination, equal to the exploration and exploitation of the search space. Each operator is assigned with a probability of occurrence:

$$\mathrm{P(S)} + \mathrm{P(D)} + \mathrm{P(R)} = 1. \tag{2.29}$$

Spreading This algorithm consists of disseminating the seed by randomly creating a new individual. On this work multiple mutations are applied to less than the half of the content of the current seed; by this mean the seed is spread while some part of it is conserved. An example of this operator is illustrated in Figure 2.24(a).

Dispersing The second algorithm is depicted in Figure 2.24(b), aims to disperse the seed to a place close to the original plant. The procedure consists in computing a degree of difference and multiply it by the seed. The distance is gradually reduced as the simulation advance. In addition to this approach, a second dispersion method that consists in mutating a small part — less than the 20 percent — of the seed content is implemented on this work.

Rolling-down The aim of the last algorithm is moving the seed to a better location. This method evaluates the weed neighborhood and just leaves the seed if a better place

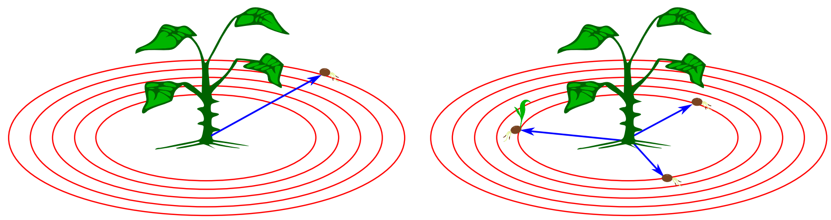

(a) Spreading operator. Seeds are spread all over the area.

(b) Dispersing operator. Seeds are dispersed in the weed neighborhood.

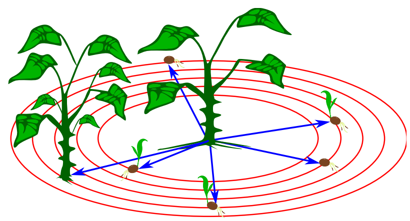

(c) Rolling-down operator. Seeds are spread and dispersed until a best solution is found.

Figure 2.24: Invasive-weed optimization operators.

is found. The neighborhood is described as places located at a distance equal to one transformation of the current plant. The implementation of this proposal creates copies of the current seed and apply random mutations, the mutated copies are evaluated and this process is repeated until a copy improves the weed fitness. The improved seeds and the ones with close but different solutions are kept while the others are dismissed. The rolling-down algorithm is shown in Figure 2.24(c).

The emulation of invasive-weeds behavior has been widely accepted by the scientific community, this methodology has solved different problems as shown in references [154–157, 165], among others. Spreading operator explores the search space, dispersion one exploits the weed location, and the rolling-down combines these methods to improve the actual solution. Altogether the invasive-weed operators permit a rapid exploration and exploitation of the search space. Similar to GA, IWO is also a metaheuristic that cannot assure the obtention of optimal values or convergence to the same solution on each simulation. The implementation of this method presents the same benefits that were mentioned for GA. In addition, mutation-based operators create new settings instead of performing crossover operations, requiring less computational effort.

CHAPTER 3

PROPOSED SOLUTION

The previous chapter described the general methodology of some optimization methods that have been used to solve the coordination process. The aim of this chapter is to describe the implementation of the algorithms used in this thesis. The original algorithms have been modified with the objective of adapting them to the coordination problem; nevertheless, slight changes can be made to the presented methodologies in order to apply them to solve different assignments.

As described in our hypothesis, the use of non-standardized inverse-time curves would reduce the tripping time for currents different than the maximum and consequently improve the coordination process. The overcurrent relays tripping time for different levels of short-circuit current is computed using Equation 2.2. This equation is conformed by five settings and the input current. The main distinctive characteristic of this work is the consideration of the five equation settings as adjustable, obtaining non-standardized inverse-time curves.

The present chapter is divided into five sections, the first one discusses the followed methodology, the next one describes the mathematical model of the coordination problem while the following sections describe the implementation of sequential quadratic programming, genetic algorithms, and invasive-weed optimization to solve the overcurrent relay coordination problem.

3.1 METHODOLOGY

The information provided by the previous chapter and condensed in Tables 1.1 and 1.2 is useful to highlight that the overcurrent and distance-relays coordination problem is a high impact problem among the protections engineering community; it is a problem that has maintained its importance and stayed current for more than thirty years, being studied by diverse research groups around the globe.

The problem has been faced through the implementation of diverse optimization algorithms; the first efforts were focused in the implementation of exact algorithms as linear and nonlinear programming, capable of obtaining optimal coordination solutions. Nevertheless the trends over the years seem to have turned toward the implementation of heuristic and metaheuristic methods capable to overcome the exact methods limitations with the — maybe negligible — drawback of not guaranteeing an optimal solution.

Genetic Algorithms are proven to perform well as denoted by different included references, considering that the main objective of this thesis is not the proposal of a new optimization method we decided to use GA just as a tool that has proven good and robust performance and permits the computation of a large amount of optimization variables.

Furthermore, as a secondary objective it was decided to implement the relatively recently developed invasive-weed optimization algorithm because it has not been reported to solve the coordination problem. In addition, the implementation of exact algorithms is explored and the sequential quadratic programming method was selected since it has been recognized as the state of the art in nonlinear programming.

Related works consider standardized inverse-time curves and a maximum of three settings — or group of settings when the characteristic curve is also a variable — as adjustable. We have not encountered any existing literature in which five adjustable settings of the OCR are used to obtain the inverse-time curve. Another point to emphasize is the fault points location used to carry out the coordination process, some works take into account either close-end and/or far-end faults but their consideration in the objective function is not clearly defined.

In this thesis we propose to coordinate OCR considering two and three different levels of short-circuit current and five adjustable settings, obtaining non-standardized inverse-time curves. The proposed objective function considers — with different weighing — close-end three-phase and far-end two-phase faults as frontier coordination currents while a third magnitude between those is also taken into account in order to prevent possible miscoordination in the central part of the inverse-time curves.

The proposal is justified by the fact that presently, some commercial relays — through software tools [166] — already allow the user to define the OCR parameters instead of simply selecting among the standardized ones [167]. However, the consideration of more adjustable settings increase the search space exponentially and consequently the problem complexity, demanding bigger computational effort and better algorithmic implementation.

Regarding the coordination of distance and overcurrent relays, the aim of all related works consist on coordination all the distance and overcurrent relays while this proposal have a different approach; it seeks to coordinate the overcurrent relays and then allocate distance ones in places where the OCR are not sensitive: improving the system reliability, reducing the costs of redundancy, and proposing a different coordination concept.

The followed methodology consists of a deep understanding of the coordination problem and optimization algorithms in order to model, adapt, and implement them to being solved through computational simulation. The next phase is the experimental design and results obtention, coming to an end with the results discussion, conclusions obtention, and further work proposition.

3.2 Mathematical Model

The general and implemented model, as well as the genetic, invasive-weed, and sequential quadratic programming algorithms are described in the following paragraphs.

3.2.1 Proposed General Model

Let f and g denote respectively the tripping time of a main and a backup overcurrent relay for determined short-circuit (a) and load (b) currents, while h is the difference between those two magnitudes.

$$f(\mathbf{x}) = \left[\frac{x^1}{\left[\frac{\mathbf{a}}{b_1 \times x^5}\right]^{x^3} - 1} + x^2 \right] \times x^4, \tag{3.1}$$

$$g(\mathbf{y}) = \left[\frac{y^1}{\left[\frac{\mathbf{a}}{b_2 \times y^5}\right]^{y^3} - 1} + y^2 \right] \times y^4, \tag{3.2}$$

$$h(x, y) = g(y) - f(x), \tag{3.3}$$

where

$$\mathbf{a} = \left(a^{\min} : a^{\max}\right)^{\intercal}, \ \mathbf{x} = \left(x^1, x^2, x^3, x^4, x^5\right)^{\intercal}, \ \mathbf{y} = \left(y^1, y^2, y^3, y^4, y^5\right)^{\intercal}, \ \mathbf{y} \subset \mathbf{x} \in \mathbb{R}.$$

Equation 3.4 shows a simplification of the proposed model for the optimization of the overcurrent relay coordination problem.

$$\underset{f,g,h}{\text{minimize}} \quad \alpha \sum_{i=1}^{\mathrm{m}} \frac{f_i(\mathbf{x}_i)}{\mathrm{m}} + \beta \sum_{j=1}^{\mathrm{n}} \frac{g_j(\mathbf{y}_j)}{\mathrm{n}} + \gamma \sum_{j=1}^{\mathrm{n}} \frac{h_j(\mathbf{x}_j, \mathbf{y}_j)}{\mathrm{n}}, \tag{3.4}$$

$$\text{subject to} \quad x^4, y^4 \geq 0.5, \tag{3.5}$$

$$x^5, y^5 \geq 1.4, \tag{3.6}$$

$$\forall a : h \geq 0.3, \tag{3.7}$$

where m and n are the total relays and the total coordination pairs in the system while α, β, γ are given weighting factors for each one of the objectives. The first two restrictions are given by conceptual limitations of the overcurrent relay [168, 169]; while x^4 keeps the TDS greater than a standardized magnitude that emulates a function of the electromechanical relay, x^5 aims to ensure that the protection would operate for ampere magnitudes greater than 1.4 times the load current . Both restrictions have upper limits but, since their magnitude is directly proportional to the tripping time, the algorithm seeks to set them as low as possible, therefore those limits are not listed in this model. The last one is the coordination restriction, it establish that for a given short-circuit magnitude the tripping time difference between the backup and main relays have to be greater than or equal to the coordination time interval.

3.2.2 Model Enhancements

The x^1, x^2, and x^3 variables, corresponding to the A, B, and p parameters, are theoretically capable of accepting any assigned magnitude; nevertheless this assumption might lead to undesired curve shapes, i.e., curves that do not present the inverse-time characteristic of the overcurrent relays. Furthermore, a more important drawback is the increase of the search space size.

Relays tripping time is augmented if the magnitude of the two remaining variables (x^4 and x^5) increases, therefore if bigger values that will not bring benefits to the problem solution are discarded the search space may be reduced. Consequently, boundaries are placed to delimitate the selection of each of the five variables. The sets of boundaries are going to be called selection ranges and will be discussed in the following chapters. Moreover the restriction $h \geq 0.3$ — responsible of relays coordination — is changed for penalty functions. The CTI is included in Equation 3.8 to redefine Equation 3.3:

$$h(x, y) = g(y) - f(x) - \mathrm{CTI}. \tag{3.8}$$

Positive magnitudes of h indicate slower operation and negative ones lack of coordination.

The first is acceptable while the last is not; in addition, the use of penalty functions may lead to undesired compensations between both kind of errors. Since lack of coordination should be avoided, those cases are harshly penalized by multiplying the exponential of their backup tripping time and coordination error by a penalty factor (ϵ) as shown in Equations 3.9 and 3.10. Meanwhile penalized versions of positive errors are equal to their original magnitudes, i.e., $h_j \leq 0 \iff g_j = g_j^p \wedge h_j = h_j^p; h_j < 0 \iff$

$$g_j^p = e^{g_j} \times \epsilon, \tag{3.9}$$

$$h_j^p = e^{|h_j|} \times \epsilon. \tag{3.10}$$

The objective function is still conformed by the operation times of the main relays, but g_j and h_j are substituted by their penalized versions. In addition, given that the apparition of negative errors is now an option, the total of miscoordinations ($\mathrm{T_{mc}}$) is considered as presented in Equation 3.11:

$$\underset{\mathrm{T_{mc}},f,g,h}{\text{minimize}} \quad \frac{\mathrm{T_{mc}}}{\mathrm{n}} + \alpha \sum_{i=1}^{\mathrm{m}} \frac{f_i(\mathbf{x}_i)}{\mathrm{m}} + \beta \sum_{j=1}^{\mathrm{n}} \frac{g_j(\mathbf{y}_j)}{\mathrm{n}} + \gamma \sum_{j=1}^{\mathrm{n}} \frac{h_j(\mathbf{x}_j, \mathbf{y}_j)}{\mathrm{n}}. \tag{3.11}$$

The coordination problem has a multi-objective nature, the computations considered as part of the objective function are desired characteristics of the protection system. In essence, each relay has to provide fast fault clearance for its main protection zone and backup protection for the adjacent lines.

An optimal solution would be constituted by zero miscoordinations and the lowest tripping times; nevertheless, both attributes are opposed and conform a *Pareto frontier* [170], obtained when an attribute cannot be improved without worsen another. Similar to other problems that involve time reduction, an optimal solution is not as useful and practical as a solution that obtain low enough times in a reasonable simulation time.

As stated before, this thesis seeks to improve coordination for different levels of short-circuit current, consequently the optimization process is carried out simultaneously considering short-circuit magnitudes caused by two and three-phase solid faults located respectively in the far and close-end bus of each main relay. Both magnitudes are considered as coordination boundaries; since the use of non standardized inverse-time curves might lead to undesirable curve shapes, a third I_{sc} magnitude equal to the average of both previous values is also used. As a consequence the coordination is performed considering three levels of short-circuit current, computing times and evaluating Equation 3.11 for each one of them.

The protection system has to ensure coordination for a maximum I_{sc} level, therefore the objective function result for other levels will be considered with smaller weights. The constants ι, κ, and τ serve as weighting constants for the different short-circuit magnitudes. The complete fitness function is then defined as the sum of the weighted OF results for minimum ($\mathrm{OF_m}$), intermediate ($\mathrm{OF_i}$), and maximum ($\mathrm{OF_M}$) short-circuit levels:

$$OF = \iota \times \mathrm{OF_m} + \kappa \times \mathrm{OF_i} + \tau \times \mathrm{OF_M}. \tag{3.12}$$

3.3 Overcurrent Relay Coordination

The following subsections will describes the GA, IWO, and SQP adaptations and implementations of the directional overcurrent relay coordination problem considering five adjustable settings. The general methodologies of these algorithms were presented in the Chapter 2.

Previous calculations have to be performed and given as an input to the following methods. The I_{pickup} is computed using Equation 2.1, therefore it is necessary to obtain the I_{load} via a load-flow analysis; the fault currents are also computed through the implementation of a fault analysis [171]; faults in intermediate points are calculated by considering the moving fault method for either balanced [172] and unbalanced [173] faults.

3.3.1 Genetic Algorithm

The population of the genetic algorithm is conformed by chromosomes, each $\mathrm{C_x}$ contain adjustable settings for the total overcurrent relays ($\mathrm{T_r}$). Supposing three AS and a five relays system, the size of each $\mathrm{C_x}$ would be $[15 \times 1]$. The population size $\mathrm{P_s}$ is given by the total considered chromosomes ($\mathrm{T_{C_x}}$); the previous example for a population size equal to 20 represent a population matrix ($\mathbf{P_{C_x}}$) of $[15 \times 20]$, containing a total of 300 genes. The arrangement of the population matrix is presented in Equation 3.13 where each column represents a chromosome and each row a relay setting.

$$\mathbf{P_{C_x}} = \left(\begin{array}{cccc} \mathrm{TDS_{1-1}} & \mathrm{TDS_{1-2}} & \dots & \mathrm{TDS_{1-T_{C_x}}} \\ \vdots & \vdots & \ddots & \vdots \\ \mathrm{TDS_{T_r-1}} & \mathrm{TDS_{T_r-2}} & \dots & \mathrm{TDS_{T_r-T_{C_x}}} \\ \hline \mathrm{P_{m1-1}} & \mathrm{P_{m1-2}} & \dots & \mathrm{P_{m1-T_{C_x}}} \\ \vdots & \vdots & \ddots & \vdots \\ \mathrm{P_{mT_r-1}} & \mathrm{P_{mT_r-2}} & \dots & \mathrm{P_{mT_r-T_{C_x}}} \\ \hline \mathrm{A_{1-1}} & \mathrm{A_{1-2}} & \dots & \mathrm{A_{1-T_{C_x}}} \\ \vdots & \vdots & \ddots & \vdots \\ \mathrm{A_{T_r-1}} & \mathrm{A_{T_r-2}} & \dots & \mathrm{A_{T_r-T_{C_x}}} \\ \hline \mathrm{B_{1-1}} & \mathrm{B_{1-2}} & \dots & \mathrm{B_{1-T_{C_x}}} \\ \vdots & \vdots & \ddots & \vdots \\ \mathrm{B_{T_r-1}} & \mathrm{B_{T_r-2}} & \dots & \mathrm{B_{T_r-T_{C_x}}} \\ \hline \mathrm{p_{1-1}} & \mathrm{p_{1-2}} & \dots & \mathrm{p_{1-T_{C_x}}} \\ \vdots & \vdots & \ddots & \vdots \\ \mathrm{p_{T_r-1}} & \mathrm{p_{T_r-2}} & \dots & \mathrm{p_{T_r-T_{C_x}}} \end{array} \right). \tag{3.13}$$

The initial population is created generating uniformly distributed random numbers, each number must be located within each setting boundaries. A coordination pair is conformed by a main relay and its backup; relays may be part of different coordination pairs either as main or backup protection.

The tripping times of all main and backup relays are computed using Equation 2.2, then the coordination errors are obtained with Equation 2.4; the negative errors are penalized through Equations 3.9 and 3.10 and thereupon all chromosomes are evaluated considering the objective function presented in Equation 3.11.

The selection process is carried out either with stochastic universal sampling or

Table 3.1: Selection probability and repeated selections of some ranked chromosomes.

Roulette-wheel selection probabilities												
Ranking	1	2	3	4	5	10	20	30	40	50	75	100
Probability (%)	19.27	9.63	6.42	4.81	3.85	1.92	0.96	0.64	0.48	0.38	0.25	0.19
Universal sampling repeated selections												
Ranking	1	2	3	4	5	6	7	8	9	10	11	12
Selections	20	9	6	5	4	3	3	2	2	2	2	2

roulette-wheel selection methods using the ranking-based approach, as described in Chapter 2. For a population size of 100 chromosomes — if the roulette-wheel is applied — the probability of selection of the $\mathrm{C_x}$ positioned in different ranks is shown in the first part of Table 3.1. On the other hand, considering a population size and total selected elements equal to 100, the total of repeated selections of the first twelve ranked chromosomes is shown.

The first twelve ranked elements of a 100 $\mathrm{C_x}$ population conforms the 60% of the individuals selected by the universal sampling method. In appearance the roulette-wheel selection would be more diversified, aiming to test this assumption a simple experiment is conducted. The experiment consists in simulating the roulette-wheel method 100,000 times to determine the population percentage occupied by the first twelve ranked elements.

The results are illustrated as a box-whiskers plot in Figure 3.1. The mean result is 59.83% while the median is 60%, almost equal to the universal sampling result. Both methods offer different advantages, while the obtention of more diversification is a strong of the roulette-wheel, the universal sampling offers less computational effort by previously defining the selected ranks.

The next step in GA is the conformation of the next generation via the genetic operators. Almost all the new generation is obtained through the crossover operator. A single point crossover methodology is implemented in this work; each group of settings is divided into two blocks, the division point is randomly set between the 25% and 75% of

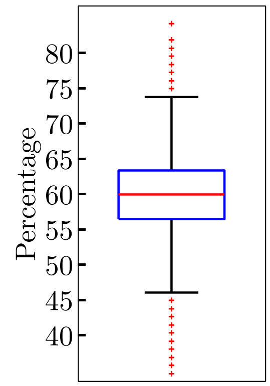

Figure 3.1: Population percentage conformed by the first twelve elements.

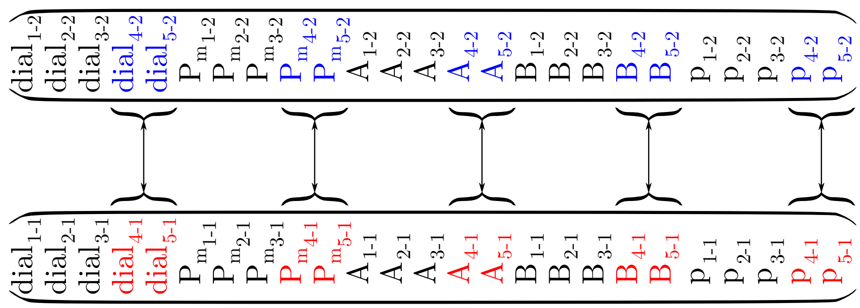

Figure 3.2: Crossover operator interchange relay settings of the two selected parents.

the total system relays. All the corresponding relays settings are interchanged to prevent loosing information. An example of the crossover methodology is depicted in Figure 3.2.

The reproduction is followed by mutation operator. The objective of this step is to diversify the population with the introduction of random setting changes. In this work a small part of the population — commonly 5% — is mutated; nevertheless a mechanism that monitors the slope of the convergence increase the mutation rate up to 40% if the slope remains horizontal after iterations. Elite mutations, consisting on exclusive modifications to the fittest elements, are also performed. The last part of the population is formed with elite parents, the fittest elements survive through the generations with the objective of ensuring that the result will not get worse over the simulation.

Around the 90% of the new generation is conformed by crossover offspring, the remaining 10% is divided into mutation, elite mutation, and elite parents. Diverse percentages and mutation rates have been tested, results will be presented in the following chapters. The described process is repeated until a stopping criteria is met. The most common criterium is the reach of the total iterations ($\mathrm{T_i}$).

3.3.2 Invasive-Weed Optimization

The initial steps of the invasive-weed optimization method are equivalent to the genetic algorithm ones. The individuals are called weeds, the weed matrix is randomly generated, the tripping times and coordination errors are computed using the same equations and the considered objective function is Equation 3.11 for different short-circuit levels.

The distinctive stages of IWO begin after the evaluation step; the weeds are sorted according to their fitness (F) and each one is allowed to leave seeds in accordance to their ranking as illustrated in Figure 3.3.

Figure 3.3: Weeds are assigned with a number of seeds in accordance with their fitness.

A seed is a clone of the actual weed that will be subjected to mutation operators. The total seeds ($\mathrm{T_S}$) assigned to each weed are computed using Equation 3.14.

$$\mathrm{T_{S_i}} = \mathrm{S_{rm}} + \left[(\mathrm{F_w} - \mathrm{F_i}) \times \frac{\mathrm{S_{rM}} - \mathrm{S_{rm}}}{\mathrm{F_w} - \mathrm{F_b}} \right], \tag{3.14}$$

where $\mathrm{S_{rm}}$ and $\mathrm{S_{rM}}$ are the minimum and maximum quantity of possible weeds, $\mathrm{F_b}$ and $\mathrm{F_w}$ are the fitness values of the best and worst elements, and $\mathrm{F_i}$ is the fitness of the actual individual. There may be some scenarios were the fitness of the worst element results infinite, so a predefined magnitude is considered as $\mathrm{F_w}$.

Spreading, dispersing, and rolling weed operators are used to explore and exploit the search space in order to find better results. Each assigned seed is subjected to one of the three operators randomly chosen. The implementation of all three operators is described in the following paragraphs.

The objective of the spreading operator is to create a new plant based on the current seed. The implementation consists in mutating up to 50% of the seed content. The second operator's objective is to disperse the seed in the surrounding neighborhoods of the weed; on this thesis the dispersion methodology faces two stages, the first one undergoes the seed to small perturbations by multiplying every setting by a maximum variation of $\pm$ 1%. The second stage mutates up to 20% of the seed elements.

The last operator creates copies of the current seed and then combines the first two mechanisms to disperse and spread the actual seed; the process is repeated until a better solution is found or the seed copies are exhausted. The mutation percentage, the perturbation magnitude, and the settings to mutate are randomly selected. Examples of the three operators can be seen in Figure 3.4.

The fitness of the current weeds and mutated seeds are sorted and the n fittest elements are selected to conform the new population. The method is initialized from the seed assignment step and this procedure is iteratively repeated until the only stopping criterium considered for this implementation — the reach of total iterations $\mathrm{T_i}$ — is met.

$$\text{Spreading}\begin{pmatrix} dial_{1\text{-}1} \\ dial_{2\text{-}1} \\ dial_{3\text{-}1} \\ dial_{4\text{-}1} \\ dial_{5\text{-}1} \\ P_{m_{1\text{-}1}} \\ P_{m_{2\text{-}1}} \\ P_{m_{3\text{-}1}} \\ P_{m_{4\text{-}1}} \\ P_{m_{5\text{-}1}} \\ A_{1\text{-}1} \\ A_{2\text{-}1} \\ A_{3\text{-}1} \\ A_{4\text{-}1} \\ A_{5\text{-}1} \\ B_{1\text{-}1} \\ B_{2\text{-}1} \\ B_{3\text{-}1} \\ B_{4\text{-}1} \\ B_{5\text{-}1} \\ p_{1\text{-}1} \\ p_{2\text{-}1} \\ p_{3\text{-}1} \\ p_{4\text{-}1} \\ p_{5\text{-}1} \end{pmatrix} \quad \text{Dispersing}\begin{pmatrix} dial_{1\text{-}2} \\ dial_{2\text{-}2} \\ dial_{3\text{-}2} \\ dial_{4\text{-}2} \\ dial_{5\text{-}2} \\ P_{m_{1\text{-}2}} \\ P_{m_{2\text{-}2}} \\ P_{m_{3\text{-}2}} \\ P_{m_{4\text{-}2}} \\ P_{m_{5\text{-}2}} \\ A_{1\text{-}2} \\ A_{2\text{-}2} \\ A_{3\text{-}2} \\ A_{4\text{-}2} \\ A_{5\text{-}2} \\ B_{1\text{-}2} \\ B_{2\text{-}2} \\ B_{3\text{-}2} \\ B_{4\text{-}2} \\ B_{5\text{-}2} \\ p_{1\text{-}2} \\ p_{2\text{-}2} \\ p_{3\text{-}2} \\ p_{4\text{-}2} \\ p_{5\text{-}2} \end{pmatrix} \bullet \begin{pmatrix} 1.008 \\ 0.999 \\ 1.005 \\ 0.994 \\ 0.990 \\ 0.993 \\ 0.992 \\ 0.994 \\ 0.999 \\ 1.001 \\ 1.003 \\ 0.995 \\ 1.005 \\ 0.997 \\ 1.007 \\ 1.008 \\ 1.009 \\ 1.006 \\ 0.995 \\ 1.005 \\ 1.007 \\ 0.999 \\ 1.009 \\ 0.991 \\ 1.009 \\ 1.010 \\ 1.001 \\ 0.997 \end{pmatrix} \quad \text{Rolling Down}\begin{pmatrix} dial_{1\text{-}2} \\ dial_{2\text{-}2} \\ dial_{3\text{-}2} \\ dial_{4\text{-}2} \\ dial_{5\text{-}2} \\ P_{m_{1\text{-}2}} \\ P_{m_{2\text{-}2}} \\ P_{m_{3\text{-}2}} \\ P_{m_{4\text{-}2}} \\ P_{m_{5\text{-}2}} \\ A_{1\text{-}2} \\ A_{2\text{-}2} \\ A_{3\text{-}2} \\ A_{4\text{-}2} \\ A_{5\text{-}2} \\ B_{1\text{-}2} \\ B_{2\text{-}2} \\ B_{3\text{-}2} \\ B_{4\text{-}2} \\ B_{5\text{-}2} \\ p_{1\text{-}2} \\ p_{2\text{-}2} \\ p_{3\text{-}2} \\ p_{4\text{-}2} \\ p_{5\text{-}2} \end{pmatrix} \bullet \begin{pmatrix} 1.007 \\ 0.993 \\ 1.003 \\ 0.998 \\ 1.995 \\ 0.994 \\ 0.993 \\ 1.004 \\ 0.997 \\ 1.005 \\ 1.004 \\ 0.999 \\ 1.002 \\ 0.996 \\ 0.007 \\ 1.001 \\ 0.990 \\ 1.007 \\ 0.997 \\ 1.002 \\ 1.003 \\ 0.997 \\ 0.996 \\ 0.993 \\ 1.007 \\ 1.001 \\ 1.008 \\ 0.995 \end{pmatrix}$$

Figure 3.4: Spreading and dispersing operators mutate respectively up to 50% and 20% of seed elements. Rolling-down combines both and selects an improved mutation.

3.3.3 Sequential Quadratic Programming

As mentioned in Chapter 2, due to the search space dimensions and also the required computation of Jacobian and Hessian matrices, the implementation of nonlinear methods may not be the best option to solve the problem addressed in this thesis. However, these methods are useful when good initial approximations are provided.

The sequential quadratic programming methods are the state of the art in nonlinear programming [107]; this method was implemented through the adaptation of the *fmincon* function [174] belonging to the *Optimization Toolbox* [175, 176] of MATLAB [177]. The boundaries that define the feasible area help SQP to make informed decisions on the search directions and step lengths, therefore SQP can often solve nonlinear constrained faster than unconstrained problems. This fact support the decision of set boundaries to all variables, stated in Section 3.2. On this thesis the SQP is applied in different stages of the GA and IWO simulations; the results will be illustrated and discussed in the following chapters.

The quasi-Newton approximation of the Hessian of the Lagrangian function is calculated using the BFGS method (see Equations 2.22 to 2.25); then, on each iteration is solved a problem of the form of Equation 2.21. The first stage of this process consists in evaluating a feasible point — it is commonly required that this point is user-provided — while the second one creates a sequence of feasible points until the stopping criteria is met. The SQP implementation combines the constraint and objective functions into a merit function when a feasible solution for the next step cannot be found. For more information about the MATLAB implementation of SQP, the Optimization Toolbox User's Guide [176] may be reviewed.

3.4 Overcurrent and Distance Relay Coordination

Overcurrent protection principle face limitations regarding the tripping times increase for current magnitudes near the pickup setting. By using non-standardized inverse-time curves inversion grades can be modified and some of those limitations may be overcome while others can remain and cause miscoordinations. In addition, there are some scenarios where $\mathrm{I_{sc}} \leq \mathrm{I_{pickup}}$ and consequently the OCR is insensitive. Making an effort to offer an integrate solution for the OCR coordination problem, a methodology that uses distance-relays to substitute overcurrent ones for conflicted coordination pairs is proposed. Three kind of coordination pairs are expected, overcurrent as main and backup (OC+OC), distance as main and OCR as backup (D+OC), and OCR as main and distance as backup (OC+D) .

The methodology is adapted to be compatible with the already described implementation; a new term that considers distance-relay coordination is included to the objective function as shown in Equation 3.15:

$$\underset{\mathrm{T_{mc}},f,g,h,d}{\text{minimize}} \quad \frac{\mathrm{T_{mc}}}{\mathrm{n}} + \alpha \sum_{i=1}^{\mathrm{m}} \frac{f_i(\mathbf{x}_i)}{\mathrm{m}} + \beta \sum_{j=1}^{\mathrm{n}} \frac{g_j^p(\mathbf{y}_j)}{\mathrm{n}} + \gamma \sum_{j=1}^{\mathrm{n}} \frac{h_j^p(\mathbf{x}_j,\mathbf{y}_j)}{\mathrm{n}} + \delta \sum_{k=1}^{\mathrm{o}} \frac{d_k(\mathbf{x}_k,\mathbf{y}_k,\mathbf{Z}_k)}{\mathrm{o}}, \tag{3.15}$$

where o represents the total distance-relays, d their penalization function, δ is a weighting factor, and $\mathbf{Z}$ is a matrix containing the distance-relays tripping time for each one of the three zones as shown in Equation 3.16, where $\mathrm{T_{dr}}$ is the total of distance-relays:

$$\mathbf{Z} = \begin{pmatrix} \mathrm{t_{z11-1}} & \mathrm{t_{z11-2}} & \cdots & \mathrm{t_{z11-T_{C_x}}} \\ \mathrm{t_{z21-1}} & \mathrm{t_{z21-2}} & \cdots & \mathrm{t_{z21-T_{C_x}}} \\ \mathrm{t_{z31-1}} & \mathrm{t_{z31-2}} & \cdots & \mathrm{t_{z31-T_{C_x}}} \\ \vdots & \vdots & \ddots & \vdots \\ \mathrm{t_{z1T_{dr}-1}} & \mathrm{t_{z1T_{dr}-2}} & \cdots & \mathrm{t_{z1T_{dr}-T_{C_x}}} \\ \mathrm{t_{z2T_{dr}-1}} & \mathrm{t_{z2T_{dr}-2}} & \cdots & \mathrm{t_{z2T_{dr}-T_{C_x}}} \\ \mathrm{t_{z3T_{dr}-1}} & \mathrm{t_{z3T_{dr}-2}} & \cdots & \mathrm{t_{z3T_{dr}-T_{C_x}}} \end{pmatrix}. \tag{3.16}$$

A distance-relay is located to replace the operation of OCRs that does not pass the sensitivity filter described by Equation 2.3. As described, there may be some scenarios where an OCR is insensitive for a specific coordination pair and sensitive for others; consequently the OCR is not completely removed, but its coordination requirements with the appointed coordination pair are discarded. The implemented penalization function for distance and overcurrent relay coordination is presented in Equation 3.17:

$$d_k = \sum_{l=1}^{\mathrm{q}} \frac{g_l^p(\mathbf{y}_l)}{\mathrm{l}} + \sum_{l=1}^{\mathrm{q}} \frac{de_l(\mathbf{x}_l,\mathbf{y}_l,\mathbf{Z}_l)}{\mathrm{l}}, \tag{3.17}$$

where q is the total coordination pairs that the current distance-relay conforms with overcurrent relays, g is the tripping time of backup OCR, and de is the coordination error when distance and OCR are considered. As represented in Figure 2.11, after a distance-relay is placed it might has to operate as backup of — and also be backed up by — OCRs; each of both cases present up to three critical points to be coordinated, a distance-relay may be part of as many coordination pairs as adjacent lines are next to its location.

The tripping times of main and backup OCRs and the coordination errors between overcurrent and distance-relays on each one of the critical points are computed. $\mathrm{CTI_d}$ is the coordination time interval when distance-relays are involved, in this work that magnitude is considered as 0.2 seconds. The coordination error between a main OCR and a backup distance-relay (de_b) is computed using Equation 3.18 while Equation 3.19 is used for the opposite case (de_m):

$$de_b = \mathbf{Z} - f(\mathbf{x}) - \mathrm{CTI_d}, \tag{3.18}$$

$$de_m = g(\mathbf{y}) - \mathbf{Z} - \mathrm{CTI_d}. \tag{3.19}$$

The total coordination error of distance and overcurrent relays (de) is conformed by the penalized versions of de_b and de_m. Negative errors are severely penalized while positive ones remain unaltered, $de_l \geq 0 \iff g_l^p = g_l \wedge de_l^p = de_l; de_l < 0 \iff$

$$g_l^p = e^{g_l} \times \epsilon, \tag{3.20}$$

$$de_l^p = e^{|de_l|} \times \epsilon. \tag{3.21}$$

There may be some scenarios where distance-relays are located in adjacent lines, the following restrictions have to be fulfilled: $\mathrm{t_{z3}} \geq \mathrm{t_{z2}} + \mathrm{CTI_d} \wedge \mathrm{t_{z2}} \geq \mathrm{t_{z1}} + \mathrm{CTI_d}$; since this restriction is considered mandatory, no penalization factor is used but distance-relays that do not meet it are discarded.

CHAPTER 4

EXPERIMENTS AND RESULTS

The coordination problem formulation is solved through the implementation of meta-heuristic methods. Genetic algorithms and invasive-weed optimization methods are used in this thesis; in addition, a sequential quadratic programming method is implemented aiming to improve the convergence process. In this chapter the experimental results obtained by the implemented routines are presented.

The first section contains present the preliminary simulations, whose results are used as input by the optimization algorithms. The next section introduce the results of the conducted experiments; those simulations were carried out with the objective of defining adequate tuning parameters for the optimization algorithms. The following sections compare the results of the proposed implementation with a base case that considers two parameters as adjustable settings.

The robustness of the proposed methodology is tested by solving the coordination problem for different power systems. The overcurrent relay coordination is obtained for five test systems of 9, 14, 30, 57, and 118 buses in this thesis. The complete bus and line data for each tested power system can be accessed from the indicated references [81, 93]. The network configuration of the 14 and 30-bus systems is shown in Figures 4.1 and 4.2.

As stated in the previous chapters, initial calculations have to be performed and given as an input to the optimization methods. A flow analysis is carried out to obtain the load current, thereupon through a fault analysis the short-circuit currents caused by two

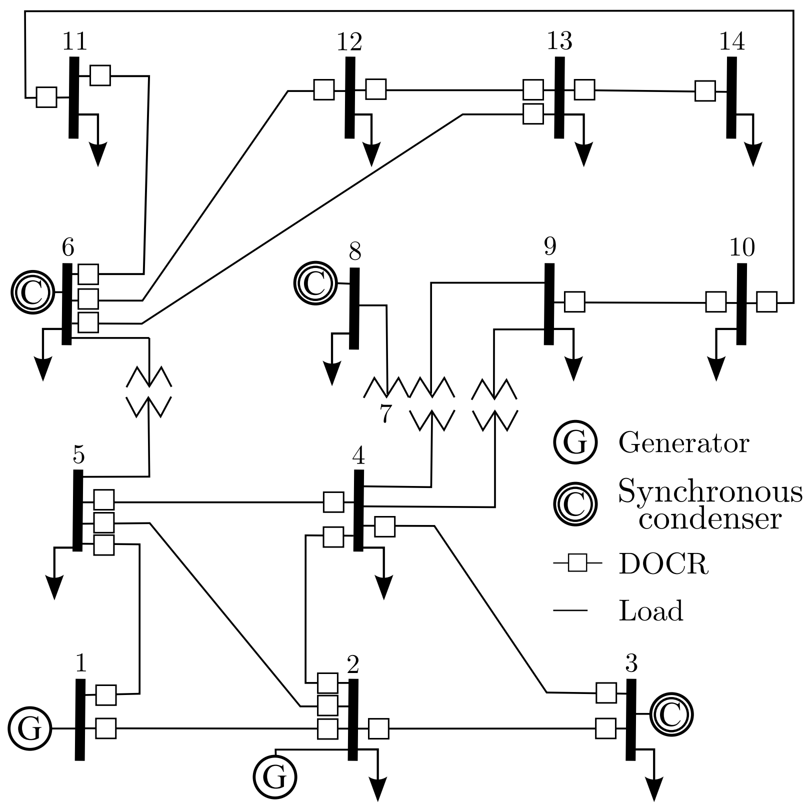

Figure 4.1: IEEE 14 Bus system one line diagram.

and three-phase faults located in the close-end, far-end [171], and intermediate [172, 173] locations — with an open end — are obtained. Both algorithms are implemented from scratch so they can be conveniently modified to analyze different system conditions.

As an example, the results obtained from the fault and flow analysis for the 14-bus system are presented in Tables 4.1 and 4.2. Table 4.1 shows the relays identification in the first column, this tag is conformed by the bus of origin and the destination one, thereby a relay located at bus 12 with the directional unit facing node 6 is identified as relay 12·6. The following columns display three levels of short circuit, contemplated as coordination current; in this work short-circuit currents caused by grounded faults are not considered in order to avoid a ground impedance guess; consequently bolted two and three-phase faults are employed. A maximum fault (I_{sc}^{M}) is contemplated as a three-phase fault located at the close-end of the line, a minimum fault (I_{sc}^{m}) is a two-phase fault located at the far-end of the line, and an intermediate level (I_{sc}^{in}) is the mean value of the previously mentioned

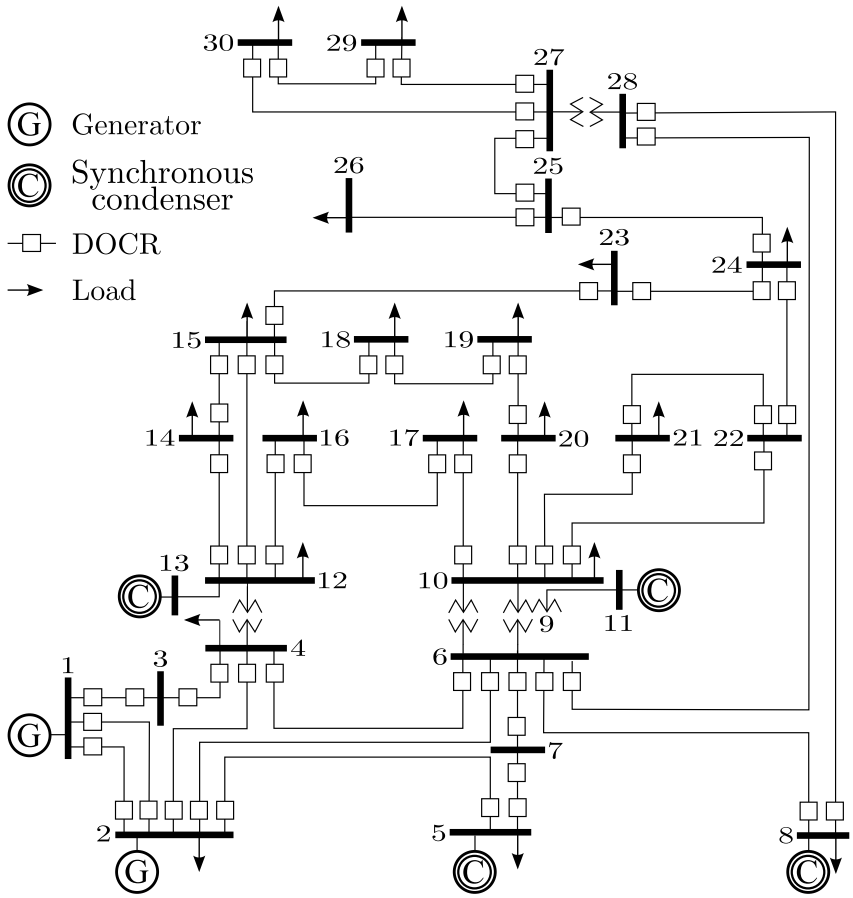

Figure 4.2: IEEE 30 Bus system one line diagram.

faults. Initial experiments led us to conclude that the use of three current magnitudes is enough to maintain an adequate inversion grade and guarantee the coordination for a curve region, avoiding computation time exponential increase.

The objective of considering a third magnitude is to prevent undesirable curve shapes between the two fault points caused by the use of five parameters as adjustable settings. Results that support this consideration will be presented in the following sections. The two following columns present the short-circuit magnitude of a three-phase fault located at the middle and at the 80% of the line; these faults positions are used to coordinate the first and second distance-relay zones. Lastly, the I_{load} seen by each relay is presented in the seventh column.

Moreover, Table 4.2 shows the short-circuit current magnitudes seen by backup re-

Table 4.1: IEEE 14-bus power system line loads and fault magnitudes seen by main relays.

Relay ID	I_{sc}^{m}	I_{sc}^{in}	I_{sc}^{M}	I_{sc}^{50}	I_{sc}^{80}	I_{load}
1·2	26007.569	39011.353	52015.138	46100.259	26147.841	776.174
2·1	26444.397	61272.328	96100.259	65728.246	44475.525	776.174
1·5	26277.266	39415.899	52554.532	11007.236	2722.286	370.343
5·1	2736.032	6871.634	11007.236	8137.377	5472.063	370.343
2·3	30273.780	45410.670	60547.560	4055.731	1042.450	359.025
3·2	1059.178	2557.455	4055.731	2993.495	2079.318	359.025
2·4	30220.038	45330.057	60440.076	8558.410	2346.393	275.616
4·2	2438.187	5498.298	8558.410	6194.338	4338.090	275.616
2·5	30147.926	45221.889	60295.852	9190.049	2517.758	204.407
5·2	2625.399	5907.724	9190.049	6594.868	4600.644	204.407
3·4	1263.774	2365.627	3467.481	2527.547	1386.148	115.902
4·3	3015.215	4522.822	6030.429	3467.481	1042.209	115.902
4·5	2229.999	3344.998	4459.998	4374.545	1677.872	306.289
5·4	2679.948	4019.922	5359.897	4374.545	1575.168	306.289
6·11	1043.612	1565.418	2087.224	1170.968	405.153	41.892
11·6	503.529	837.249	1170.968	1007.058	517.168	41.892
6·12	1201.050	1801.574	2402.099	986.418	386.821	40.291
12·6	457.217	721.817	986.418	914.434	532.327	40.291
6·13	1166.133	1749.199	2332.266	1148.625	466.472	94.671
13·6	581.747	872.620	1163.493	1148.625	593.113	94.671
9·10	1126.891	1690.336	2253.781	1042.078	341.577	30.624
10·9	402.119	722.099	1042.078	804.239	471.916	30.624
9·14	1189.273	1783.910	2378.546	994.479	322.850	48.276
14·9	373.165	683.822	994.479	746.329	466.991	48.276
10·11	823.258	1234.887	1646.516	1143.684	417.605	21.937
11·10	558.081	850.882	1143.684	1116.161	472.549	21.937
12·13	524.797	787.195	1049.593	954.148	472.524	9.026
13·12	862.675	1294.012	1725.350	1050.721	383.444	9.026
13·14	754.023	1131.034	1508.046	1050.721	383.444	29.983
14·13	516.658	783.689	1050.721	1033.316	439.059	29.983

lays. The first and second columns allude the main and backup relays that conform a coordination pair while the following columns enlist the current seen by the backup after a minimum, intermediate, and maximum fault occurrence.

Lastly, the sixth and seventh columns show the short-circuit level seen by the backups considering a three-phase fault located in the middle and at 80% of the main line. Similar data is obtained for each one of the test systems, nevertheless that information is not illustrated in this document.

Table 4.2: IEEE 14-bus power system faults magnitudes seen by the backup relays.

Main	Backup	I_{sc}^{m}	I_{sc}^{in}	I_{sc}^{M}	I_{sc}^{50}	I_{sc}^{80}
1·2	5·1	963.745	1285.274	1606.804	1584.603	1543.236
2·1	3·2	1863.462	2058.167	2252.871	1918.684	1741.352
2·1	4·2	1960.285	2217.899	2475.514	2126.375	1935.761
2·1	5·2	2002.632	2251.857	2501.083	2165.971	1979.492
1·5	2·1	1461.318	4217.126	6972.935	3861.454	2569.620
5·1	2·5	915.267	1383.643	1852.019	1823.087	1780.008
5·1	4·5	1252.608	2436.588	3620.568	3473.633	1956.695
2·3	1·2	854.660	4045.298	7235.935	2610.213	1389.624
2·3	4·2	1012.024	1049.124	1086.224	855.128	796.874
2·3	5·2	903.381	1045.404	1187.427	922.054	851.970
3·2	4·3	1003.620	1091.651	1179.681	1131.867	1090.469
2·4	1·2	741.773	3988.767	7235.762	3821.354	2470.492
2·4	3·2	1008.136	1069.798	1131.460	967.233	878.793
2·4	5·2	1082.336	1170.883	1259.429	1045.983	919.334
4·2	3·4	636.808	1082.805	1528.802	1416.347	1199.001
4·2	5·4	838.997	1898.995	2958.993	2938.613	1902.474
2·5	1·2	1667.953	4451.785	7235.617	3926.226	2579.230
2·5	3·2	970.057	1109.543	1249.029	1077.861	985.151
2·5	4·2	1070.789	1224.015	1377.241	960.844	913.946
5·2	1·5	678.229	1136.421	1594.613	1521.932	1519.673
5·2	4·5	844.482	1940.160	3035.837	3013.785	1868.530
3·4	2·3	929.379	1091.828	1254.278	1245.081	1056.375
4·3	2·4	884.680	1331.963	1779.245	1325.712	962.366
4·3	5·4	777.839	1395.295	2012.752	1326.611	1130.388
4·5	2·4	1371.712	1493.560	1615.407	1440.413	1205.588
4·5	3·4	1116.421	1222.669	1328.916	1082.419	984.009
5·4	1·5	1337.088	1469.538	1601.987	1307.273	1089.315
5·4	2·5	950.336	1355.606	1760.876	1454.445	1177.038
6·11	12·6	351.180	397.093	443.006	378.401	307.566
6·11	13·6	285.946	416.244	546.542	430.382	332.832
11·6	10·11	324.620	386.869	449.118	436.784	384.702
6·12	11·6	289.486	382.604	475.722	366.932	294.059
6·12	13·6	301.282	356.715	412.148	337.290	272.606
12·6	13·12	255.426	305.030	354.633	347.017	325.699
6·13	11·6	276.994	383.946	490.898	408.444	337.647
6·13	12·6	313.704	320.680	327.655	309.858	271.656
13·6	12·13	324.278	346.270	368.262	347.711	330.717
13·6	14·13	257.591	308.146	358.701	339.420	338.017
9·10	14·9	345.400	386.852	428.304	324.703	255.323
10·9	11·10	277.838	348.181	418.525	367.204	355.268
9·14	10·9	304.497	452.682	600.867	394.800	288.059
14·9	13·14	249.346	300.902	352.457	343.368	315.015
10·11	9·10	325.348	476.241	627.134	477.437	367.404
11·10	6·11	247.838	371.428	495.018	448.812	370.818
12·13	6·12	323.019	361.017	399.014	388.514	361.646
13·12	6·13	290.277	386.583	482.890	431.886	381.981
13·12	14·13	311.048	338.338	365.628	314.595	268.393
13·14	6·13	255.256	406.670	558.084	431.835	373.730
13·14	12·13	295.784	355.856	415.928	368.264	301.566
14·13	9·14	261.265	353.489	445.713	387.745	386.620

4.1 Conducted Experiments

One of the advantages of metaheuristic methods is their capacity of being adapted to solve several different problems, the parameters involved in the solution process must be previously tuned in order to improve algorithm performance and achieve better results. The parameters to tune in the coordination process include the total iterations, population size, parameter selection range, weighting factors of the objective function as well as those for the different levels of short-circuit current, the probability of occurrence of each genetic or weed operator, and the iteration number where the SQP is applied.

Initial experiments testing different configurations of each one of the mentioned parameters were conducted considering the 9, 14, 30, 57, and 118-bus systems [81, 93], however after initial simulations the first system did not present notorious variations before parameters modifications and consequently it was discarded for this stage; furthermore since several parameters combinations are tested and the experiments are repeated, the 57 and 118-bus systems are also discarded because of their high simulation time.

The tuning process is consequently carried out considering the 14 and 30-bus systems while the 9, 57, and 118-bus systems are included in the final simulations. Most of the results shown on this section belong to the 14-bus system simulations, nevertheless a comparison between the results of both systems is used to select one of the cases as base case in further experiments.

The first set of experiments aim to test A, B, and p parameters selection ranges; the experiment consists in allowing the algorithm to select any intermediate magnitude of each parameter for each relay. The boundaries of the first set of ranges are defined considering the minimum and maximum values of the three IEEE standardized inverse-time curves presented in Table 2.1. The following ranges are obtained by combining diverse boundaries that extent or reduce the base selection range. A total of 85 cases illustrated in Table 4.3 are tested.

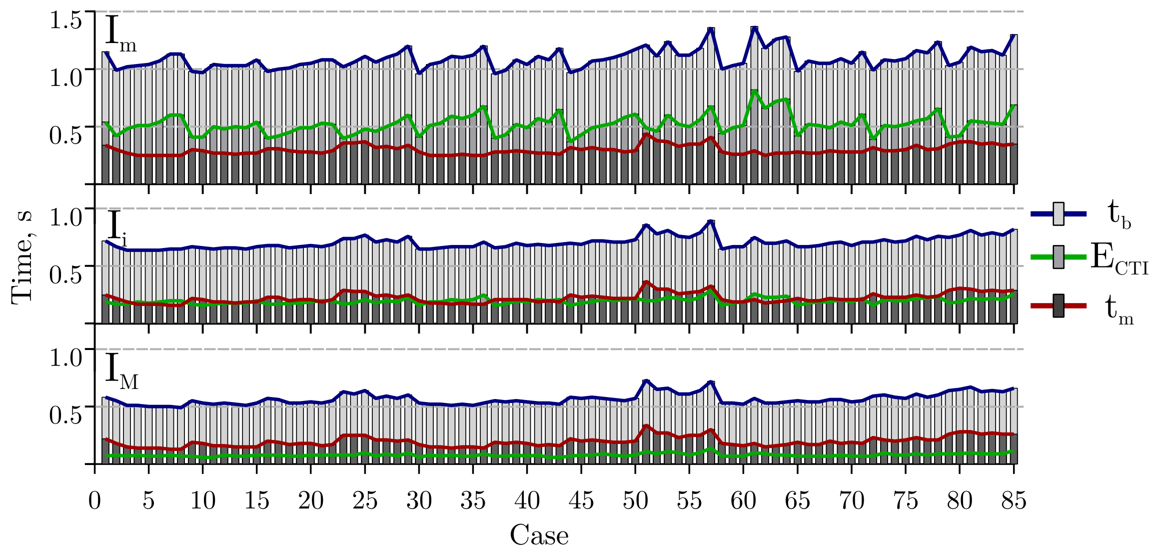

(a) Tripping times and coordination errors.

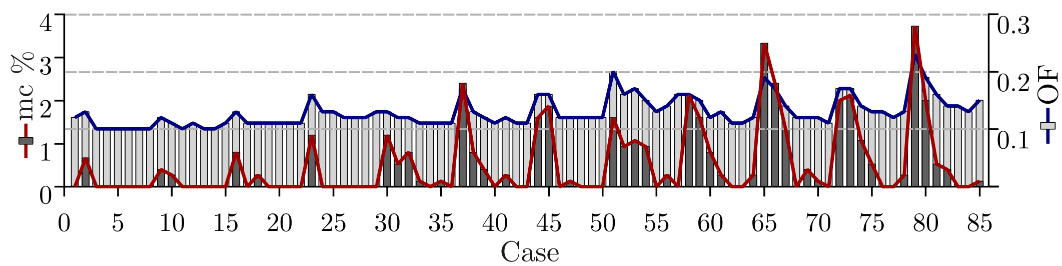

(b) Miscoordination percentage and fitness.

Figure 4.3: Testing parameters selection ranges.

The significant results obtained by these experiments considering the 14-bus system are illustrated in Figures 4.3(a) and 4.3(b). The first figure shows the mean tripping time of the main t_m and backup t_b relays as well as the coordination error E_{CTI} for minimum, intermediate, and maximum short-circuit levels. Moreover, Figure 4.3(b) depicts the miscoordination percentage and the fitness obtained by each case. The results of the following experiments will be presented in a similar way.

Observation of the first experimental results allow us to note that the algorithm is obtaining adequate parameters to define the relay operation; the tripping times decrease as the short-circuit levels increase, maintaining the relays inverse characteristic. The results are worsen as the boundaries are extended, this is an expected result since the boundaries expansion enlarge the solution space size and consequently the problem complexity. Better results are obtained by those cases when B and p parameters are restricted to small magnitudes; cases three to eight obtained practically identical results.

Similar outcome is obtained by the experiment conducted considering the 30-bus power system — not shown —, where the best results are obtained by the cases four to seven. From now on case number five of the first set of experiments will be used as base case, it is important to remark the similarity of this case with the number one, the parameters boundaries are just slightly extended while parameter B is allowed to select magnitudes equal to zero.

The objective of the second experiment is to test the objective function weighting constants α, β, and γ. On each case the sum of the constants is equal to one, the increments are equal to $\frac{1}{20}$, and no constant is allowed to take a magnitude equal to zero. Initial simulations demonstrated the importance of α and β, consequently these constants are prevented to take values lesser than 0.25. Table 4.4 presents the 51 cases tested in this analysis.

The set of Figures 4.4 illustrate the results obtained by the second experiment. Better tripping times are obtained as α is weighted heavily; this experiment enlightens that the main relay tripping time reduction causes the backup to have a better chance to adapt its operation time in order to fulfill the coordination requirements, preventing penalizations and consequently improving individual fitness. Since it obtained the best results for both analyzed systems, case 48 will be used as base case.

The next variables to test are the total iterations and the population size. The total iterations are varied from 300 to 1500 while the population size takes values from 50 to 500. A total of thirty cases are analyzed in this experiment and the results can be observed in Figure 4.5. Neglecting slight variations it can be said that increasing both variables leads to better algorithmic performance, a well defined slope in the tripping times can be seen in Figure 4.5(a). All cases eradicate the total of miscoordinations for the 14-bus system while the objective function results present minor variations.

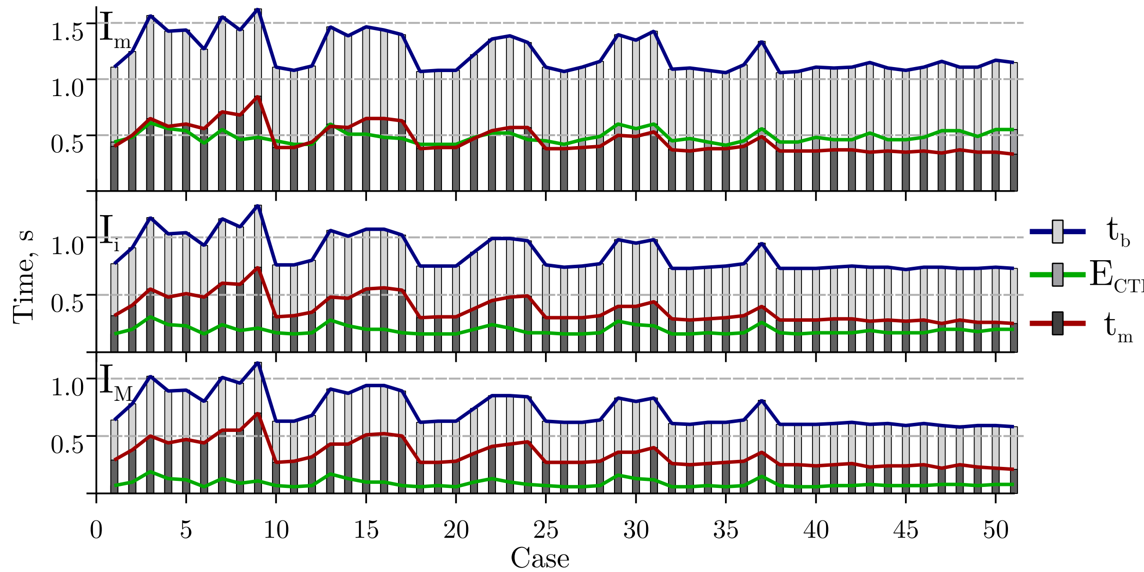

(a) Tripping times and coordination errors.

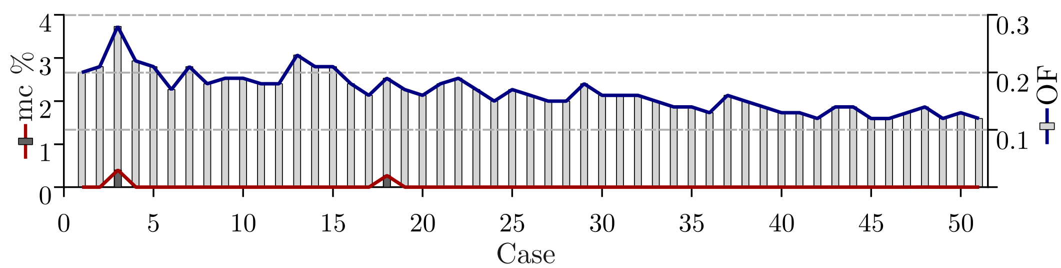

(b) Miscoordination percentage and fitness.

Figure 4.4: Testing objective function weighting factors.

The decision factor in this experiment is given by Figure 4.5(b), where the simulation time of each scenario for the 14 and 30-bus systems is shown; it can be appreciated that the increase of both variables is directly proportional to the simulation time. Since the objective of this thesis is not online coordination, this proposal is not time-aware; nevertheless given that each case is simulated at least five times and several cases are analyzed, a solution that obtains good results in a reasonable amount of time is considered as better.

The simulation time of case 30 is more than ten times greater than in case 14, obtaining a fitness reduction of almost 0.01 reflected in operation time reductions in the order of one to five cycles — considering a 60 Hertz frequency —. This tripping time reduction is great and useful for the protection system, nevertheless the simulation time increase is not justified for this stage. As a result of this analysis, 700 iterations and a population size of 100 elements, i.e. case 14, is going to be considered as base case.

The following experiment consists of testing ι, κ, and τ constants. The sum of the three of them must be equal to one, no constant can be set to zero, and the increase between samples is set to $\frac{1}{20}$. Since the protection system must guarantee correct operations for maximum faults, τ is set to be greater than the other constants in all cases. A total of 52 scenarios are analyzed, the settings for each case are shown in Table 4.6.

The experimental results are illustrated in Figure 4.6. As can be noted in Figure 4.6(a) the tripping time for a maximum short circuit present minor variations while those changes are accentuated for lower currents. Figure 4.6(b) demonstrates that the first cases obtain better OF results, this behaviour is presented because they are practically neglecting the impact of coordination for currents lower than the maximum. By reducing the importance of low currents, minor improvements are obtained for maximum magnitudes, nevertheless one of the objectives of this thesis consists in upgrading the relay performance for currents different than the maximum — which are more common —; in consequence, for this set of experiments the fitness obtained by the objective function evaluation is not a complete indicator of better solutions. Case 35 achieve intermediate results, reducing tripping times for minimum and intermediate I_{sc} and maintaining good results for maximum currents, therefore it will be selected as base case in the following experiments.

Metaheuristics improve the population fitness through the implementation of genetic or mutation operators; the spreading, dispersing, and rolling-down operators are used by the invasive-weed optimization method. The next experiment seeks to test operator's probability of occurrence. Initial simulation demonstrated that the rolling-down operator influences the most in the final results, consequently it is set to be always greater than the remaining two and it is not allowed to take values under 0.5. The sum of the three probabilities is equal to one on each case. A total of 52 listed in Table 4.7 are tested and results are illustrated in Figure 4.7.

The increase in the rolling-down operator probability of occurrence presents improvements to the coordination problem. Since this operator combines the other two and ensures a slope change in the algorithm convergence, this result is expected. The counterpart is that the simulation time increase caused by the operator complexity. One of the best fitness and tripping time results for both systems is obtained by case 32, obtaining also an intermediate simulation time, therefore this case is used as base case.

On previous chapters the complexity of the coordination problem was described; the combinatorial explosion makes difficult or almost impossible to find a solution using only exact methods. One of the contributions of this thesis is the implementation of a hybrid algorithm capable to combine a metaheuristic method with a nonlinear programming algorithm.

The last experiment of this section is testing the sequential quadratic programming frequency of occurrence. The considerations of these experiments are that SQP can be run from one to three times in a simulation. The nonlinear method use as initial variables the settings of one and up to five randomly selected individuals at the determined iteration. The iteration occurrence of the 43 analyzed cases is presented in Table 4.8, while the results are illustrated in Figure 4.8. The first iterations give fitness results in the order of millions, since SQP is sensitive to initial guesses, its convergence is not achieved for bad candidates; consequently, after initial simulations the first SQP occurrence is set to iteration number eight.

The SQP implementation present minor improvements in the coordination results; nevertheless the simulation time is not harshly affected by its presence. In consequence, some of these cases will be used to compare results in the following section.

Similar tuning processes are carried out for the genetic algorithm implementation and for the algorithm that coordinates overcurrent and distance-relays. For the sake of simplicity, the experiments results are not illustrated on this document.

Table 4.3: Tested cases varying sets of parameters selection ranges.

Case	A		B		p		Case	A		B		p	
1	0.0515	28.2	0.114	0.491	0.02	2	44	0.01	5	0	2	0.01	5
2	0.01	5	0	0.5	0.01	2	45	0.01	10	0	2	0.01	5
3	0.01	10	0	0.5	0.01	2	46	0.01	20	0	2	0.01	5
4	0.01	20	0	0.5	0.01	2	47	0.01	30	0	2	0.01	5
5	0.01	30	0	0.5	0.01	2	48	0.01	40	0	2	0.01	5
6	0.01	40	0	0.5	0.01	2	49	0.01	50	0	2	0.01	5
7	0.01	50	0	0.5	0.01	2	50	0.01	100	0	2	0.01	5
8	0.01	100	0	0.5	0.01	2	51	0.01	5	0	5	0.01	5
9	0.01	5	0	1	0.01	2	52	0.01	10	0	5	0.01	5
10	0.01	10	0	1	0.01	2	53	0.01	20	0	5	0.01	5
11	0.01	20	0	1	0.01	2	54	0.01	30	0	5	0.01	5
12	0.01	30	0	1	0.01	2	55	0.01	40	0	5	0.01	5
13	0.01	40	0	1	0.01	2	56	0.01	50	0	5	0.01	5
14	0.01	50	0	1	0.01	2	57	0.01	100	0	5	0.01	5
15	0.01	100	0	1	0.01	2	58	0.01	5	0	0.5	0.01	10
16	0.01	5	0	2	0.01	2	59	0.01	10	0	0.5	0.01	10
17	0.01	10	0	2	0.01	2	60	0.01	20	0	0.5	0.01	10
18	0.01	20	0	2	0.01	2	61	0.01	30	0	0.5	0.01	10
19	0.01	30	0	2	0.01	2	62	0.01	40	0	0.5	0.01	10
20	0.01	40	0	2	0.01	2	63	0.01	50	0	0.5	0.01	10
21	0.01	50	0	2	0.01	2	64	0.01	100	0	0.5	0.01	10
22	0.01	100	0	2	0.01	2	65	0.01	5	0	1	0.01	10
23	0.01	5	0	5	0.01	2	66	0.01	10	0	1	0.01	10
24	0.01	10	0	5	0.01	2	67	0.01	20	0	1	0.01	10
25	0.01	20	0	5	0.01	2	68	0.01	30	0	1	0.01	10
26	0.01	30	0	5	0.01	2	69	0.01	40	0	1	0.01	10
27	0.01	40	0	5	0.01	2	70	0.01	50	0	1	0.01	10
28	0.01	50	0	5	0.01	2	71	0.01	100	0	1	0.01	10
29	0.01	100	0	5	0.01	2	72	0.01	5	0	2	0.01	10
30	0.01	5	0	0.5	0.01	5	73	0.01	10	0	2	0.01	10
31	0.01	10	0	0.5	0.01	5	74	0.01	20	0	2	0.01	10
32	0.01	20	0	0.5	0.01	5	75	0.01	30	0	2	0.01	10
33	0.01	30	0	0.5	0.01	5	76	0.01	40	0	2	0.01	10
34	0.01	40	0	0.5	0.01	5	77	0.01	50	0	2	0.01	10
35	0.01	50	0	0.5	0.01	5	78	0.01	100	0	2	0.01	10
36	0.01	100	0	0.5	0.01	5	79	0.01	5	0	5	0.01	10
37	0.01	5	0	1	0.01	5	80	0.01	10	0	5	0.01	10
38	0.01	10	0	1	0.01	5	81	0.01	20	0	5	0.01	10
39	0.01	20	0	1	0.01	5	82	0.01	30	0	5	0.01	10
40	0.01	30	0	1	0.01	5	83	0.01	40	0	5	0.01	10
41	0.01	40	0	1	0.01	5	84	0.01	50	0	5	0.01	10
42	0.01	50	0	1	0.01	5	85	0.01	100	0	5	0.01	10
43	0.01	100	0	1	0.01	5							

Table 4.4: Tested cases varying objective-function weighting parameters.

Case	α	β	γ	Case	α	β	γ	Case	α	β	γ	Case	α	β	γ
1	0.25	0.7	0.05	14	0.3	0.45	0.25	27	0.4	0.45	0.15	40	0.5	0.35	0.15
2	0.25	0.6	0.15	15	0.3	0.4	0.3	28	0.4	0.4	0.2	41	0.5	0.3	0.2
3	0.25	0.55	0.2	16	0.3	0.3	0.4	29	0.4	0.35	0.25	42	0.5	0.25	0.25
4	0.25	0.5	0.25	17	0.3	0.25	0.45	30	0.4	0.3	0.3	43	0.55	0.4	0.05
5	0.25	0.45	0.3	18	0.35	0.6	0.05	31	0.4	0.25	0.35	44	0.55	0.35	0.1
6	0.25	0.4	0.35	19	0.35	0.55	0.1	32	0.45	0.5	0.05	45	0.55	0.3	0.15
7	0.25	0.35	0.4	20	0.35	0.5	0.15	33	0.45	0.45	0.1	46	0.55	0.25	0.2
8	0.25	0.3	0.45	21	0.35	0.45	0.2	34	0.45	0.4	0.15	47	0.6	0.35	0.05
9	0.25	0.25	0.5	22	0.35	0.4	0.25	35	0.45	0.35	0.2	48	0.6	0.3	0.1
10	0.3	0.65	0.05	23	0.35	0.3	0.35	36	0.45	0.3	0.25	49	0.6	0.25	0.15
11	0.3	0.6	0.1	24	0.35	0.25	0.4	37	0.45	0.25	0.3	50	0.65	0.3	0.05
12	0.3	0.55	0.15	25	0.4	0.55	0.05	38	0.5	0.45	0.05	51	0.7	0.25	0.05
13	0.3	0.5	0.2	26	0.4	0.5	0.1	39	0.5	0.4	0.1				

Table 4.5: Tested cases varying total iterations and population size.

Case	$\mathrm{T_i}$	$\mathrm{P_s}$	Case	$\mathrm{T_i}$	$\mathrm{P_s}$	Case	$\mathrm{T_i}$	$\mathrm{P_s}$	Case	$\mathrm{T_i}$	$\mathrm{P_s}$	Case	$\mathrm{T_i}$	$\mathrm{P_s}$
1	300	50	7	500	50	13	700	50	19	1000	50	25	1500	50
2	300	100	8	500	100	14	700	100	20	1000	100	26	1500	100
3	300	200	9	500	200	15	700	200	21	1000	200	27	1500	200
4	300	300	10	500	300	16	700	300	22	1000	300	28	1500	300
5	300	400	11	500	400	17	700	400	23	1000	400	29	1500	400
6	300	500	12	500	500	18	700	500	24	1000	500	30	1500	500

Table 4.6: Tested cases varying short-circuit levels weighting factors.

Case	ι	κ	τ	Case	ι	κ	τ	Case	ι	κ	τ	Case	ι	κ	τ
1	0.05	0.05	0.9	14	0.1	0.3	0.6	27	0.2	0.15	0.65	40	0.3	0.15	0.55
2	0.05	0.1	0.85	15	0.1	0.35	0.55	28	0.2	0.2	0.6	41	0.3	0.2	0.5
3	0.05	0.15	0.8	16	0.1	0.4	0.5	29	0.2	0.25	0.55	42	0.3	0.25	0.45
4	0.05	0.2	0.75	17	0.15	0.05	0.8	30	0.2	0.3	0.5	43	0.3	0.3	0.4
5	0.05	0.25	0.7	18	0.15	0.1	0.75	31	0.2	0.35	0.45	44	0.35	0.05	0.6
6	0.05	0.3	0.65	19	0.15	0.15	0.7	32	0.25	0.05	0.7	45	0.35	0.1	0.55
7	0.05	0.35	0.6	20	0.15	0.2	0.65	33	0.25	0.15	0.6	46	0.35	0.15	0.5
8	0.05	0.4	0.55	21	0.15	0.25	0.6	34	0.25	0.2	0.55	47	0.35	0.2	0.45
9	0.05	0.45	0.5	22	0.15	0.3	0.55	35	0.25	0.25	0.5	48	0.35	0.25	0.4
10	0.1	0.05	0.85	23	0.15	0.35	0.5	36	0.25	0.3	0.45	49	0.4	0.05	0.55
11	0.1	0.1	0.8	24	0.15	0.4	0.45	37	0.25	0.35	0.4	50	0.4	0.1	0.5
12	0.1	0.15	0.75	25	0.2	0.05	0.75	38	0.3	0.05	0.65	51	0.4	0.15	0.45
13	0.1	0.2	0.7	26	0.2	0.1	0.7	39	0.3	0.1	0.6	52	0.45	0.05	0.5

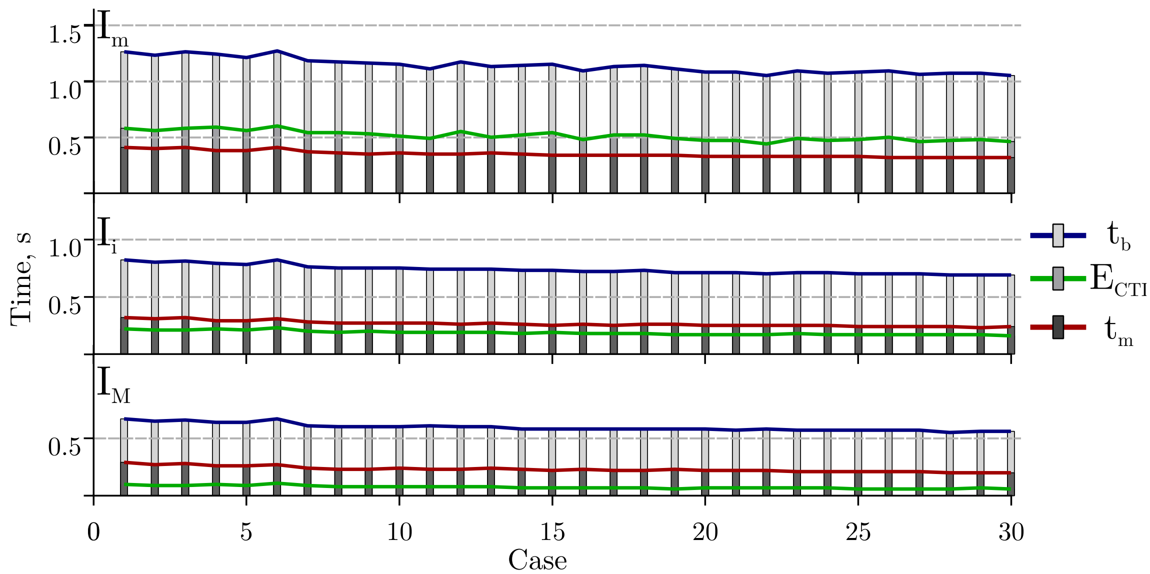

(a) Tripping times and coordination errors.

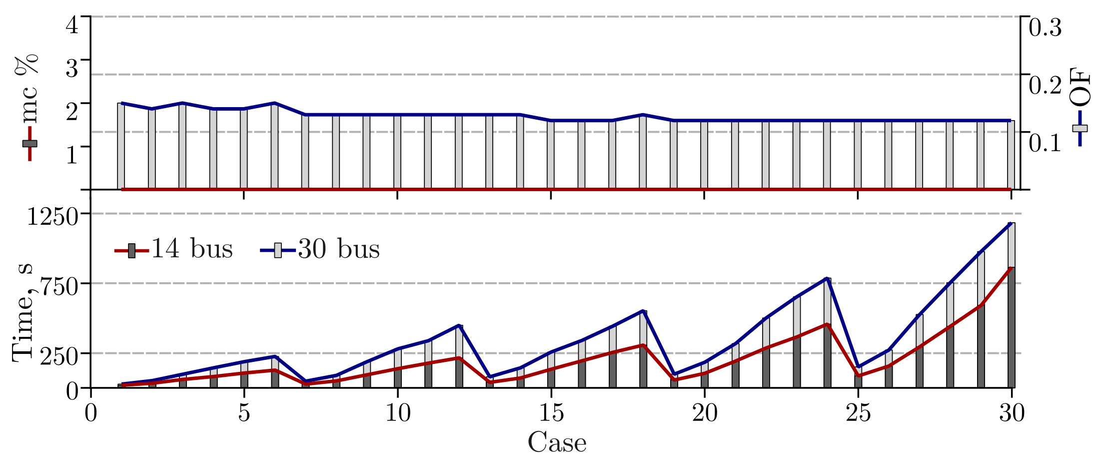

(b) Miscoordination percentage, fitness, and simulation time.

Figure 4.5: Testing total iterations and population size.

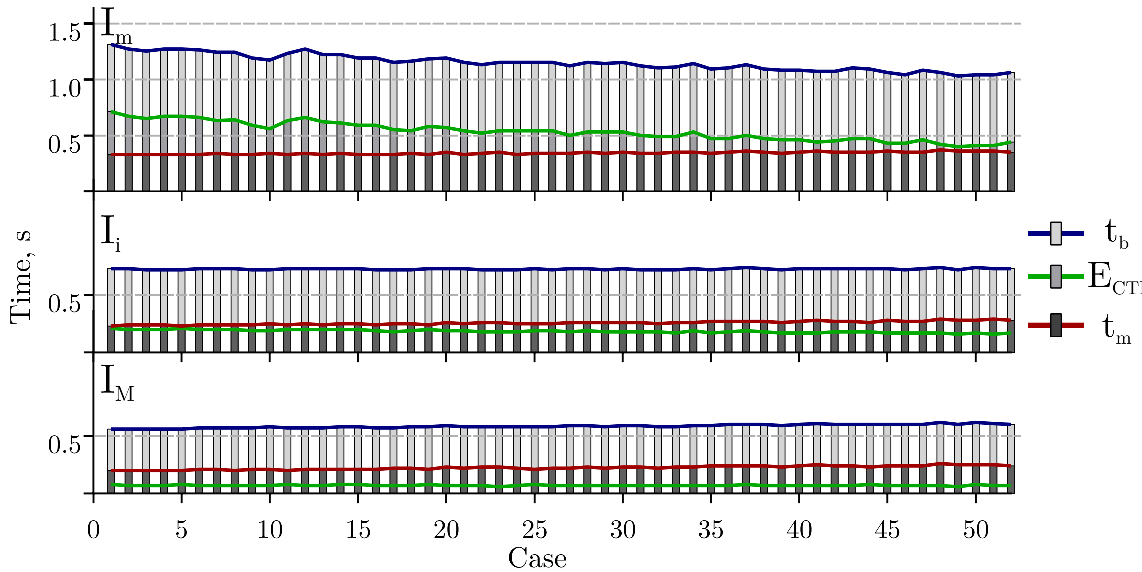

(a) Tripping times and coordination errors.

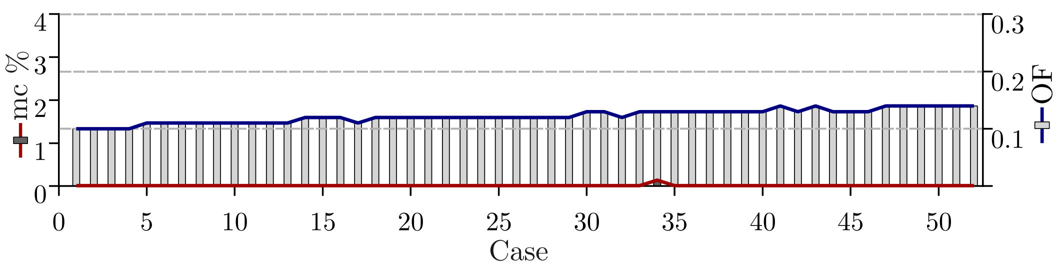

(b) Miscoordination percentage and fitness.

Figure 4.6: Testing short-circuit levels weighting factors.

Table 4.7: Probability of occurrence of tested operators.

Case	P(S)	P(D)	P(R)	Case	P(S)	P(D)	P(R)	Case	P(S)	P(D)	P(R)	Case	P(S)	P(D)	P(R)
1	0.05	0.05	0.9	14	0.1	0.3	0.6	27	0.2	0.15	0.65	40	0.3	0.15	0.55
2	0.05	0.1	0.85	15	0.1	0.35	0.55	28	0.2	0.2	0.6	41	0.3	0.2	0.5
3	0.05	0.15	0.8	16	0.1	0.4	0.5	29	0.2	0.25	0.55	42	0.3	0.25	0.45
4	0.05	0.2	0.75	17	0.15	0.05	0.8	30	0.2	0.3	0.5	43	0.3	0.3	0.4
5	0.05	0.25	0.7	18	0.15	0.1	0.75	31	0.2	0.35	0.45	44	0.35	0.05	0.6
6	0.05	0.3	0.65	19	0.15	0.15	0.7	32	0.25	0.05	0.7	45	0.35	0.1	0.55
7	0.05	0.35	0.6	20	0.15	0.2	0.65	33	0.25	0.15	0.6	46	0.35	0.15	0.5
8	0.05	0.4	0.55	21	0.15	0.25	0.6	34	0.25	0.2	0.55	47	0.35	0.2	0.45
9	0.05	0.45	0.5	22	0.15	0.3	0.55	35	0.25	0.25	0.5	48	0.35	0.25	0.4
10	0.1	0.05	0.85	23	0.15	0.35	0.5	36	0.25	0.3	0.45	49	0.4	0.05	0.55
11	0.1	0.1	0.8	24	0.15	0.4	0.45	37	0.25	0.35	0.4	50	0.4	0.1	0.5
12	0.1	0.15	0.75	25	0.2	0.05	0.75	38	0.3	0.05	0.65	51	0.4	0.15	0.45
13	0.1	0.2	0.7	26	0.2	0.1	0.7	39	0.3	0.1	0.6	52	0.45	0.05	0.5

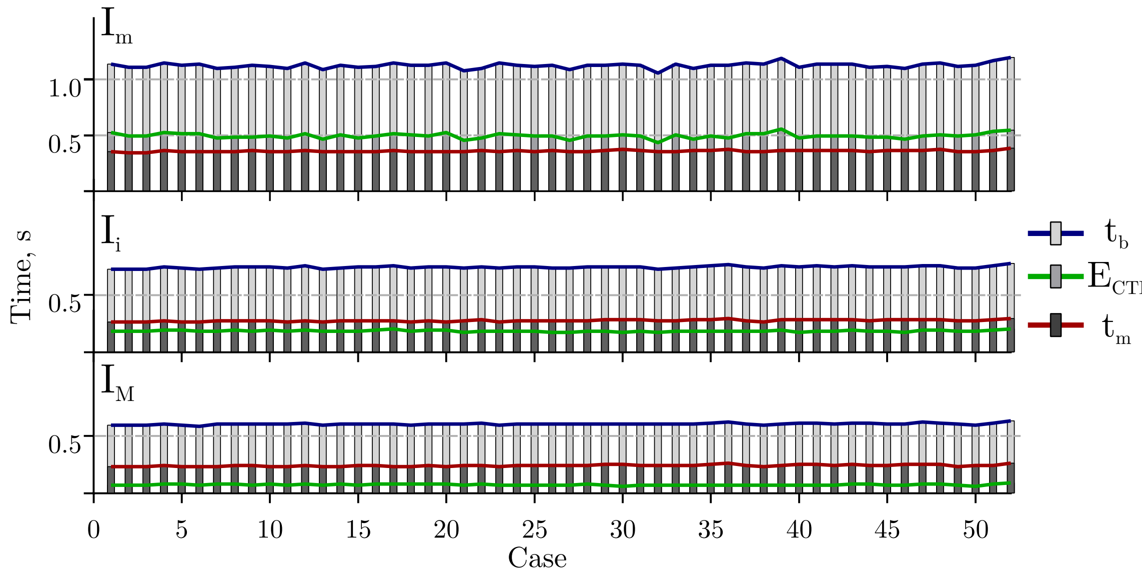

(a) Tripping times and coordination errors.

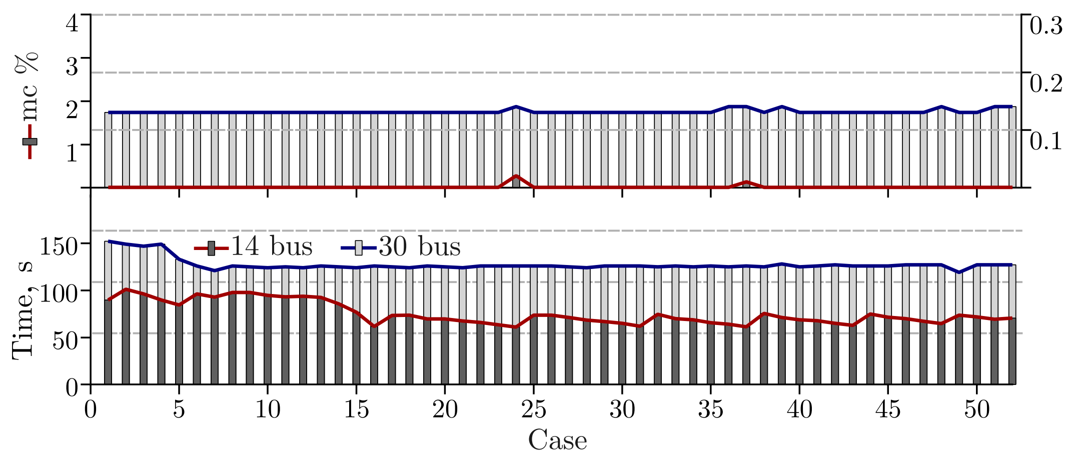

(b) Miscoordination percentage, fitness, and simulation time.

Figure 4.7: Testing operators probability of occurrence.

Table 4.8: Tested sequential quadratic programming occurrence.

Case	Iteration	Case	Iteration	Case	Iteration	Case	Iteration	Case	Iteration
1		10	8, 32	19	32, 256	28	8, 32, 128	37	16, 128, 256
2	8	11	8, 128	20	32, 700	29	8, 32, 256	38	16, 128, 700
3	16	12	8, 256	21	128, 256	30	8, 32, 700	39	16, 256, 700
4	32	13	8, 700	22	128, 700	31	8, 128, 256	40	32, 128, 256
5	128	14	16, 32	23	256, 700	32	8, 128, 700	41	32, 128, 700
6	256	15	16, 128	24	8, 16, 32	33	8, 256, 700	42	32, 256, 700
7	700	16	16, 256	25	8, 16, 128	34	16, 32, 128	43	128, 256, 700
8	8, 8	17	16, 700	26	8, 16, 256	35	16, 32, 256		
9	8, 16	18	32, 128	27	8, 16, 700	36	16, 32, 700		

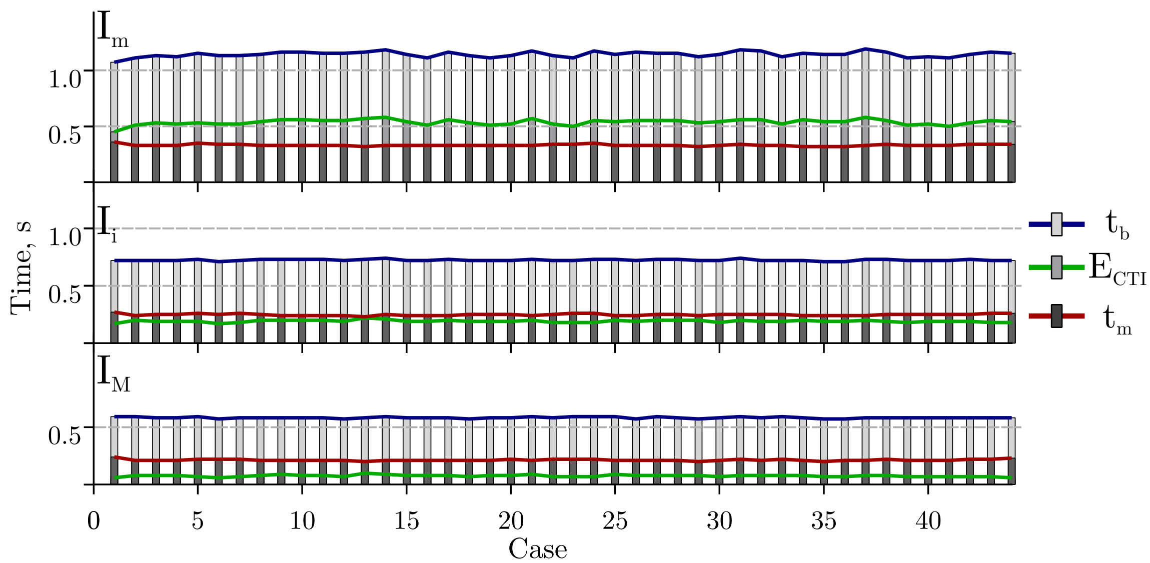

(a) Tripping times and coordination errors.

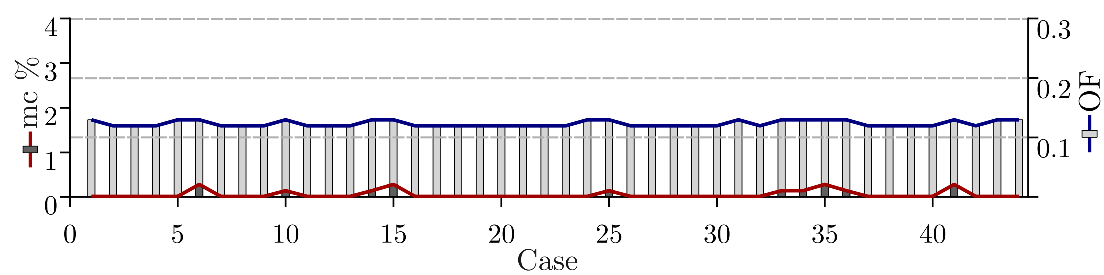

(b) Miscoordination percentage, fitness, and simulation time.

Figure 4.8: Testing the SQP implementation.

4.2 OVERCURRENT RELAY COORDINATION RESULTS

The previous section illustrate the experiments carried out in order to tune the parameters used by genetic algorithms and invasive-weed optimization. Meanwhile this section aims to compare the results obtained by the proposed methodology in comparison with four different cases that exemplify the considerations followed by different researchers through the last 30 years.

After experimental tuning, the magnitudes used by each parameter of both algorithms are listed in Table 4.9. The table is divided in three groups of parameters, the first part comprehend columns one to three and enlists settings that are used by an specific algorithm. The probability of occurrence of IWO operators remains unaltered during simulation, nevertheless the GA implementation is subjected to alterations in accordance with the slope decrease; if the best fitness is not improved after $\frac{\mathrm{T_i}}{20}$ iterations, the probabilities P(C), P(M), and P(E) are respectively modified to 0.55, 0.45, 0.05 until the algorithm escapes the local minima.

The second and third set of parameters indicates settings that are shared by both methods. While α, β, γ, ι, κ, and τ are fixed, both algorithms are allowed to define a continuous magnitude inside the defined boundaries for TDS, $\mathrm{P_m}$, A, B, and p. An adequate selection of those adjustable settings may lead to a relay coordination problem solution.

Five coordination approaches are compared in this section. The first case is the proposed method, five parameters that conform the overcurrent relay curve are considered as adjustable settings and the objective function aims to achieve coordination and time reduction for three different levels of short-circuit current. The first proposal is reached by allowing the relays to select continuous curve settings between a predefined boundaries while the second one consists in weighting the objective function as indicated in Equation 3.11 in Chapter 3.

Table 4.9: Selection ranges of each adjustable setting.

						Boundaries	
Parameter	GA	IWO	Parameter	Setting	Parameter	Minimum	Maximum
T_i	2000	700	α	0.60	TDS	0.50	5
P_s	200	100	β	0.30	P_m	1.40	2
P(C)	0.85	-	γ	0.10	A	0.01	30
P(M)	0.10	-	ι	0.25	B	0	0.50
P(E)	0.05	-	κ	0.25	p	0.01	2
P(S)	-	0.25	τ	0.50			
P(D)	-	0.05					
P(R)	-	0.70					

The remaining four cases are selected since they correspond to common practices conducted by researchers in all the related work cited in the previous chapters, they seek to achieve coordination while two — in cases three and five — and three — in cases two and four — inverse-time curve parameters are contemplated as adjustable. The IEEE very inverse-time curve is predefined for all relays in cases three and five, while in cases two and four each relay is allowed to choose one of the eight curve types presented in Table 2.1. The selection of a curve type involves the unaltered use of their A, B, and p parameters. Another difference is related to the objective function weighting factors, cases two and three seek to achieve coordination for minimum and maximum fault currents while cases four and five pursuits the same objective considering just a maximum level of short-circuit current. The five cases parameters are resumed in Table 4.10.

The overcurrent relay coordination results for the 9, 14, 30, 57, and 118-bus systems obtained by the genetic algorithm are presented in Table 4.11. Each one of the five table sections belongs to each tested power system, sections are identical and only the obtained results vary from one system to another. The fitness, miscoordination percentage (mc%), average main and backup tripping times, and coordination errors are the results to be compared and they are illustrated in columns one and two. Operation times and coordination errors for different short-circuit magnitudes are shown individually while fitness and miscoordination percentage represent the global result.

Table 4.10: Selection ranges of each adjustable setting.

	Case				
Parameter	1	2	3	4	5
TDS	[0.50 - 5]				
P_m	[1.4 - 2]				
A	[0.01 - 30]	8 curves	19.60	8 curves	19.60
B	[0 - 0.50]		0.49		0.49
p	[0.01 - 2]		2		2
ι	0.25	0.25	0.25	0.00	0.00
κ	0.25	0.00	0.00	0.00	0.00
τ	0.50	0.75	0.75	1.00	1.00

Columns three to seven exhibit the results obtained by each one of the five cases. Lastly, columns eight to eleven show in percentage the improvement obtained by case one in comparison with cases two to five. Negative magnitudes in those columns indicate a case that obtained a better result. In addition, Figure 4.9 illustrates the same results in a set bar plots for better appreciation.

The total coordination pairs of each test system is respectively 12, 50, 124, 220, and 906; after the sensitivity filter the total pairs is reduced to 10, 47, 118, 206, and 884; since three coordination points are considered for each pair, these values are multiplied by three to obtain the total coordination points of each system. Therefore, if cases three to five obtained a miscoordination percentage of 6.67 for the the 9-bus system, it means that coordination is not achieved for two out of 30 coordination pairs. GA achieves full coordination for the small 9-bus power system, nevertheless the miscoordination percentage increase as the systems grow. This behavior is shared by all five cases and it is an expected result considering the complexity increase.

The results of the first three systems are fully dominated by the proposed case, improvements from 7% to more than 90% are achieved. Since the miscoordination percentage is improved or at least maintained equal in comparison with standardized cases, the curves compatibilities are not compromised by using unstandardized adjusts. The situation is different for more complex systems, some results obtained by the standard cases are better than the proposed case; even considering these disadvantages the proposed case fitness is better than the others, indicating that its overall result is the best among all scenarios. This statement can be better appreciated by observing the 57 and 118-bus systems results in Figure 4.9, some scenarios achieve less miscoordinations but they fail to obtain fast tripping times for all short-circuit currents. The improvement average considering all cases, measurements and systems is equal to 44.01%.

Results presented in Table 4.12 and illustrated in Figure 4.10 are obtained by the implementation of the invasive-weed optimization method. They are arranged in the same order and contain the same information as previously analyzed GA results. An important fact to highlight is that in these simulations all results are fully dominated by the proposed case, improvements from 1% to 96% are achieved, obtaining an improvement average for all cases, measurements, and systems of 51.60%, 7% more than GA average.

The total iterations is increased to 1000 and 1500 for the 57 and 118-bus systems. The proposed methodology achieves coordination for all 618 pairs in the 57-bus power system with better tripping times for all short-circuit levels, the same performance is also obtained for smaller systems. The standardized cases also obtained better results in comparison with genetic algorithms. Furthermore, 118-bus system is successfully coordinated presenting just 0.44% of miscoordinations. This results are outstanding considering the magnitude, interconnection, and complexity of this power system where 2718 pairs are being coordinated and the relays function as backups for up to seven main relays. The tripping times and coordination errors are also improved by the base case.

The average convergence of both algorithms after 10 ten experimental repetitions, solving the coordination for the 57-bus system is illustrated in Figure 4.11, 700 IWO iterations obtained similar results in comparison with 2000 GA iterations. GA total iterations were increased during some experiments in order to perform a better comparison, nevertheless the algorithm did not improved IWO solutions. Table 4.13 compares the results obtained by both algorithms, it can be noted that IWO improves all but one measurements, reducing total of miscoordinations as well as tripping times and coordination errors.

Table 4.11: OCR coordination results obtained by GA.

Results		Case 1	Case 2	Case 3	Case 4	Case 5	Improvement 2	Improvement 3	Improvement 4	Improvement 5	
	f	0.10	0.18	0.56	0.21	0.56	42.14	81.79	52.49	81.87	9-bus system
	mc%	0.00	0.00	6.67	6.67	6.67	/	100	100	100	
	t_m	0.27	0.46	0.97	0.49	0.98	41.98	72.72	46.04	72.93	
I_{sc}^{m}	E_{CTI}	0.64	0.89	5.30	1.56	5.30	27.70	87.89	58.85	87.88	
	t_{bu}	1.21	1.65	6.42	2.27	6.42	26.63	81.18	46.84	81.19	
	t_m	0.12	0.32	0.50	0.30	0.50	60.98	75.44	58.25	75.47	
I_{sc}^{in}	E_{CTI}	0.18	0.30	2.06	0.42	2.06	37.89	91.04	55.95	91.05	
	t_{bu}	0.61	0.91	2.82	1.01	2.82	33.44	78.45	40.07	78.48	
	t_m	0.09	0.26	0.38	0.23	0.38	67.64	77.80	63.62	77.78	
I_{sc}^{M}	E_{CTI}	0.03	0.12	1.07	0.18	1.08	76.84	97.33	84.22	97.34	
	t_{bu}	0.41	0.69	1.76	0.72	1.76	39.76	76.46	42.19	76.49	
	f	0.14	0.18	3.67	0.25	3.72	21.84	96.24	44.69	96.30	14-bus system
	mc%	2.13	2.13	11.35	6.38	13.48	0.00	81.25	66.67	84.21	
	t_m	0.28	0.37	0.68	0.38	0.66	24.92	59.07	26.21	57.78	
I_{sc}^{m}	E_{CTI}	0.77	0.83	3.70	2.18	2.81	7.33	79.15	64.60	72.60	
	t_{bu}	1.31	1.48	4.48	2.75	3.61	11.48	70.69	52.35	63.63	
	t_m	0.15	0.24	0.47	0.21	0.45	36.74	68.11	27.21	66.87	
I_{sc}^{in}	E_{CTI}	0.23	0.32	0.70	0.36	0.69	28.98	67.61	37.36	67.13	
	t_{bu}	0.66	0.86	1.41	0.86	1.40	23.39	53.41	23.68	53.29	
	t_m	0.11	0.19	0.43	0.16	0.41	42.20	73.78	28.71	72.73	
I_{sc}^{M}	E_{CTI}	0.10	0.17	0.35	0.15	0.31	39.34	70.55	33.05	67.40	
	t_{bu}	0.50	0.67	1.03	0.62	1.01	25.45	51.71	19.21	50.59	
	f	0.22	0.25	1.43	0.58	1.60	10.98	84.32	61.70	86.05	30-bus system
	mc%	5.37	5.93	20.34	8.47	15.25	9.52	73.61	36.67	64.81	
	t_m	0.43	0.50	0.87	0.59	0.88	13.43	50.48	27.03	50.88	
I_{sc}^{m}	E_{CTI}	0.78	0.81	1.77	1.45	1.59	3.49	55.74	45.93	50.61	
	t_{bu}	1.44	1.55	2.58	2.19	2.46	6.80	44.00	33.91	41.27	
	t_m	0.27	0.33	0.62	0.35	0.69	17.85	55.98	21.41	60.37	
I_{sc}^{in}	E_{CTI}	0.33	0.41	1.00	0.60	0.61	20.43	67.21	45.56	46.40	
	t_{bu}	0.87	1.01	1.72	1.22	1.40	14.17	49.63	28.65	38.00	
	t_m	0.22	0.27	0.57	0.27	0.65	18.42	60.99	18.44	65.52	
I_{sc}^{M}	E_{CTI}	0.17	0.24	0.41	0.29	0.26	30.24	58.34	41.29	34.81	
	t_{bu}	0.67	0.80	1.10	0.86	1.02	15.97	39.36	22.18	34.60	
	f	0.38	0.42	1.58	2.18	5.24	7.71	75.66	82.40	92.66	57-bus system
	mc%	14.89	13.92	35.44	14.24	28.16	-6.98	57.99	-4.55	47.13	
	t_m	0.55	0.74	2.42	0.68	2.65	24.80	77.06	18.90	79.06	
I_{sc}^{m}	E_{CTI}	1.09	1.77	63.92	5.72	4.74	38.13	98.29	80.91	76.93	
	t_{bu}	1.71	2.54	64.94	6.45	5.56	32.67	97.37	73.47	69.23	
	t_m	0.47	0.48	1.89	0.35	1.88	0.17	74.86	-33.97	74.72	
I_{sc}^{in}	E_{CTI}	0.34	0.64	0.50	0.73	0.39	47.04	32.59	53.27	13.26	
	t_{bu}	0.90	1.23	1.35	1.30	1.13	27.28	33.70	31.17	21.12	
	t_m	0.44	0.41	1.76	0.28	1.75	-9.07	74.69	-59.93	74.62	
I_{sc}^{M}	E_{CTI}	0.23	0.44	0.27	0.36	0.17	46.87	12.10	34.71	-40.60	
	t_{bu}	0.75	0.98	1.03	0.88	0.90	22.75	27.05	14.73	16.25	
	f	0.62	0.66	5.61	1.99	3.57	6.26	88.99	68.88	82.70	118-bus system
	mc%	26.58	24.81	33.14	20.29	26.81	-7.14	19.80	-31.04	0.84	
	t_m	0.86	0.82	1.18	0.94	1.25	-5.59	27.07	8.39	30.77	
I_{sc}^{m}	E_{CTI}	2.09	3.27	3.85	21.84	4.52	35.93	45.56	90.41	53.65	
	t_{bu}	2.79	4.03	4.67	21.84	5.36	30.87	40.36	87.24	48.03	
	t_m	0.65	0.61	0.97	0.59	0.99	-7.68	32.95	-11.21	33.93	
I_{sc}^{in}	E_{CTI}	0.77	1.08	0.77	1.27	0.66	28.73	-0.19	39.06	-16.38	
	t_{bu}	1.37	1.72	1.53	1.85	1.47	20.58	10.65	25.98	6.84	
	t_m	0.59	0.54	0.93	0.49	0.94	-10.22	36.32	-20.54	36.80	
I_{sc}^{M}	E_{CTI}	0.55	0.82	0.55	0.81	0.43	32.62	-1.09	31.67	-30.46	
	t_{bu}	1.12	1.41	1.29	1.35	1.22	20.44	13.51	17.07	8.39	

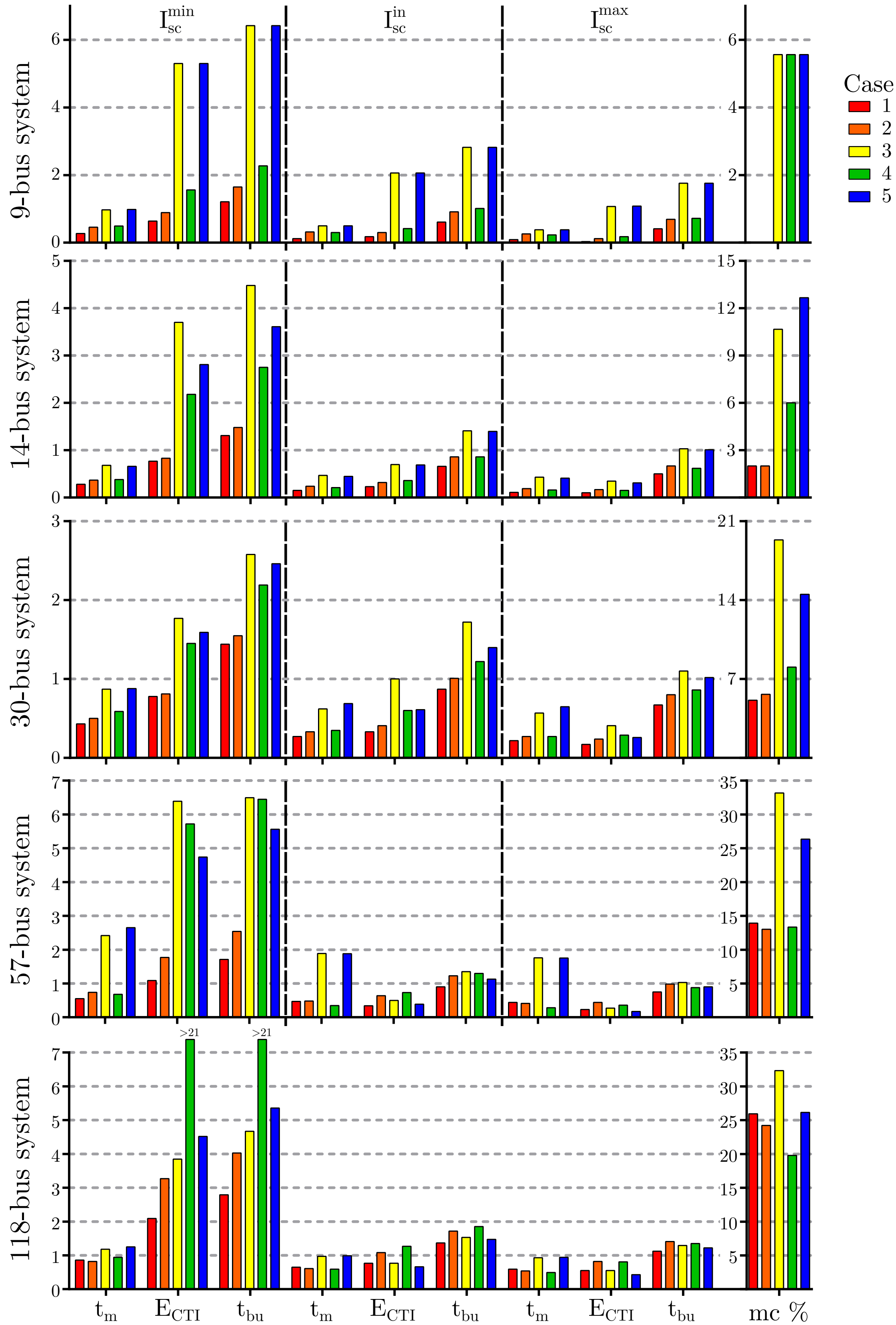

Figure 4.9: Tripping times, errors, and miscoordination percentage using GA.

Table 4.12: OCR coordination results obtained by IWO.

Results		Case 1	Case 2	Case 3	Case 4	Case 5	Improvement 2	Improvement 3	Improvement 4	Improvement 5	System
	f	0.07	0.15	0.20	0.14	0.21	54.06	66.10	53.05	68.01	9-Bus system
	mc%	0	0	0	0	0	/	/	/	/	
I_{sc}^{m}	t_m	0.19	0.46	0.69	0.44	0.73	59.66	72.99	57.77	74.58	
	E_{CTI}	0.46	0.63	0.82	0.74	0.91	26.74	44.18	38.12	49.49	
	t_{bu}	0.93	1.38	1.77	1.48	1.91	32.65	47.33	36.96	51.36	
I_{sc}^{in}	t_m	0.08	0.32	0.42	0.29	0.42	74.63	80.52	72.34	80.88	
	E_{CTI}	0.14	0.24	0.44	0.27	0.51	42.14	68.66	48.28	73.18	
	t_{bu}	0.52	0.85	1.14	0.85	1.23	39.57	54.92	39.40	58.10	
I_{sc}^{M}	t_m	0.05	0.27	0.35	0.24	0.35	80.63	85.05	78.45	85.05	
	E_{CTI}	0.00	0.10	0.24	0.10	0.30	95.81	98.32	96.01	98.65	
	t_{bu}	0.35	0.66	0.88	0.63	0.94	46.43	59.95	44.16	62.57	
	f	0.10	0.13	0.30	0.14	0.29	24.62	68.61	30.41	67.39	14-Bus system
	mc%	0	0	4.26	0	2.13	/	100	/	100	
I_{sc}^{m}	t_m	0.24	0.34	0.69	0.35	0.71	29.42	65.44	32.31	66.47	
	E_{CTI}	0.42	0.59	1.36	0.86	1.55	29.41	69.11	51.22	72.90	
	t_{bu}	0.93	1.21	2.30	1.48	2.47	22.86	59.46	36.98	62.16	
I_{sc}^{in}	t_m	0.15	0.21	0.52	0.21	0.52	30.40	71.57	29.21	71.55	
	E_{CTI}	0.17	0.25	0.50	0.30	0.53	30.40	65.56	42.45	67.90	
	t_{bu}	0.61	0.75	1.29	0.80	1.32	18.60	52.46	23.15	53.70	
I_{sc}^{M}	t_m	0.12	0.18	0.49	0.17	0.48	30.94	75.21	28.32	74.97	
	E_{CTI}	0.07	0.12	0.26	0.14	0.29	45.42	74.39	53.18	76.49	
	t_{bu}	0.49	0.60	1.02	0.61	1.04	18.31	52.45	19.99	53.31	
	f	0.13	0.20	0.50	0.18	0.49	32.92	73.28	26.86	72.64	30-Bus system
	mc%	0	0	5.93	0.28	3.67	/	100	100	100	
I_{sc}^{m}	t_m	0.37	0.57	0.95	0.49	1.11	35.09	61.25	24.54	66.68	
	E_{CTI}	0.48	0.86	1.11	0.88	1.38	43.73	56.57	45.25	65.00	
	t_{bu}	1.11	1.68	2.11	1.62	2.49	33.91	47.22	31.45	55.40	
I_{sc}^{in}	t_m	0.25	0.37	0.76	0.29	0.87	31.81	67.13	12.77	71.16	
	E_{CTI}	0.26	0.48	0.48	0.46	0.54	46.44	46.40	44.38	52.71	
	t_{bu}	0.78	1.13	1.34	1.03	1.53	30.95	41.86	24.60	49.24	
I_{sc}^{M}	t_m	0.21	0.30	0.72	0.22	0.82	29.93	71.08	5.54	74.47	
	E_{CTI}	0.16	0.32	0.26	0.30	0.29	50.78	40.64	47.31	46.94	
	t_{bu}	0.64	0.90	1.08	0.81	1.24	29.35	41.26	21.11	48.43	
	f	0.15	0.27	0.99	0.70	1.43	43.63	84.48	78.06	89.23	57-Bus system
	mc%	0	0.65	13.75	0.97	13.27	100	100	100	100	
I_{sc}^{m}	t_m	0.36	0.79	2.25	0.89	2.48	54.66	84.10	59.77	85.58	
	E_{CTI}	0.68	1.51	1.52	3.37	2.31	54.89	55.23	79.77	70.51	
	t_{bu}	1.35	2.39	2.57	4.30	3.29	43.39	47.43	68.52	58.92	
I_{sc}^{in}	t_m	0.29	0.52	1.93	0.50	1.92	43.61	84.68	40.99	84.61	
	E_{CTI}	0.26	0.54	0.33	0.81	0.37	52.29	21.14	68.34	30.88	
	t_{bu}	0.86	1.22	1.27	1.57	1.29	29.19	31.72	45.09	32.81	
I_{sc}^{M}	t_m	0.27	0.44	1.82	0.40	1.81	38.35	85.12	32.37	85.03	
	E_{CTI}	0.17	0.36	0.21	0.50	0.25	52.98	21.19	66.81	32.32	
	t_{bu}	0.75	0.97	1.10	1.18	1.11	22.73	32.21	36.86	32.93	
	f	0.16	0.41	0.89	0.51	1.52	60.18	81.75	68.03	89.25	118-Bus system
	mc%	0.44	2.22	13.88	2.30	13.73	80.15	96.82	80.81	96.78	
I_{sc}^{m}	t_m	0.35	0.77	1.33	0.74	1.38	54.44	73.60	52.49	74.66	
	E_{CTI}	0.72	2.37	1.57	3.66	1.83	69.67	54.24	80.34	60.64	
	t_{bu}	1.28	3.18	2.55	4.40	2.75	59.65	49.63	70.81	53.36	
I_{sc}^{in}	t_m	0.28	0.55	1.12	0.49	1.11	48.50	74.74	42.44	74.54	
	E_{CTI}	0.28	0.99	0.54	0.97	0.54	71.70	48.19	71.31	48.14	
	t_{bu}	0.80	1.67	1.44	1.61	1.43	52.32	44.82	50.61	44.08	
I_{sc}^{M}	t_m	0.26	0.47	1.07	0.42	1.05	46.04	76.05	39.13	75.68	
	E_{CTI}	0.18	0.70	0.39	0.64	0.37	74.75	54.40	72.48	52.35	
	t_{bu}	0.67	1.34	1.28	1.23	1.25	49.60	47.16	45.32	45.89	

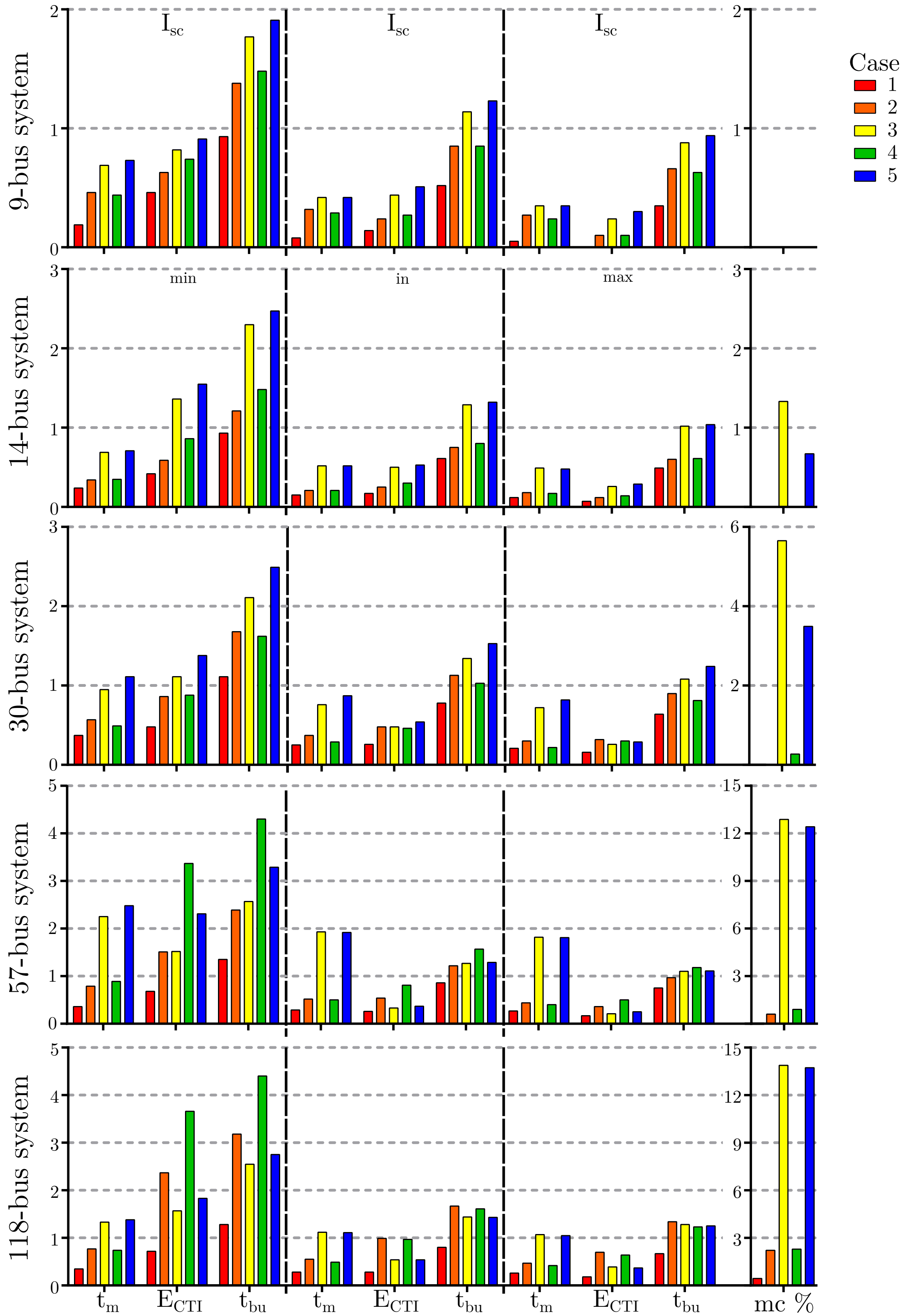

Figure 4.10: Tripping times, errors, and miscoordination percentage using IWO.

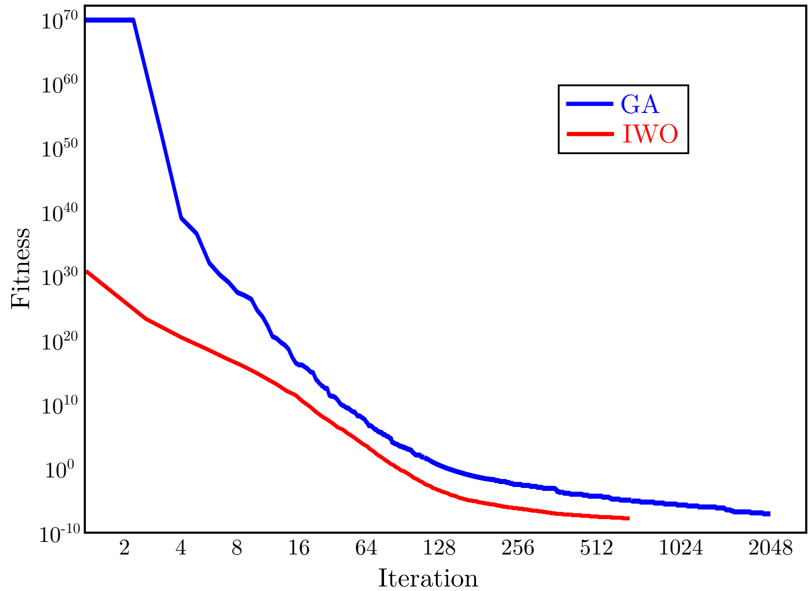

Figure 4.11: GA and IWO fitness convergence for OCR coordination.

Table 4.13: IWO and GA results comparison and IWO percentage of improvement.

Results		9-Bus System			14-Bus System			30-Bus System			57-Bus System			118-Bus System		
		IWO	GA	%	IWO	GA	%	IWO	GA	%	IWO	GA	%	IWO	GA	%
	f	0.07	0.10	33.32	0.10	0.14	31.00	0.13	0.22	40.07	0.15	0.38	59.90	0.26	0.62	58.57
	mc%	0	0	/	0	2.13	100	0	5.37	100	0	14.91	100	0.53	26.58	98.01
I_{sc}^{m}	t_m	0.19	0.27	29.82	0.24	0.28	13.66	0.37	0.43	14.60	0.36	0.55	35.47	0.58	0.86	32.73
	E_{CTI}	0.46	0.64	28.51	0.42	0.77	45.61	0.48	0.78	38.65	0.68	1.09	37.66	1.30	2.09	37.72
	t_{bu}	0.93	1.21	22.91	0.93	1.31	28.92	1.11	1.44	23.10	1.35	1.71	20.92	2.05	2.79	26.59
I_{sc}^{in}	t_m	0.08	0.12	34.21	0.15	0.15	0.25	0.25	0.27	8.40	0.29	0.47	37.83	0.46	0.65	29.07
	E_{CTI}	0.14	0.18	25.24	0.17	0.23	24.97	0.26	0.33	21.73	0.26	0.34	24.21	0.53	0.77	31.58
	t_{bu}	0.52	0.61	15.10	0.61	0.66	6.55	0.78	0.87	10.46	0.86	0.90	3.39	1.20	1.37	12.61
I_{sc}^{M}	t_m	0.05	0.09	39.32	0.12	0.11	-7.44	0.21	0.22	7.05	0.27	0.44	39.07	0.42	0.59	29.00
	E_{CTI}	0.00	0.03	85.84	0.07	0.10	33.92	0.16	0.17	8.34	0.17	0.23	28.31	0.36	0.55	35.76
	t_{bu}	0.35	0.41	14.59	0.49	0.50	2.32	0.64	0.67	4.79	0.75	0.75	1.04	0.99	1.12	11.16

Last results to show in this section correspond to sequential quadratic programming implementation. Since nonlinear optimization methods require a good initial guess in order to converge, SQP has been implemented to initialize after eight IWO iterations. The simulation results are shown in Table 4.14, IWO+SQP improvement percentage in comparison with IWO is also reported. Certain tripping times are worsen in some scenarios but fitness and consequently most measurements are slightly improved in all systems. The average fitness convergency after ten simulations of each case is illustrated in Figure 4.12.

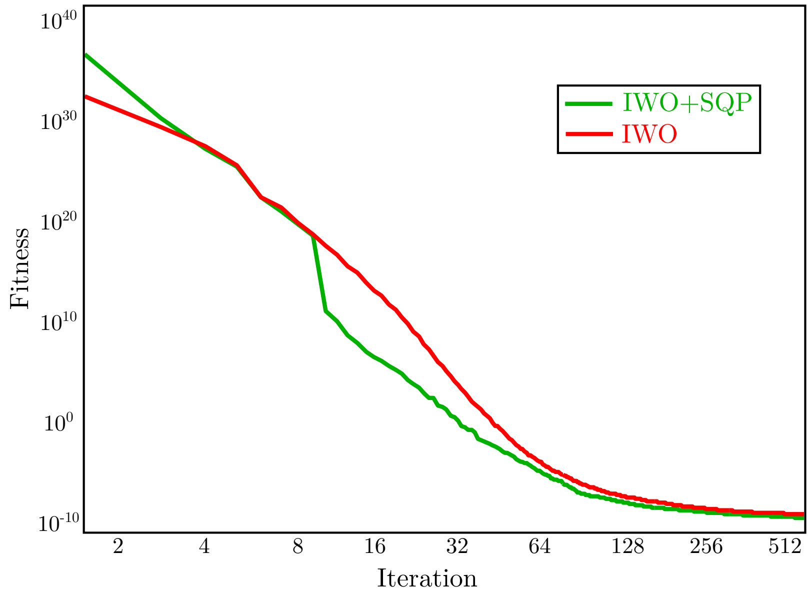

Figure 4.12: IWO and IWO+SQP average fitness convergency for OCR coordination.

Table 4.14: IWO+SQP and IWO results compared.

Results		9-Bus System			14-Bus System			30-Bus System			57-Bus System			118-Bus System		
		SQP	IWO	%	SQP	IWO	%	SQP	IWO	%	SQP	IWO	%	SQP	IWO	%
	f	0.07	0.07	1.76	0.09	0.10	5.87	0.11	0.13	19.87	0.15	0.15	0.29	0.16	0.16	4.71
	mc%	0	0	/	0	0	/	0	0	/	0	0	/	0.37	0.44	16.67
	t_m	0.17	0.19	6.47	0.22	0.24	6.89	0.29	0.37	22.44	0.36	0.36	0.44	0.34	0.35	3.71
I_{sc}^{m}	E_{CTI}	0.45	0.46	1.39	0.42	0.42	0.21	0.52	0.48	-8.48	0.69	0.68	-1.48	0.66	0.72	8.74
	t_{bu}	0.91	0.93	1.91	0.92	0.93	1.69	1.07	1.11	3.71	1.36	1.35	-0.82	1.21	1.28	6.01
	t_m	0.08	0.08	-0.45	0.13	0.15	12.39	0.16	0.25	34.94	0.29	0.29	1.85	0.27	0.28	4.31
I_{sc}^{in}	E_{CTI}	0.13	0.14	4.76	0.17	0.17	1.66	0.23	0.26	8.46	0.27	0.26	-4.81	0.27	0.28	2.91
	t_{bu}	0.51	0.52	1.61	0.59	0.61	3.19	0.67	0.78	13.65	0.87	0.86	-1.11	0.78	0.80	2.76
	t_m	0.05	0.05	-2.71	0.10	0.12	15.65	0.12	0.21	41.02	0.26	0.27	2.73	0.24	0.26	4.55
I_{sc}^{M}	E_{CTI}	0.00	0.00	52.89	0.06	0.07	7.57	0.12	0.16	25.12	0.17	0.17	-1.61	0.17	0.18	3.53
	t_{bu}	0.35	0.35	0.57	0.46	0.49	4.54	0.52	0.64	18.92	0.75	0.75	0.10	0.66	0.67	2.85

4.3 Overcurrent and Distance Relay Coordination Results

The previous section presented overcurrent relay coordination results using genetic algorithms and invasive-weed optimization for the 9, 14, 30, 57, and 118-bus systems. In four systems IWO accomplished coordination of all coordination pairs that involved relays capable of being coordinated, i.e., relays that pass the sensitivity filter described by Equation 2.3; the implemented algorithm failed failed to coordinate 0.44% of the total coordination pairs of the 118-bus system. Since overcurrent relays cannot detect certain short-circuit magnitudes, relays that do not pass the filter are impossible to coordinate; this limitation is caused by the protection principle and is not related to any specific methodology or algorithm.

The coordination pairs are conformed in accordance with the bus connection data of each system, after fault and flow analysis coordination pairs pass through the sensitivity filter. The total pairs removed from the coordination process for each system is respectively equal to 2, 3, 6, 14, and 22 pairs. According to reported literature researchers have implemented algorithms to solve the OCR coordination, nevertheless nothing has been done about the insensitive relays; furthermore some works propose distance and OCR coordination offering a redundant solution by placing both protection principles on every bus. In this work, distance-relays are used to substitute insensitive overcurrent ones, aiming to offer a better solution to OCR coordination.

Inserted distance-relays conform new hybrid coordination pairs with all their related OCR, Figure 4.13 illustrate the coordination points considered in this section of the thesis, when distance-relay is used as main or backup protection. The programmed algorithm is capable to handle different total zones and zone coverage percentage, however for this thesis distance-relays first zone is set to cover 80% of the main line while their second zone is expected to cover the remaining 20% and the 100% of the adjacent one, the third zone is deactivated. As highlighted in the figure, each kind of coordination pair — dis-

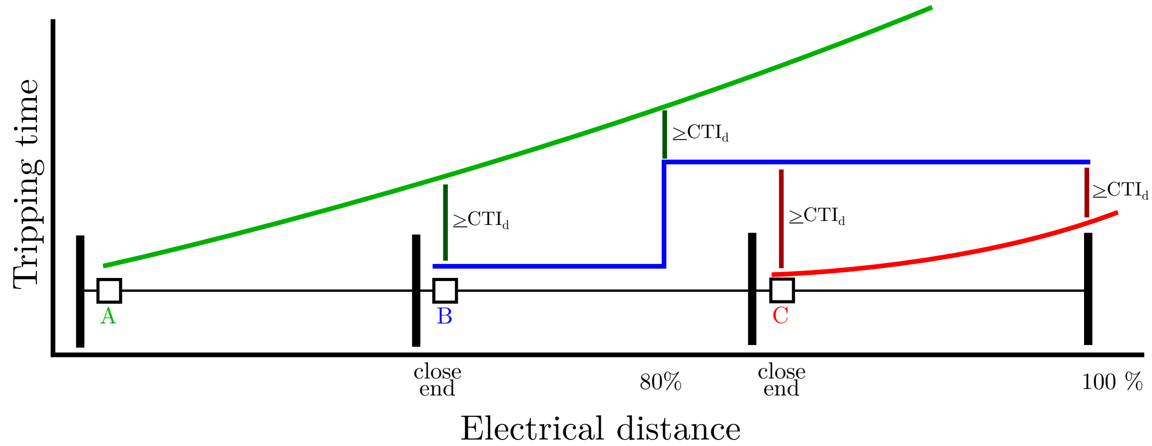

Figure 4.13: Distance and overcurrent relays coordination points.

tance as main and overcurrent as backup (D+OC) or vice versa (OC+D) — aims to fulfill coordination requirements for two coordination points. The distance coordination time interval is set to 0.2 seconds.

The total overcurrent and distance coordination pairs for each tested system is respectively equal to 4, 11, 25, 49, and 123 pairs; since in this approach each pair involve two coordination points, the total points is twice the total pairs. GA have been implemented to complete this part of the thesis however it presented difficulties to converge and was finally discarded for this section.

The objective function is described by Equation 3.15, and the weighting factors are set to α, β, γ, and δ are respectively set to 0.5, 0.15, 0.25, and 0.1. Excluding these adjustments, the remaining IWO parameters shown in Table 4.9 and the five cases illustrated in Table 4.10 are considered in the following simulations.

Overcurrent and distance-relay coordination results are shown in Table 4.15; the table is organized in the same manner presented in the previous section, being the distance miscoordination percentage ($\mathrm{mc_d}$%) the only addition. In addition, Figure 4.14 illustrates the system results as a set of box plots. Similar to previously presented results, the proposed methodology dominated almost all categories obtaining lower tripping times and lesser miscoordinations in comparison with the remaining four cases, which in addition failed to converge in some simulations.

Table 4.15: IWO results for overcurrent and distance-relay coordination.

Results		Case					Improvement				
		1	2	3	4	5	2	3	4	5	
	f	0.11	0.43	0.37	0.28	0.39	74.13	70.11	60.26	71.53	9-Bus system
	mc%	0	0	0	0	0	/	/	/	/	
	mc_d%	0	37.50	25.00	12.50	25.00	100.00	100.00	100.00	100.00	
I_{sc}^{m}	t_m	0.36	0.82	0.81	0.61	0.77	56.39	55.90	41.71	53.63	
	E_{CTI}	0.51	1.72	1.06	0.96	1.74	70.53	52.27	47.11	70.84	
	t_{bu}	1.15	2.86	2.20	1.93	2.83	59.74	47.72	40.46	59.33	
I_{sc}^{in}	t_m	0.22	0.64	0.67	0.44	0.60	65.71	67.40	49.94	63.69	
	E_{CTI}	0.20	0.63	0.47	0.40	0.75	68.41	57.52	51.11	73.69	
	t_{bu}	0.70	1.58	1.44	1.20	1.64	56.01	51.53	41.75	57.56	
I_{sc}^{M}	t_m	0.18	0.56	0.63	0.36	0.56	68.64	72.23	51.41	68.35	
	E_{CTI}	0.06	0.31	0.24	0.21	0.40	79.80	73.68	71.08	84.61	
	t_{bu}	0.52	1.19	1.16	0.93	1.24	56.27	55.41	44.01	58.08	
	f	0.19	0.48	0.44	0.55	0.45	59.57	56.06	64.67	56.99	14-Bus system
	mc%	0	0	0.67	5.33	0.67	/	100	100	100	
	mc_d%	4.55	63.64	22.73	31.82	27.27	92.86	80.00	85.71	83.33	
I_{sc}^{m}	t_m	0.37	0.74	0.91	0.58	0.85	49.41	59.00	36.19	55.98	
	E_{CTI}	0.75	1.18	1.35	2.24	1.86	36.11	44.20	66.52	59.68	
	t_{bu}	1.40	2.10	2.50	3.04	2.97	33.63	44.23	54.12	52.97	
I_{sc}^{in}	t_m	0.23	0.58	0.78	0.37	0.69	59.61	70.07	36.81	66.41	
	E_{CTI}	0.45	0.50	0.46	0.70	0.58	11.56	3.39	36.48	23.71	
	t_{bu}	0.96	1.29	1.51	1.37	1.56	25.44	36.27	29.56	38.17	
I_{sc}^{M}	t_m	0.19	0.51	0.75	0.30	0.65	62.80	74.39	36.16	70.83	
	E_{CTI}	0.30	0.34	0.24	0.46	0.31	11.33	-26.16	35.24	4.80	
	t_{bu}	0.78	1.07	1.26	1.06	1.25	27.18	38.17	26.99	37.81	
	f	0.31	0.79	0.73	0.71	0.76	60.12	57.12	55.79	58.90	30-Bus system
	mc%	2.42	14.25	7.80	9.41	8.06	83.02	68.97	74.29	70.00	
	mc_d%	8.00	24.00	24.00	22.00	16.00	66.67	66.67	63.64	50.00	
I_{sc}^{m}	t_m	0.51	0.52	0.99	0.64	1.09	3.00	48.94	20.90	53.82	
	E_{CTI}	0.49	1.32	1.31	1.30	1.37	63.22	62.90	62.74	64.64	
	t_{bu}	1.22	1.99	2.33	2.10	2.45	38.66	47.59	41.73	50.07	
I_{sc}^{in}	t_m	0.38	0.40	0.85	0.42	0.93	7.25	55.88	11.15	59.63	
	E_{CTI}	0.27	0.66	0.55	0.68	0.62	58.43	50.07	59.49	55.51	
	t_{bu}	0.90	1.24	1.48	1.34	1.60	27.43	38.96	32.57	43.49	
I_{sc}^{M}	t_m	0.33	0.36	0.81	0.35	0.89	9.80	60.03	6.54	63.36	
	E_{CTI}	0.18	0.42	0.30	0.46	0.37	57.66	40.28	60.67	51.27	
	t_{bu}	0.77	0.98	1.20	1.06	1.32	21.62	36.37	27.84	41.93	
	f	0.31	0.80	1.13	1.01	1.18	61.30	72.75	69.55	73.96	57-Bus system
	mc%	1.06	8.94	13.18	8.03	13.33	88.14	91.95	86.79	92.05	
	mc_d%	7.14	21.43	19.39	9.18	17.35	66.67	63.16	22.22	58.82	
I_{sc}^{m}	t_m	0.50	1.06	1.95	0.95	2.01	52.43	74.21	47.09	75.00	
	E_{CTI}	0.85	1.30	0.97	2.46	1.45	35.02	12.39	65.60	41.71	
	t_{bu}	1.66	2.05	1.99	3.28	2.52	19.21	16.87	49.58	34.35	
I_{sc}^{in}	t_m	0.42	0.96	1.90	0.73	1.95	56.48	77.87	42.23	78.44	
	E_{CTI}	0.35	0.63	0.35	0.78	0.44	43.78	-0.76	54.65	19.55	
	t_{bu}	1.07	1.28	1.33	1.51	1.47	16.02	19.57	28.96	27.11	
I_{sc}^{M}	t_m	0.39	0.93	1.88	0.66	1.93	58.14	79.42	41.47	79.91	
	E_{CTI}	0.24	0.47	0.26	0.53	0.30	49.33	8.47	55.23	21.46	
	t_{bu}	0.92	1.07	1.23	1.22	1.32	14.17	25.17	24.31	30.31	
	f	0.35	1.14	1.40	1.65	1.55	69.46	75.15	78.95	77.70	118-Bus system
	mc%	2.91	17.44	18.32	24.32	18.95	83.33	84.14	88.05	84.66	
	mc_d%	4.47	17.48	20.33	25.61	18.29	74.42	78.00	82.54	75.56	
I_{sc}^{m}	t_m	0.45	0.62	1.25	0.89	1.33	27.40	63.76	49.54	66.01	
	E_{CTI}	1.00	2.25	1.26	3.05	1.87	55.79	20.92	67.32	46.65	
	t_{bu}	1.64	2.89	2.23	3.70	2.86	43.39	26.70	55.78	42.79	
I_{sc}^{in}	t_m	0.38	0.55	1.21	0.76	1.22	31.07	68.66	49.84	69.04	
	E_{CTI}	0.36	0.89	0.59	1.22	0.66	59.35	38.09	70.40	45.27	
	t_{bu}	0.96	1.48	1.53	1.84	1.64	35.36	37.53	48.05	41.47	
I_{sc}^{M}	t_m	0.35	0.52	1.20	0.71	1.20	32.37	70.80	50.71	70.85	
	E_{CTI}	0.24	0.70	0.48	0.95	0.50	66.16	51.09	75.10	52.93	
	t_{bu}	0.81	1.26	1.43	1.54	1.47	35.92	43.21	47.47	44.86	

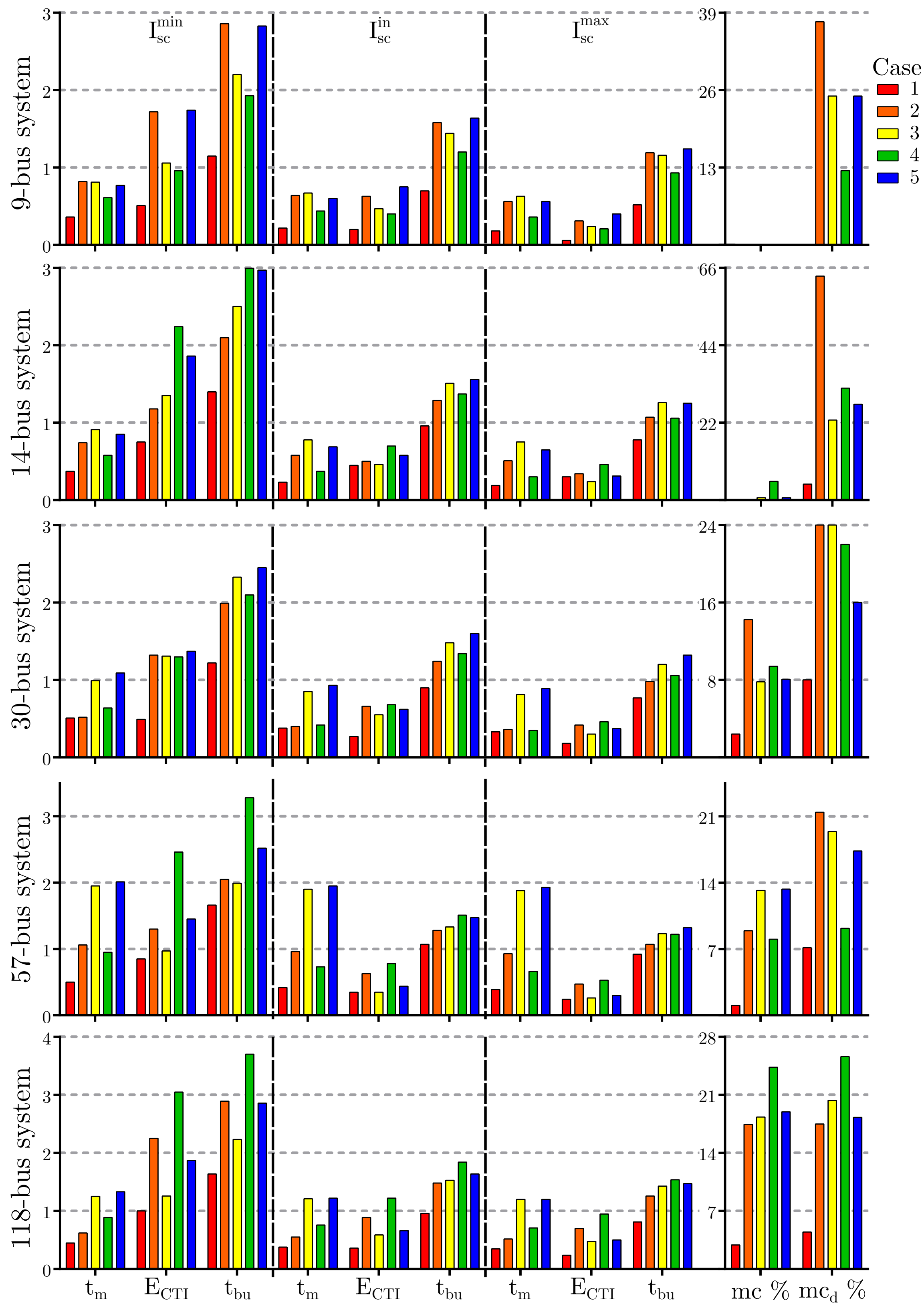

Figure 4.14: Overcurrent and distance-relays coordination results.

Let us make a supposition and tag insensitive relays as miscoordinations for the case presented in the previous section — when only overcurrent relays are coordinated —. Table 4.16 shows the total coordination points and total miscoordinations of both approaches. The total and percentage of miscoordinations is then shown in the fourth and fifth rows. The second group of results is obtained by overcurrent and distance-relays coordinations, the total coordination points (TCP) is the sum of OC+OC, OC+D, and D+OC coordination points. As can be appreciated in the last two rows, the inclusion of distance-relays decreases the miscoordination percentage if insensitive relays are considered in four out of five cases.

On the other hand distance-relays introduction increases OCR mean tripping times; since the total coordination points and variables grow, this is an expected result.

Table 4.16: Total pairs and miscoordinations comparing both approaches.

	OCR					OCR + Distance				
System	9	14	30	57	118	9	14	30	57	118
TCP	36	150	372	660	2718	38	163	404	716	2898
mc	6	9	18	42	80	0	1	12	13	90
mc%	16.67	6.00	4.84	6.36	2.87	0.00	0.61	2.97	1.82	3.11

CHAPTER 5

CONCLUSIONS

Protective relaying is an art that has been constantly studied, modeled, characterized, and improved over the years. Several researchers have contributed to increase the power system security and reliability through the development and implementation of new protection approaches capable of dealing with day to day events that can harm the power system and users. New protection schemes are also designed to face the system behaviour changes caused by the introduction of state of the art technologies.

The important contribution of researchers from all over the world has ease the protections engineer job and most of all it has maintained the protective relaying through the path of becoming a science. In this chapter the conclusions reached during these years of thesis development are presented, in addition the achieved contributions are listed and further work is proposed. The reached conclusions are itemized in the following paragraphs:

- Protective relay coordination is a complex task that requires not just the protection engineer expertise but also software and technology aid.
- Conceptual expertise and software and algorithmic development knowledge is mandatory while working on protective relaying improvements. Optimization theory can be vastly exploited in this research area.
- The requirements of good initial guess and modelling in exact optimization methods present important disadvantages in comparison with metaheuristic methods. The

latter are proposed to carry out most coordination process while nonlinear methods might help to focus the search direction and improve results obtention.

- Protective relaying requires the protection system to clear the fault condition as fast as possible while the coordination time interval between coordination pairs is respected, avoiding sympathy trips and miscoordinations. This fact lead to conclude that the obtention of global optimal results is not a protection requirement. This conclusion is based in two simple affirmations: the power systems size and complexity produces a search space that tents to infinite size, consequently the global optimum obtention is almost impossible to be demonstrated by exhaustive search or exact methods; heuristics on the other hand cannot guarantee the convergency to an optimal result. Secondly, the slower obtention of global optimum settings that might modestly improve coordination results might not be as useful as local optimum results obtained in a reasonable small amount of time.

- The design of an algorithmic parameters tuning process is needed to correctly select a base case for the proposed methodology. The more simulations carried out and the better the experiments design, the most certainty of a correct selection. Powerful computers capable of performing fast simulations would be an advantageous tool in this research step.

- As briefly described, relay coordination is a multiobjective task that requires the improvement of contradictory parameters. The problem is consequently characterised as a pareto front conformed by tripping times a total miscoordinations, where a better solution for one of them cannot be found without degrading the other. The implemented methodology and mainly the objective function weighting parameters can be modified to obtain the required system characteristics.

- Three short-circuit magnitudes are enough to maintain a compatible inversions grade, guaranteeing that coordination is carried out for a region of the curve. The inclusion of more coordination points may be considered in accordance with computational capacities in order to satisfy specific coordination requirements.

- The consideration of unstandardized inverse-time curves improves the overcurrent relay performance and consequently the relay coordination results. The curves compatibilities might be compromised if preventive mechanisms as restrictions are not adopted. The coordination for multiple short-circuit current levels helps to improve the reliability and avoid curve crosses for currents lower than the maximum. This contemplation also reduces the tripping times for the left part of the OCR inverse-time curves.

- Developed methods should be tested in big, widely interconnected, and complex power systems in order to demonstrate robustness and adaptability. The proposed method obtain better results in comparison with conventional approaches using standardized inverse-time curves. The algorithm is tested in five different power systems obtaining important improvements in all of them.

- The inclusion of distance-relays to replace insensitive overcurrent ones suppose a coordination complexity increase. The proposed method obtained positive results, representing a new approach that aims to offer an integral solution for overcurrent relay coordination.

5.1 Contributions

The developed contributions are listed as follows:

- A new protection approach that considers unconventional inverse-time curves has been developed and proven to obtain better results than the use of conventional curves.

- An objective function that considers the overcurrent relay coordination desired characteristics is introduced.

- Coordination for different short-circuit levels is considered in the proposed objective function, multiple intermediate points may be defined in order to ensure coordination for a complete range of currents instead of certain points.

- A software tool capable of carry out the coordination problem is developed from scratch in Matlab. The tool was successfully tested in different power systems and can be modified to fulfil different system requirements.
- Invasive-weed optimization method is implemented to solve power system protection problems for the first time. This method improved genetic algorithm results when tested for different power systems.
- A sequential quadratic programming nonlinear method is used to cooperate with metaheuristic methods, this implementation obtained slight improvements.
- A new coordination approach that replaces insensitive overcurrent relays with distance ones is introduced an proven to obtain positive results.

5.2 Further Work

There are some topics that emerged during this thesis development and might be of interest to perform as further work, those are listed in the following paragraphs:

- The computational capabilities increase would reduce the simulation time, making possible to obtain a solution for bigger power systems, increase the total of iterations, test broader ranges of parameters selection, and consequently obtain improves in the coordination results.
- A perturbation routine can be developed in order to ensure that there is not a better solution in the actual solution surroundings.
- The overcurrent and distance-relay coordination routine can be adapted to offer a protection scheme of full redundancy, considering overcurrent and distance-relays in all system buses and non standardized inverse-time curves.

- The SQP methodology can also be adapted to cooperate in the overcurrent and distance-relay coordination solution.

- The proposed methodology using five adjustable settings and obtaining nonstandardised inverse-time curves might be helpful to compute relay settings for industrial relay applications.

- The development of a user friendly software application that combines different optimization algorithms and protection principles may be the most interesting and sophisticated further work idea emerged from this thesis. This application may receive power system data as an input and recommend protective relaying principles and settings for all system buses as an output.

BIBLIOGRAPHY

[1] P. Kundur, N. J. Balu, and M. G. Lauby. *Power System Stability and Control*. EPRI power system engineering series. McGraw-Hill, New York, first edition, 1994.

[2] A. von Meier. *Electric Power Systems: a Conceptual Introduction*. John Wiley & Sons, New Jersey, USA, first edition, 2006.

[3] M. H. Brown and R. P. Sedano. *Electricity Transmission A Primer*. National Council on Electric Policy, first edition, 2004.

[4] E. Mollick. Establishing Moore's law. *IEEE Annals of the History of Computing*, 28(3):62–75, June 2006.

[5] G. E. Radke. A Method for Calculating Time-Overcurrent Relay Settings by Digital Computer. *IEEE Transactions on Power Apparatus and Systems Special Supplement*, 2(3):303–307, February 1963.

[6] R. E. Albrecht, M. J. Nisja, W. E. Feero, G. D. Rockefeller, and C. L. Wagner. Digital Computer Protective Device Coordination Program. *IEEE Transactions on Power Apparatus and Systems*, 83(4):402–410, April 1964.

[7] H. Y. Tsien. An Automatic Digital Computer Program for Setting Transmission Line Directional Overcurrent Relays ORepreurentation. *IEEE Transactions on Power Apparatus and Systems*, 83(10):1048–1053, October 1964.

[8] R. A. Kennedy and L. E. Curtis. Overcurrent protective device coordination by computer. *IEEE Transactions on Industry Applications*, 1(5):445–456, October 1982.

[9] J. P. Whiting and D. Lidgate. Computer prediction of IDMT relay settings and performance for interconnected power systems. In *IEEE Proceedings on Generation, Transmission and Distribution*, volume 130, pages 139–147, May 1983.

[10] A. J. Urdaneta, R. Nadira, and L. G. Pérez. Optimal coordination of directional overcurrent relays in interconected power systems. *IEEE Transactions on Power Delivery*, 3(3):903–910, July 1988.

[11] A. J. Urdaneta, H. Restrepo, S. Márquez, and J. Sánchez. Coordination of directional overcurrent relay timing using linear programming. *IEEE Transactions on Power Delivery*, 11(1):122–128, January 1996.

[12] A. J. Urdaneta and L. G. Pérez. Optimal coordination of directional overcurrent relays considering dynamic changes in the network topology. *IEEE Transactions on Power Delivery*, 12(4):1458–1464, October 1997.

[13] C. W. So, K. K. Li, K. T. Lai, and K. Y. Fung. Application of Genetic Algorithm for Overcurrent Relay Coordination. In *In Proceedings of the Sixth International Conference on Developments in Power System Protection*, number 434, pages 66–69, March 1997.

[14] C. W. So, K. K. Li, K. T. Lai, and K. Y. Fung. Application of Genetic Algorithm to Overcurrent Relay Grading Coordination. In *In Proceedings of the Fourth International Conference on Advances in Power System Control, Operation and Management*, number 450, pages 283–287, November 1997.

[15] C. W. So and K. K. Li. Overcurrent relay coordination by evolutionary programming. *Electric Power Systems Research*, 53(2):83–90, February 2000.

[16] A. J. Urdaneta, L. G. Pérez, J. F. Gómez, B. Feijoo, and M. González. Presolve analysis and interior point solutions of the linear programming coordination problem of directional overcurrent relays. *International Journal of Electrical Power and Energy Systems*, 23(8):819–825, October 2001.

[17] H. K. Karegar, H. A. Abyaneh, V. Ohis, and M. Meshkin. Pre-processing of the optimal coordination of overcurrent relays. *Electric Power Systems Research*, 75 (2-3):134–141, June 2005.

[18] H. Zeienldin, E. F. El-Saadany, and M. A. Salama. A novel problem formulation for directional overcurrent relay coordination. In *In Proceedings of the Large Engineering Systems Conference on Power Engineering*, pages 48–52, July 2004.

[19] H. Zeineldin, E. F. El-Saadany, and M. A. Salama. Optimal coordination of directional overcurrent relay coordination. In *Proceedings of the IEEE Power Engineering Society General Meeting*, volume 2, pages 1101–1106, June 2005.

[20] H. Zeineldin, E. F. El-Saadany, and M. A. Salama. Optimal coordination of overcurrent relays using a modified particle swarm optimization. *Electric Power Systems Research*, 76(11):988–995, January 2006.

[21] J. Gholinezhad, K. Mazlumi, and P. Farhang. Overcurrent relay coordination using MINLP technique. *19th Iranian Conference on Electrical Engineering*, 2:1–1, May 2011.

[22] D. Birla, R. P. Maheshwari, and H. O. Gupta. A new nonlinear directional overcurrent relay coordination technique, and banes and boons of near-end faults based approach. *IEEE Transactions on Power Delivery*, 21(3):1176–1182, July 2006.

[23] D. Birla, R. P. Maheshwari, and H. O. Gupta. An approach to tackle the threat of sympathy trips in directional overcurrent relay coordination. *IEEE Transactions on Power Delivery*, 22(2):851–858, April 2007.

[24] C. H. Lee and C. R. Chen. Using genetic algorithm for overcurrent relay coordination in industrial power system. In *In Proceedings of the International Conference on Intelligent Systems Applications to Power Systems*, November 2007.

[25] F. Razavi, H. A. Abyaneh, M. Al-Dabbagh, R. Mohammadi, and H. Torkaman. A new comprehensive genetic algorithm method for optimal overcurrent relays coordination. *Electric Power Systems Research*, 78(4):713–720, June 2008.

[26] S. S. H. Kamangar, H. A. Abyaneh, R. M. Chabanloo, and F. Razavi. A new genetic algorithm method for optimal coordination of overcurrent and earth fault relays in networks with different levels of voltages. In *Proceedings of the IEEE Bucharest PowerTech: Innovative Ideas Toward the Electrical Grid of the Future*, pages 1–5, June 2009.

[27] D. Uthitsunthorn and T. Kulworawanichpong. Optimal over-current relay coordination using Genetic Algorithms. *International Review of Electrical Engineering*, 7(4):162–166, September 2010.

[28] P. P. Bedekar, S. R. Bhide, and V. S. Kale. Coordination of overcurrent relays in distribution system using linear programming technique. In *Proceedings of the International Conference on Control, Automation, Communication and Energy Conservation*, pages 4–7, June 2009.

[29] P. P. Bedekar, S. R. Bhide, and V. S. Kale. Optimum coordination of overcurrent relays in distribution system using dual simplex method. In *Proceedings of the Second International Conference on Emerging Trends in Engineering and Technology*, pages 555–559, June 2009.

[30] A. S. Noghabi, J. Sadeh, and H. R. Mashhadi. Considering different network topologies in optimal overcurrent relay coordination using a hybrid GA. *IEEE Transactions on Power Delivery*, 24(4):1857–1863, October 2009.

[31] A. S. Noghabi, H. R. Mashhadi, and J. Sadeh. Optimal coordination of directional overcurrent relays considering different network topologies using interval linear programming. *IEEE Transactions on Power Delivery*, 25(3):1348–1354, July 2010.

[32] P. P. Bedekar and S. R. Bhide. Optimum coordination of directional overcurrent relays using the hybrid GA-NLP approach. *IEEE Transactions on Power Delivery*, 26(1):109–119, January 2011.

[33] P. P. Bedekar and S. R. Bhide. Optimum coordination of overcurrent relay timing using continuous genetic algorithm. *Expert Systems with Applications*, 38(9): 11286–11292, September 2011.

[34] Y. Damchi, H. R. Mashhadi, J. Sadeh, and M. Bashir. Optimal coordination of directional overcurrent relays in a microgrid system using a hybrid particle swarm optimization. In *Proceedings of the International Conference on Advanced Power System Automation and Protection*, volume 2, pages 1135–1138, October 2011.

[35] M. Singh, B. K. Panigrahi, and A. R. Abhyankar. Optimal overcurrent relay coordination in distribution system. In *Proceedings of the International Conference on Energy, Automation and Signal*, number 2, pages 822–827, December 2011.

[36] R. Mohammadi, H. A. Abyaneh, H. M. Rudsari, S. H. Fathi, and H. Rastegar. Overcurrent relays coordination considering the priority of constraints. *IEEE Transactions on Power Delivery*, 26(3):1927–1938, July 2011.

[37] M. Ezzeddine and R. Kaczmarek. A novel method for optimal coordination of directional overcurrent relays considering their available discrete settings and several operation characteristics. *Electric Power Systems Research*, 81(7):1475–1481, February 2011.

[38] J. Moirangthem, K. R. Krishnanand, and N. Saranjit. Optimal coordination of overcurrent relay using an enhanced discrete differential evolution algorithm in a distribution system with DG. In *Proceedings of the International Conference on Energy, Automation and Signal*, pages 251–256, December 2011.

[39] D. Uthitsunthorn. Optimal overcurrent relay coordination using artificial bees colony algorithm. In *Proceedings of the Power Engineering and Power Systems Convention*, number 2, pages 901–904, May 2011.

[40] M. El-Mesallamy, W. El-Khattam, A. Hassan, and H. Talaat. Coordination of Directional Overcurrent Relays using artificial bee colony. *Proceedings of the 22nd International Conference and Exhibition on Electricity Distribution*, 5(1):64–71, June 2013.

[41] R. Thangaraj, T. R. Chelliah, and M. Pant. Overcurrent relay coordination by Differential Evolution algorithm. In *Proceedings of the IEEE International Conference on Power Electronics, Drives and Energy Systems*, pages 1–6, December 2012.

[42] M. Singh, B. K. Panigrahi, and R. Mukherjee. Optimum Coordination of overcurrent relays using CMA-ES algorithm. *Proceedings of the IEEE International Conference on Power Electronics, Drives and Energy Systems*, pages 1–6, March 2012.

[43] J. A. Sueiro, E. Diaz-Dorado, E. Míguez, and J. Cidrás. Coordination of directional overcurrent relay using evolutionary algorithm and linear programming. *International Journal of Electrical Power and Energy Systems*, 42(1):299–305, March 2012.

[44] A. Mahari and H. Seyedi. An analytic approach for optimal coordination of overcurrent relays. *IET Generation, Transmission & Distribution*, 7(7):674–680, February 2013.

[45] C. R. Chen, C. H. Lee, and C. J. Chang. Optimal overcurrent relay coordination in power distribution system using a new approach. *International Journal of Electrical Power and Energy Systems*, 45(1):217–222, August 2013.

[46] F. B. Bottura, W. M. S. Bernardes, M. Oleskovicz, E. N. Asada, S. A. Souza, and M. J. Ramos. Coordination of directional overcurrent relays in meshed power systems using hybrid genetic algorithm optimization. In *Proceedings of the 12th IET International Conference on Developments in Power System Protection*, pages 1–6, March 2013.

[47] F. B. Bottura, M. Oleskovicz, D. V. Coury, S. de Souza, and M. Ramos. Hybrid Optimization Algorithm for Directional Overcurrent Relay Coordination. *Proceedings of the IEEE/PES General Meeting, Conference & Exposition*, pages 1–5, July 2014.

[48] M. H. Hussain, S. R. A. Rahim, and I. Musirin. Optimal overcurrent relay coordination: A review. *Procedia Engineering*, 53:332–336, March 2013.

[49] Y. Lu and J. L. Chung. Detecting and solving the coordination curve intersection problem of overcurrent relays in subtransmission systems with a new method. *Electric Power Systems Research*, 95:19–27, August 2013.

[50] M. Singh, B. K. Panigrahi, A. R. Abhyankar, and S. Das. Optimal coordination of directional over-current relays using informative differential evolution algorithm. *Journal of Computational Science*, 5(2):269–276, March 2014.

[51] M. Singh and B. K. Panigrahi. Minimization of Operating Time Gap Between Primary Relays at Near and Far Ends in Overcurrent Relay Coordination. In *Proceedings of the North American Power Symposium*, September 2014.

[52] T. R. Chelliah, R. Thangaraj, S. Allamsetty, and M. Pant. Coordination of directional overcurrent relays using opposition based chaotic differential evolution algorithm. *International Journal of Electrical Power and Energy Systems*, 55:341–350, December 2014.

[53] M. H. Hussain, I. Musirin, A. F. Abidin, and S.R.A. Rahim. Directional overcurrent relay coordination problem using modified swarm firefly algorithm considering the effect of population size. In *IEEE 8th International Power Engineering and Optimization Conference*, pages 591–596, March 2014.

[54] M. Y. Shih, A. Conde Enríquez, and L. M. Torres Treviño. On-line coordination of directional overcurrent relays: Performance evaluation among optimization algorithms. *Electric Power Systems Research*, 110:122–132, January 2014.

[55] O. Arreola Soria, A. Conde Enríquez, and L. A. Trujillo Guajardo. Overcurrent relay with unconventional curves and its application in industrial power systems. *Electric Power Systems Research*, 110:113–121, January 2014.

[56] R. B. Gastineau, R. H. Harris, W. L. Woodside, and W. V. Scribner. Using the computer to set transmission line phase distance and ground back-up relays. *IEEE Transactions on Power Apparatus and Systems*, 96(2):478–484, March 1977.

[57] M. J. Damborg, R. Ramaswami, and S. S. Venkata. Computer Aided Transmission Protection System Design Part I: Algorithms. *IEEE Transactions on Power Apparatus and Systems*, 103(1):51–59, January 1984.

[58] R. Ramaswami, S. S. Venkata, M. J. Damborg, and J. M. Postforoosh. Computer Aided Transmission Protection System Design Part II: Implementations and Results. *IEEE Transactions on Power Apparatus and Systems*, 103(1):60–65, January 1984.

[59] D. E. Schultz and S. S. Waters. Computer-Aided Protective Device Coordination, A Case Study. *IEEE Transactions on Power Apparatus and Systems*, 103(11): 3295–3301, November 1984.

[60] R. Ramaswami, M. J. Damborg, S. S. Venkata, A. K. Jamp, and J. Postforoosh. Enhanced Algorithms for Transmission Protective Relay Coordination. *IEEE Transactions on Power Delivery*, 6(1):280–287, January 1986.

[61] L. G. Pérez and A. J. Urdaneta. Optimal computation of distance relays second zone timing in a mixed protection scheme with directional overcurrent relays. *IEEE Transactions on Power Delivery*, 16(3):385–388, July 2001.

[62] M. Khederzadeh. Back-up protection of distance relay second zone by directional overcurrent relays with combined curves. *2006 IEEE Power Engineering Society General Meeting*, pages 1–6, June 2006.

[63] L. A. Kojovic and J. F. Witte. A new method in reducing the overcurrent protection response times at high fault currents to protect equipment from extended stress. In *Proceedings of the IEEE/PES Transmission and Distribution Conference and Exposition*, volume 1, pages 65–70, October 2001.

[64] R. M. Chabanloo, H. A. Abyaneh, S. S. H. Kamangar, and F. Razavi. A new genetic algorithm method for optimal coordination of overcurrent relays in a mixed protection scheme with distance relays. *Proceedings of the Universities Power Engineering Conference*, 08:569–573, December 2008.

[65] J. Sadeh, V. Aminotojari, and M. Bashir. Optimal coordination of overcurrent and distance relays with hybrid genetic algorithm. In *Proceedings of the 10th International Conference on Environment and Electrical Engineering*, pages 1–5, May 2011.

[66] J. Sadeh, V. Amintojjar, and M. Bashir. Coordination of overcurrent and distance relays using hybrid particle swarm optimization. In *Proceedings of the International Conference on Advanced Power System Automation and Protection*, volume 2, pages 1130–1134, October 2011.

[67] R. M. Chabanloo, H. A. Abyaneh, S. S. H. Kamangar, and F. Razavi. Optimal combined overcurrent and distance relays coordination incorporating intelligent overcurrent relays characteristic selection. *IEEE Transactions on Power Delivery*, 26 (3):1381–1391, July 2011.

[68] M. Singh, B. K. Panigrahi, and A. R. Abhyankar. Combined optimal distance to overcurrent relay coordination. In *Proceedings of the IEEE International Conference on Power Electronics, Drives and Energy Systems*, pages 1–6, December 2012.

[69] Z. Moravej, M. Jazaeri, and M. Gholamzadeh. Optimal coordination of distance and over-current relays in series compensated systems based on MAPSO. *Energy Conversion and Management*, 56:140–151, November 2012.

[70] D. S. Nair and S. Reshma. Optimal coordination of protective relays. In *Proceedings of the International Conference on Power, Energy and Control*, pages 239–244, February 2013.

[71] M. Farzinfar, M. Jazaeri, and F. Razavi. A new approach for optimal coordination of distance and directional over-current relays using multiple embedded crossover PSO. *International Journal of Electrical Power & Energy Systems*, 61:620–628, May 2014.

[72] A. R. Haron, A. Mohamed, and H. Shareef. Coordination of Overcurrent, Directional and Differential Relays for the Protection of Microgrid System. *Procedia Technology*, 11:366–373, January 2013.

[73] C. R. Mason. *The Art and Science of Protective Relaying*. John Wiley & Sons, first edition, 1956.

[74] W. A. Elmore. *Protective Relaying Theory and Applications*. Marcel Dekker, second edition, 2004.

[75] J. Lewis Blackburn and Thomas J. Domin. *Protective Relaying: Principles and Applications*. CRS Press, third edition, 2006.

[76] S. H. Horowitz and A. G. Phadke. *Power System Relaying*. John Wiley & Sons, New Jersey, USA, third edition, 2008.

[77] B. Lundqvist. 100 years of relay protection, the Swedish ABB relay history. ABB *Automation Products, Substation Automation Divisio*, 2005.

[78] IEEE. Inverse Time Characteristic Equations for Overcurrent Relays. *IEEE standard C37.112-1996*, 1997.

[79] AREVA. Directional and non directional overcurrent protection. Technical data sheet. Technical report, August 2015.

[80] International Electrotechnical Commission. IEC 60255:2001 Electrical Relays International Standard. *International Standards*, 2001.

[81] R. Christie. Power systems test case archive, August 2015. URL `http://www.ee.washington.edu/research/pstca`.

[82] M. Affenzeller, S. Winkler, S. Wagner, and A. Beham. *Genetic Algorithms and Genetic Programming: Modern Concepts and Practical Applications*. Chapman & Hall/CRC, London, UK, first edition, 2009.

[83] J. W. Chinneck. *Practical optimization: a gentle introduction*. Carleton University, Ottawa, Canada, first edition, 2012.

[84] D. E. Goldberg. *Genetic Algorithms in Search, Optimization, and Machine Learning*. Addison-Wesley, Reading, USA, second edition, 1989.

[85] Eugene Lawler. *Combinatorial Optimization: Networks and Matroids*. Saunders College Publishing, TX, USA, first edition, 1976.

[86] C. H. Papadimtriou and K Steiglitz. *Combinatorial Optimization: Algorithms and Complexity*. Prentice-Hall, New Jersey, USA, first edition, 1982.

[87] W. J. Cook, W. H. Cunningham, W. R. Pulleyblank, and A. Schrijver. *Combinatorial Optimization*. John Wiley & Sons, New York, USA, first edition, 1998.

[88] Eugene Lawler. *The Traveling Salesman Problem: A Guided Tour of Combinatorial Optimization*. John Wiley & Sons, New York, USA, first edition, 1985.

[89] Z. Michalewicz and D. B. Fogel. *How to solve it: Modern Heuristics*. Springer, Berlin, Germany, first edition, 2000.

[90] Indiana University. Understanding measures of supercomputer performance and storage system capacity. `https://kb.iu.edu/d/apeq`, August 2015.

[91] the list Top 500. China's tianhe-2 supercomputer takes no. 1 ranking on top 500 list. `http://www.top500.org/blog/lists/2013/06/press-release/`, August 2015.

[92] J. Dongarra. Visit to the national university for defense technology changsha, china. Technical report, University of Tennessee, August 2013.

[93] F. Gonzalez-Longatt. Test case p. m. anderson power system. `http://fglongatt.org/OLD/Test\_Case\_Anderson.html`, August 2015.

[94] V Task Studio. Free software tools: Qwikmark 0.4. `http://www.vtaskstudio.com/support.php#tools`, August 2015.

[95] S. Kirkpatrick, C. D. Gelatt, and M. P. Vecchi. Optimization by simulated annealing. *Science*, 220(4598):671–680, May 1983.

[96] S. Ólafsson. *Handbook on Simulation*. Handbooks in Operations Research and Management Science VII. Elsevier, 2006.

[97] S. Sumathi, Hamsapriya T., and Surekha P. *Evolutionary intelligence : an introduction to theory and applications with Matlab*. Springer, Berlin, Germany, first edition, 2008.

[98] D. P. Bertsekas. *Nonlinear Programming*. Athena Scientific, Cambridge, USA, second edition, 1999.

[99] M. S. Bazaraa, H. D. Sherali, and C. M. Shetty. *Nonlinear Programming: Theory and Applications*. John Wiley & Sons, Hoboken, NJ, third edition, 2006.

[100] D. Luenberger and Y. Ye. *Linear and Nonlinear Programming*. Springer, New York, USA, third edition, 2008.

[101] I. Griva, S. G. Nash, and A. Sofer. *Linear and Nonlinear Optimization*. Society for Industrial and Applied Mathematics, Pennsilvania, USA, second edition, 2009.

[102] H. K. Khalil. *Nonlinear Systems*. Prentice Hall, New Jersey, USA, first edition, 2002.

[103] H. A. Taha. *Operations Research: An Introduction*. Pearson Prentice Hall, New Jersey, USA, eighth edition, 2007.

[104] E. Goodarzi, Ziaei M., and Hosseinipour E. Z. *Introduction to Optimization Analysis in Hydrosystem Engineering*. Springer International Publishing, Switzerland, first edition, 2014.

[105] S. P. Bradley, A. C. Hax, and T. L. Magnanti. *Applied Mathematical Programming*. Addison-Wesley, Reading, USA, first edition, 1977.

[106] C. G. Broyden. Quasi-Newton Methods and their Application to Function Minimisation. *Mathematics of Computation*, 21(99):368–381, June 1967.

[107] K. Schittkowski. NLPQL: A fortran subroutine solving constrained nonlinear programming problems. *Annals of Operations Research*, 5(2), 1986.

[108] P. T. Boggs and J. W. Tolle. Quasi-Newton Methods and their Application to Function Minimisation. *Acta Numerica, Cambridge University Press*, 4(1):1–54, January 1995.

[109] R. Fletcher. The sequential quadratic programming method. In Gianni Di Pillo and Fabio Schoen, editors, *Nonlinear Optimization*, Lecture Notes in Mathematics, pages 165–214. Springer, 2010.

[110] P. E. Gill and E. Wong. Sequential quadratic programming methods. In J. Lee and S. Leyffer, editors, *Mixed Integer Nonlinear Programming*, volume 154 of *Volumes in Mathematics and its Applications*, pages 147–224. Springer, New York, USA, 2012.

[111] R. B. Wilson. *A Simplicial Algorithm for Concave Programming*. PhD thesis, Graduate School of Business Administration, Harvard University, Cambridge, USA, 1963.

[112] K. C. B. Steer, A. Wirth, and S. K. Halgamuge. The rationale behind seeking inspiration from nature. In R. Chiong, editor, *Nature-Inspired Algorithms for Optimisation*, volume 193 of *Studies in Computational Intelligence*, pages 51–76. Springer, Berlin, Germany, 2009.

[113] G. Rozenberg, T. Bäck, and J. N. Kok. *Handbook of Natural Computing*. Springer, Berlin, Germany, first edition, 2012.

[114] D. W. Corne, K. Deb, J. D. Knowles, and X Yao. Selected aspects of natural computing. In *Handbook of Natural Computing*, pages 1737–1801. Springer, Berlin, Germany, first edition, 2012.

[115] D. B. Fogel, T Bäck, and Z. Michalewicz, editors. *Handbook of Evolutionary Computation*. Taylor & Francis, New York, USA, first edition, 1997.

[116] P. J. Bentley, editor. *Evolutionary Design by Computers*. Morgan Kaufmann, California, USA, first edition, 1999.

[117] A. E. Eiben and J. E. Smith, editors. *Introduction to Evolutionary Computing*. Springer, Berlin, Germany, first edition, 2003.

[118] D. B. Fogel, editor. *Evolutionary Computation, Toward a New Philosophy of Machine Intelligence*. John Wiley & Sons, New Jersey, USA, third edition, 2006.

[119] C. Darwin. *The origin of species by means of natural selection, or the preservation of favoured races in the struggle for life*. John Murray, London, UK, sixth edition, 1859.

[120] A. M. Turing. *Mechanical Intelligence*. Collected works of A. M. Turing. Elsevier Science Publishers, Amsterdam, Netherlands, November 1992.

[121] C. S. Webster. Alan Turing's unorganized machines and artificial neural networks: his remarkable early work and future possibilities. *Evolutionary Intelligence*, 5(1): 35–43, March 2012.

[122] J. H. Holland. Outline for a logical theory of adaptive systems. *Journal of The Association for Computing Machinery*, 9(3):297–314, July 1962.

[123] J. H. Holland. Genetic algorithms and the optimal allocation of trials. *Journal on Computation of the Society for Industrial and Applied Mathematics*, 2(2):88–105, August 1973.

[124] J. H. Holland. *Adaptation in Natural and Artificial Systems*. MIT Press, Cambridge, USA, second edition, 1992.

[125] L. J. Fogel. Autonomous automata. *Industrial Research*, 4:14–19, February 1962.

[126] L. J. Fogel. *On the organization of intellect*. PhD thesis, University of California Los Angeles, California, USA, 1964.

[127] L. J. Fogel, A. J. Owens, and M. J. Walsh. *Artificial Intelligence Through Simulated Evolution*. John Wiley & Sons, California, USA, first edition, 1966.

[128] H. P. Schwefel. *Kybernetische Evolution als Strategie der exprimentellen Forschung in der Strömungstechnik. Master's Thesis (in German)*. PhD thesis, Technical University of Berlin, Berlin, Germany, 1965.

[129] I. Rechenberg. *Evolutionsstrategie — Optimierung technischer Systeme nach Prinzipien der biologischen Evolution (in German)*. Frommann-Holzboog Verlag, Stuttgart, Germany, first edition, 1973.

[130] H. P. Schwefel. *Evolution and Optimum Seeking: The Sixth Generation*. John Wiley & Sons, New York, USA, first edition, 1993.

[131] T. Bäck. Evolution strategies: An alternative evolutionary algorithm. In Jean-Marc Alliot, Evelyne Lutton, Edmund Ronald, Marc Schoenauer, and Dominique Snyers, editors, *Artificial Evolution*, volume 1063 of *Lecture Notes in Computer Science*, pages 1–20. Springer, June 1996.

[132] H. G. Beyer. *The Theory of Evolution Strategies*. Natural Computing Series. Springer, Berlin, Germany, first edition, 2001.

[133] H. G. Beyer and H. P. Schwefel. Evolution strategies – a comprehensive introduction. *Natural Computing*, 1(1):3–52, March 2002.

[134] F.L. Minku and T.B. Ludermir. Evolutionary strategies and genetic algorithms for dynamic parameter optimization of evolving fuzzy neural networks. In *Proceedings of the IEEE Congress on Evolutionary Computation*, volume 3, pages 1951–1958, September 2005.

[135] J. R. Koza. *Genetic Programming: On the Programming of Computers by Means of Natural Selection*. MIT Press, Cambridge, USA, first edition, 1992.

[136] J. R. Koza. *Genetic Programming II: Automatic Discovery of Reusable Programs*. MIT Press, Cambridge, USA, first edition, 1994.

[137] J. R. Koza, D. Andre, F. H. Bennett, and M. A. Keane. *Genetic Programming III: Darwinian Invention & Problem Solving*. Morgan Kaufmann Publishers, California, USA, first edition, 1999.

[138] J. R. Koza. *Genetic Programming IV: Routine Human-Competitive Machine Intelligence*. Kluwer Academic Publishers, Cambridge, USA, first edition, 2003.

[139] R. Storn and K. Price. Minimizing the real functions of the ICEC'96 contest by differential evolution. In *Proceedings of the IEEE International Conference on Evolutionary Computation*, pages 842–844, May 1996.

[140] R. Storn and K. Price. Differential evolution – a simple and efficient heuristic for global optimization over continuous spaces. *Journal of Global Optimization*, 11 (4):341–359, December 1997.

[141] R. Storn. On the usage of differential evolution for function optimization. In *Proceedings of the Biennial Conference of the North American Fuzzy Information Processing Society*, pages 519–523, June 1996.

[142] R. Storn. System design by constraint adaptation and differential evolution. *IEEE Transactions on Evolutionary Computation*, 3(1):22–34, April 1999.

[143] K. V. Price, R. Storn, and J. A. Lampinen. *Differential Evolution - A Practical Approach to Global Optimization*. Natural Computing. Springer, first edition, January 2006.

[144] H. Bersini, M. Dorigo, S. Langerman, G. Seront, and L. Gambardella. Results of the first international contest on evolutionary optimisation (1st iceo). In *Proceedings of the IEEE International Conference on Evolutionary Computation*, pages 611–615, May 1996.

[145] J. Kennedy and R. Eberhart. Particle swarm optimization. In *Proceedings of the IEEE International Conference on Neural Networks*, volume 4, pages 1942–1948, November 1995.

[146] Y. Shi and R. Eberhart. A modified particle swarm optimizer. In *Proceedings of the IEEE World Congress on Computational Intelligence*, pages 69–73, May 1998.

[147] J. Kennedy and R. C. Eberhart. *Swarm Intelligence*. Morgan Kaufmann Publishers, CA, USA, first edition, 2001.

[148] R. Poli. Analysis of the publications on the applications of particle swarm optimisation. *Journal of Artificial Evolution and Applications*, 2008(1):1–10, November 2007.

[149] M. Dorigo and T. Stützle. *Ant Colony Optimization*. MIT Press, Cambridge, USA, first edition, 2004.

[150] M. Dorigo and K. Socha. An introduction to ant colony optimization. Approximation Algorithms and Metaheuristics. CRC Press, Brussels, Belgium, first edition, 2007.

[151] M. Dorigo, M. Birattari, and T. Stützle. Ant colony optimization– artificial ants as a computational intelligence technique. *IEEE Computational Intelligence Magazine*, September 2006.

[152] M. Dorigo and T. Stützle. Ant colony optimization: Overview and recent advances. In M. Gendreau and J. Y. Potvin, editors, *Handbook of Metaheuristics*, volume 146 of *International Series in Operations Research & Management Science*, pages 227–263. Springer US, first edition, 2010.

[153] M. Dorigo. *Optimization, Learning and Natural Algorithms*. PhD thesis, Politecnico di Milano, Milano, Italy, 1992.

[154] A. R. Mehrabian and C. Lucas. A novel numerical optimization algorithm inspired from weed colonization. *Ecological Informatics*, 1(4):355–366, July 2006.

[155] H. S. Rad and C. Lucas. A recommender system based on invasive weed optimization algorithm. In *Proceedings of the IEEE Congress on Evolutionary Computation*, pages 4297–4304, September 2007.

[156] A. H. Nikoofard, H. Hajimirsadeghi, A. Rahimi-Kian, and C. Lucas. Multiobjective invasive weed optimization: Application to analysis of pareto improvement models in electricity markets. *Applied Soft Computing*, 12(1):100–112, January 2012.

[157] H. Josiński, D. Kostrzewa, A. Michalczuk, and A. Świtoński. The expanded invasive weed optimization metaheuristic for solving continuous and discrete optimization problems. *The Scientific World Journal*, 2014(1):1–14, January 2006.

[158] M. Mitchell. *An Introduction to Genetic Algorithms*. MIT Press, Cambridge, USA, fifth edition, 1999.

[159] J. Bronowski. *The Ascent of Man*. British Broadcasting Corporation, London, UK, 1973.

[160] A. R. Wallace. *My Life; A Record of Events and Opinions*. Chapman & Hall, London, UK, first edition, 1905.

[161] M. Gen, R. Cheng, and L. Lin. *Network Models and Optimization: Multiobjective Genetic Algorithm Approach (Decision Engineering)*. Springer, first edition, 2008.

[162] D. E. Goldberg and K. Deb. A comparative analysis of selection schemes used in genetic algorithms. In *Foundations of Genetic Algorithms*, pages 69–93. Morgan Kaufmann, 1991.

[163] J. E. Baker. Reducing bias and inefficiency in the selection algorithm. In *Proceedings of the Second International Conference on Genetic Algorithms on Genetic Algorithms and Their Application*, pages 14–21, New Jersey, USA, 1987. Erlbaum Associates Inc.

[164] H. G. Baker, G. L. Stebbins, and International Union of Biological Sciences. *The genetics of colonizing species: proceedings*. Academic Press, New York, USA, 1965.

[165] Y. Zhou, Q. Luo, and H. Chen. A novel differential evolution invasive weed optimization algorithm for solving nonlinear equations systems. *Journal of Applied Mathematics*, 2013(4):1–18, November 2013.

[166] Siemens. Reydisp evolution, configuration software for Reyrolle protection devices. `http://w3.siemens.com/smartgrid/global/en/products-systems-solutions/Protection/Engineering-Evaluation-Diagnostic-Software/Pages/reydisp-evolution.aspx`, August 2015.

[167] Siemens. Reyrolle protection devices. `http://www.energy.siemens.com/hq/en/automation/power-transmission-distribution/protection/reyrolle`, August 2015.

[168] K. Chen. *Industrial Power Distribution and Illuminating Systems*. Electrical and Computer Engineering. Taylor & Francis, New York, USA, 1990.

[169] A. F. Sleva. *Protective Relay Principles*. Taylor & Francis, New York, USA, first edition, 2009.

[170] W. Mock. Pareto optimality. In D. K. Chatterjee, editor, *Encyclopedia of Global Justice*, pages 808–809. Springer Netherlands, 2011.

[171] H. Saadat. *Power Systems Analysis*. McGraw-Hill series in electrical and computer engineering. McGraw-Hill, New York, USA, 2002.

[172] G. Olguin. *Voltage Dip (Sag) Estimation in Power Systems based on Stochastic Assessment and Optimal Monitoring*. PhD thesis, Chalmers University of Technology, Göteborg, Sweden, 2005.

[173] M. Wämundson. *Calculating voltage dips in power systems using probability distributions of dip durations and implementation of the Moving Fault Node method. Master's Thesis*. PhD thesis, Chalmers University of Technology, Göteborg, Sweden, 2007.

[174] MATLAB. Find minimum of constrained nonlinear multivariable function. `http://www.mathworks.com/help/optim/ug/fmincon.html`, August 2015.

[175] MATLAB. Optimization toolbox. `http://www.mathworks.com/products/optimization`, August 2015.

[176] MATLAB. Optimization toolbox user's guide. `http://www.mathworks.com/help/pdf_doc/optim/optim_tb.pdf`, August 2015.

[177] MATLAB. The language of technical computing. `http://www.mathworks.com/products/optimization/`, August 2015.

INDEX

AUTOBIOGRAPHY

M.C. Carlos Alberto Castillo Salazar

Candidato al grado de Doctor en Ingeniería Eléctrica

Universidad Autónoma de Nuevo León

Facultad de Ingeniería Mecánica y Eléctrica

Tesis:

DISTANCE AND OVERCURRENT RELAY COORDINATION CONSIDERING NON STANDARDIZED INVERSE TIME CURVES

Nací en Octubre de 1987 en Monterrey, Nuevo León, México. Soy el cuarto hijo de Luis Javier Castillo Granados y Rosa Laura Salazar Macías (†), e hijo adoptivo de Alma Chávez. Obtuve el título de Ingeniero Mecánico Eléctrico en Octubre de 2009, fui asesorado por la Dra. Elisa Schaeffer para desarrollar mi trabajo de tesis titulado “Optimización de costos de reemplazo en redes sensoras inalámbricas”. Desde inicios de 2010 trabajé en la industria hasta que en Agosto del mismo año ingresé a realizar estudios de posgrado. Aprobé las materias cursadas y asesorado por el Dr. Arturo Conde realicé el trabajo de tesis titulado “Coordinación de relevadores de sobrecorriente mediante algoritmos de optimización utilizando curvas de tiempo no convencionales”, obteniendo el grado de Maestro en Ciencias de la Ingeniería Eléctrica con orientación en Sistemas Eléctricos de Potencia en Julio de 2012. Desde ese momento y hasta la fecha he desarrollado estudios doctorales, teniendo además la oportunidad de realizar una estancia de investigación en Aalto University, en Espoo, Finlandia; asimismo me he desempeñado como profesor de diversas asignaturas en universidades locales.